Design of Controllers and Analysis of PEM Fuel Cell System

A thesis submitted in partial fulfillment of the requirement

for the award of the degree of

DOCTOR OF PHILOSOPHY

in

CHEMICAL ENGINEERING

By

Mr. SRINIVASARAO DIVI

(Roll No.715056)

Under the supervision of

Prof. SHIRISH HARI SONAWANE

DEPARTMENT OF CHEMICAL ENGINEERING

NATIONAL INSTITUTE OF TECHNOLOGY

WARANGAL – 506004 (T.S), INDIA.

MAY 2020

DEDICATED TO

MY PARENTS & FAMILY

NATIONAL INSTITUTE OF TECHNOLOGY-WARANGAL

Warangal - 506 004, Telangana, INDIA.

CERTIFICATE

This is to certify that the thesis entitled "**Design of Controllers and Analysis of PEM Fuel Cell System**" being submitted by **Mr. SrinivasaraoDivi**for the award of the degree of Doctor of Philosophy (**Ph.D.**) in the Department of Chemical Engineering, National Institute of Technology, Warangal, Telangana, India is a record of the bonafide research work carried out by him under my supervision. The thesis has fulfilled the requirements according to the regulations of this Institute and in my opinion it has reached the standards for submission. The results embodied in the thesis have not been submitted to any other University or Institute for the award of any degree or diploma.

Date:

(**Dr. SHIRISHH. SONAWANE**)
Research Supervisor
Professor & Head
Department of Chemical Engineering
National Institute of Technology, Warangal, India.

DECLARATION

This is to certify that the work presented in the thesis entitled "**Design of Controllers and Analysis of PEM Fuel Cell System**" is a bonafide work done by me under the supervision of **Dr. Shirish H. Sonawane** and was not submitted elsewhere for award of any degree.

I declare that this written submission represents my ideas in my own words and where others ideas or words have been included; I have adequately cited and referenced the original sources. Ialso declare that I have adhered to all principles of academic honesty and integrity and have not misrepresented or fabricated or falsified any idea/data/fact/source in my submission. I understand that any violation of the above will be a cause for disciplinary action by the institute and can also evoke penal action from the sources which have thus not been properly cited or from whom proper permission has not been taken when needed.

SRINIVASARAO DIVI

Roll No.: 715056

ACKNOWLEDGEMENTS

At this moment firstly I would take privilege to express my gratitude and extend accomplishment, to my respected guide, ***Dr. Shirish H. Sonawane,*** Professor, Department of Chemical Engineering, National Institute of Technology Warangal, India. This work would not have been possible without his guidance, support and encouragement. His knowledge and guidance is an invaluable tool throughout my work. Under his guidance I have successfully completed this work and learned a lot from him.

I extend my thanks to the Director, ***Prof. N.V. Ramana Rao,*** National Institute of Technology Warangal, India for giving me this opportunity to carry out the work and allowing me to submit this work in the form of thesis.

I would like to extend my thanks to ***Prof. Shirish H. Sonawane,*** HOD, Department of Chemical Engineering, National Institute of Technology, Warangal, India for their encouragement and valuable suggestions throughout my research period.

I would like to express my sincere and whole hearted thanks to my doctoral scrutiny committee (DSC) members ***Prof. A. SarathBabu***, Professor, Dept. of Chemical Engineering, ***Dr. S. Srinath,*** Associate Professor, Dept. of Chemical Engineering, ***Dr. G. Uday Bhaskar Babu,*** Assistant Professor, Dept. of Chemical Engineering, ***Dr. Ch. Venkaiah,*** Associate Professor, Dept. of Electrical Engineering, National Institute of Technology, Warangal for their helpful suggestions and encouragement for successful completion of research work.

I would like to extend my thanks to all the faculty members in Department of Chemical Engineering especially ***Dr. T. Sunil Kumar*** and ***Prof. M Chidambaram*** for their valuable suggestions, support and encouragement.

I am also thankful to all the supporting and technical staff of the Department who has directly or indirectly helped me during my research period at NIT Warangal.

I would like to express my sincere thanks to ***Prof. Shantanu Das,*** RCSDS, E&I Group, Bhabha Atomic Research Center (BARC), Mumbai, India for his valuable suggestions and constant encouragement.

It is my great pleasure to acknowledge and extend my gratitude to ***Prof. M. Chidambaram,*** **Department of Chemical Engineering, Indian Institute of Technology, Chennai (IIT Madras), India** for his valuable guidance and support.

I take this opportunity to sincerely acknowledge the Ministry of Human Resource Development (MHRD), Government of India, New Delhi for providing financial assistance in the form of Stipend for the stay at NIT Warangal from 2015 to 2019.

I am thankful to all my fellow research scholars and lab mates specially ***Dr. M. Suresh Kumar, Dr. Bhaskar Bethi, Dr.Shabana Shaik, Dr. Prashant L. Suryawanshi, Dr. D. Uday Bagley, Dr. P. Rajesh Kumar, Mr. M Yadagiri, Mr. P. Narsimha, Mr. Swapnil Adsul, Mr. Vikas Hakke, Mrs. Vividha, Mrs. Shital Potdar, Mr. Dilip Kumar, Mr. D.Kishore, Mr. Purushotam, and Mr. Shekhar, Mr. Ameer Khan*** for their encouragement and support during my stay at NIT Warangal.

I invariably feel short of words to express my deep sense of gratitude to my family for their constant support, co-operation, love and affection whose blessings made my journey worth effort. My special appreciation is to my parents (***Smt. Bhagya Lakshmi*** and ***Mr. RadhakrishnaMurty*****)** and my brother ***Mr. D. Chandra Sekhar*** who has been a constant source of encouragement for my higher studies and believed me in all the work I do. A special appreciation is to my better half ***Smt. D. Bhavani,*** my children ***Sahithi, Meghana and Gopi Krishna*** for their love and affection and continuous support. I express my gratitude towards my brother-in-law, sister-in-law families for their love and support. I take this opportunity to express my gratitude to all my teachers who helped me to be the person I am and supported me to reach this position. I immensely thank them all from core of my heart.

SrinivasaraoDivi

Table of Contents

List of Figures

List of Tables

ABBREVATIONS

FC	Fuel Cell
GHG	Green House gases
PEM	Proton Exchange Membrane
PEMFC	Proton Exchange Membrane Fuel Cell
AFC	Alkaline fuel cell
MCFC	Molten Carbonate fuel cell
OCV	open circuit voltage
PAFC	Phosphoric Acid fuel cell
SOFC	Solid oxide fuel cell
DMFC	Direct Methanol fuel cell
MEA	Membrane Electrode Assembly
MIMO	Multi Input Multi Output
MISO	Multi Input Single Output
LQR	Linear Quadratic Regulator
LQG	Linear Quadratic Gaussian
SMO	Sliding Mode Observer
SMC	Sliding Mode Controller
GLC	Globally Linearizing Controller
PI	Proportional Integral
PD	Proportional Derivative
PID	Proportional Integral Derivative
MPC	Model Predictive Control
IT2FPID	Interval Type 2 Fuzzy PID
T1FPID	Type 1 Fuzzy PID
UDE	Uncertainty and Disturbance Estimation
IOPID	Integer Order PID
FOPI	Fractional Order PI
FOPID	Fractional Order PID

MATLAB	MATrixLABoratory
FOPTD	First Order Plus Time Delay
SOPTD	Second Order Plus Time Delay
ISE	Integral Square Error
IAE	Integral Absolute Error
ITAE	Integral Time Absolute Error
TV	Total Variance (or) Total Variation
IMC	Internal Model Control
SIMC	Skogestad IMC
GA	Genetic Algorithm
SP	Setpoint
LD	Load Disturbance
NDT	Non Dimensional Tuning
TITO	Two input Two output
ZN	Ziegler- Nichols
AMIGO	Approximate M-constrained Integral Gain Optimization
Ms	Maximum sensitivity
FLC	Fuzzy Logic Control
FPID	Fuzzy PID
IT2FPID	Interval Type 2 Fuzzy PID
DC	Direct current
AC	Alternative current

NOMENCLATURE

Symbol	Meanings
A_T	Cathode outlet throttle area
C_D	Cathode outlet throttle discharge coefficient
C_P	Specific heat of air
dB	Decibels
F	Faraday's constant
H_2	Hydrogen
H_2O	Water
I_{stack}	Stack current
J_{cp}	Compressor and motor inertia
$K_{ca,in}$	Cathode inlet orifice constant
K_d	Derivative constant
K_i	Integral constant
K_p	Proportional constant
K_t	Motor constant
K_v	Motor constant
L	Time delay
$M_{a,atm}$	Molar mass of air
M_{N2}	Molar mass of nitrogen
M_{O2}	Molar mass of oxygen
M_V	Molar mass of vapor
n	Number of cells in fuel cell stack
O_2	Oxygen
P_{atm}	Atmospheric pressure
PH_2	Partial pressure of hydrogen
PO_2	Partial pressure of oxygen
P_{sat}	Saturation pressure
P_{sm}	Supply manifold pressure
R	Universal gas constant

R_{cm}	Compressor motor resistance
T	Time constant
T(Tou)	Normalized dead time
T_{atm}	Atmospheric temperature
T_D	Derivative Time
T_{fc}	Temperature of fuel cell
T_i	Integral time
V_{ca}	Cathode volume
V_{comp}	Compressor voltage
V_{sm}	Supply manifold volume

Greek Letters

λ	Order of Integrator
λ_{O2}	Oxygen Excess Ratio
$y_{O2,atm}$	Oxygen mole fraction
μ	Order of Derivative
γ	Air-specific heat ratio
ϕ_{atm}	Average ambient air relative humidity
η_{cm}	Compressor efficiency
η_{cp}	Compressor motor mechanical efficiency

Abstract

A fuel cell is a electrochemical device which converts the chemical form of energy into electrical form of energy. A Proton Exchange Membrane (PEM) fuel cell is one type of fuel cell which produces electricity continuously through the reaction between the supplied fuel i.e hydrogen and an oxidant i.e oxygen and produces water and heat are as its byproducts. If the load increases, it needs more power and the load current of the fuel cell rises. The chemical reactions should accelerate to give the required power to the load, by supplying more oxygen or air feed on cathode side. If oxygen supply is not regulated properly which leads damage to the membrane, decrease in stack voltage and oxygen starvation. Therefore, it is necessary to design a suitable controller to maintain the pressure in the supply manifold on cathode side and to regulate proper oxygen excess ratio of PEM fuel cell system. In this regard, proposed analysis and design of controllers for the PEM fuel cell system to improve the fast and efficient response.

In this thesis work, higher order PEM fuel cell model is approximated to FOPTD model for analysis and control design using one of the model reduction methods. The analysis of uncertainty for the FOPTD model was carried out to know the uncertainty of plant transfer function with varying operating conditions. From FOPTD model, Smith predictor controller was designed and compared with other tuning methods such as ZN-PI, Skogestad Internal Model Control (SIMC)-PI, Improved SIMC-PID. Model Predictive Controller was designed for the linearized SISO system of higher order model of PEM fuel cell to control the supply manifold pressure. Decentralized PI controller was designed for the linearized MIMO system to know the interactions of the plant outputs.

Fractional order PI/PID controllers are designed using approximated FOPTD model for the control of supply manifold pressure of PEM fuel cell system based on minimization of IAE and maximum sensitivity to improve the performance. Optimization based PID and fractional order PID controllers were designed using Genetic Algorithm for the control of supply manifold pressure of PEM fuel cell system. Simulations show that Fractional order controllers give superior performance than integer order controllers in terms of IAE and TV. Fuzzy self tuning PID controller was applied for the original model of the PEM fuel cell system to control the oxygen excess ratio and compared with classical PID controller. Fuzzy based PID controllers provide better performance than classical PID.

Chapter 1
Introduction and objectives

1.1Fuel cell and its classification

Energy is a fundamental determinant of the economy and plays an important part in industrial growth of any country. At the same time the present and future global energy demand is related to the problem of climate change which constitutes a major challenge that must be addressed. It is widely known that the usage of energy in the worldwide getting higher. In order to meet the increased energy demand, reserves of fossil fuels used, which are gradually diminishing. On the other hand the use of fossil fuels is a source of greenhouse gasses and other pollutants that cause global warming with very serious and irreversible effects on the environment. In order to keep climate change below 2^{o}C, specific targets are set towards the reduction of green house gas (GHG) emissions. More specifically, Europe and G-8 have committed to diminish their GHG emissions by 80-95% by 2050 and in the shorter term by 2020, to decrease GHG by 20% and rise the share of renewable to 20% (European Commission, 2011). Due to the high efficiency, being renewable, lower emissions thus less polluting the environment as well as using methanol, hydrogen and so on as fuel, fuel cells (FC) are specially considered in recent researchers on renewable energies [1].

A fuel cell is an electrochemical device, which converts the chemical form of energy into electrical form of energy by reaction between hydrogen and oxidants (air or oxygen) and generates water and heat as byproduct of the reactions shown in Figure 1.1.

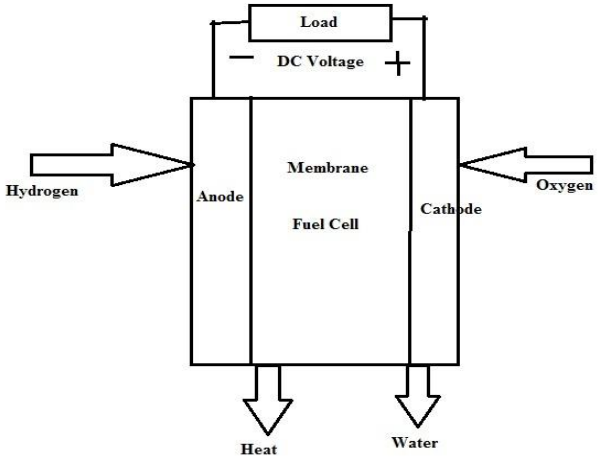

Figure 1.1 Schematic diagram of a fuel cell Inputs and outputs.

In 1960's, the first fuel cell was developed and used in the U.S space applications. Since then, usage of fuel cells increased for global applications. Fuel cell have more feasible for the number of applications, steadily developed, and commercialized. In late 1990's and early 2000's, all the main automotive manufacturers were build on their prototype fuel cell vehicles which are undergoing the tests in the Japan, Europe and United States. Above 2500 fuel cells for stationary power applications established globally. There are many challenges for fuel cell commercialization. The major obstructions for development of fuel cells are their cost and operating reliability. Recently, there is a momentum of increase in the fuel cells technology and commercialization due to its many advantages over conventional energy sources.

Fuel cell is a "clean" energy device because of its byproducts such as water and heat. They operate silently as there are no moving parts. In addition, fuel cells have high efficiency, high power density in electric power production. The power efficiency of the fuel cells are above 40% which is more than the combustion engines and it produce heat which employed for the heating purposes of fuel cell. Fuel cells will operate on a number of fuels such as hydrogen, methanol, ethanol and the natural gas etc. The hydrogen can be produced from the variety of renewable energy sources. Because of above advantages, there is less dependence on foreign oil and it leads to increase in the Indian energy security and economy. Fuel cells categorized based on type of electrolyte being employed. The following list gives the type of fuel cell based on kind of electrolyte is used. [2,3].

a) Alkaline fuel cell (AFC)
b) Solid Oxide fuel cell (SOFC)
c) Direct Methanol fuel cell (DMFC)
d) Phosphoric Acid fuel cell (PAFC)
e) Molten Carbonate fuel cell (MCFC)
f) Proton Exchange/ Polymer Electrolyte Membrane fuel cell (PEMFC)

The research work presenting in this thesis mainly focuses on PEM fuel cells because of their ability to work at low operating temperature and utilize easily in application of transport vehicles, residences and offices.

1.2 Proton Exchange Membrane (PEM) fuel cell system

The Proton exchange membrane (PEM)fuel cell as well-known as polymer electrolyte membrane fuel cell (or) solid polymer fuel cell. The name came from its kind of electrolyte is used i.e a polymeric membrane with high proton conductivity [5]**.** Most commonly used polymer in PEM fuel cell is the Nafion membrane build by Du pont (USA), which is manufactured with chemically stabilized perfluorosulfonic acid copolymer[6]. A PEM fuel cell comprise of two electrodes and electrolyte membrane which is inserted between anode and cathode electrodes, bipolar plates and current collectors.

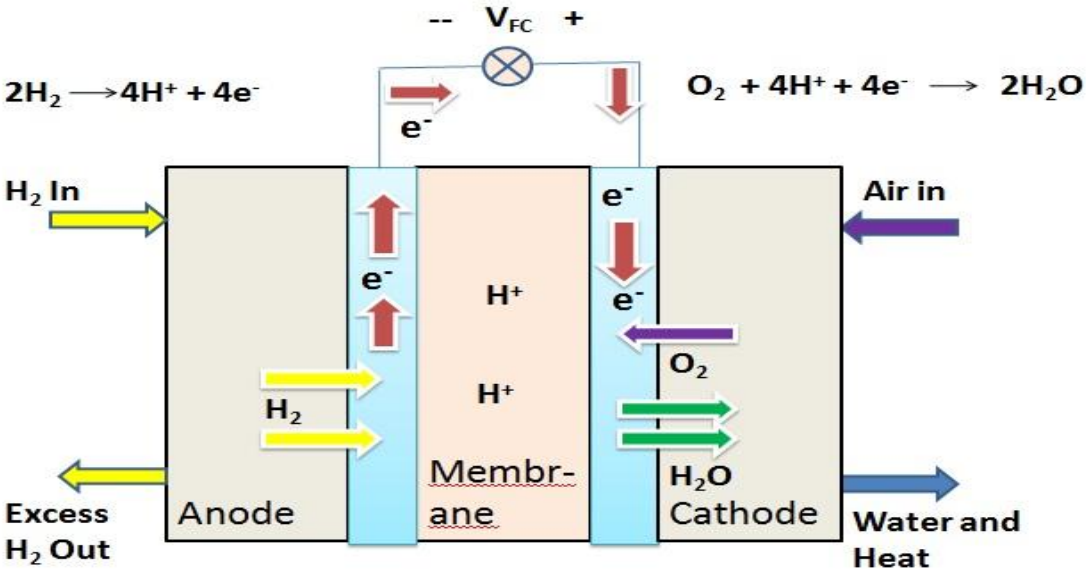

Figure 1.2 Representation of PEM fuel cell electrochemical reaction and flow gases.

The Membrane Electrode Assembly (MEA) is the heart of the PEM fuel cell which is combination of the electrodes, polymer membrane and gas diffusion layers. When hydrogen pressurized to anode side of the membrane, the catalyst causes the hydrogen atoms to produce their electrons as well as Protons (H^+ ions) which is shown in Figure 1.2

$$2H_2 \rightarrow 4H^+ + 4e^- \quad (1.1)$$

The proton exchange membrane (PEM) only permits the H^+ ions to go through it and reaches the cathode. While the produced electrons from the anode side are passes through an external electrical circuit and reach the cathode side to produce electricity. On the cathode side, the diffused hydrogen ions and electrons from the external circuit are combines with the oxygen to form water and due to reaction heat will produced

$$O_2 + 4H^+ + 4e^- \rightarrow H_2O \quad (1.2)$$

The formed water should be exhaust from the cell to stop the cell being flooded. In addition, the unused hydrogen and oxygen gases are exhausted from their respective outlets. To produce the continuous electricity, the produced electrons from the anode must pass through the electrical path, protons must diffuse from membrane and reacts with oxygen at cathode side of membrane as shown in Figure 1.2. Due to the reaction in the PEM fuel cell, it generates around 0.7V output voltage. To produce desired output voltage, number of fuel cells are arranged in series to get a fuel cell stack [7]. The PEM fuel cells can be work effectively at an operating temperature of the range 50 – 100^{o}C and it results in less start up time for the operation.

Therefore, it is especially suitable for transportation applications because of its high power density, extended stack life, solid electrolyte and less corrosion. Other positives of fuel cells are [2]:

a) Clean by-products,
b) Zero emissions,
c) High energy efficiency in electric power production

Consequently, PEM fuel cells are apt for the use in power automobiles, home and small offices and rechargeable batteries. The major drawback of PEM fuel cell technology is its high cost because Platinum is used as electro-catalyst.

1.2.1 Fuel cell Open Circuit Voltage (OCV)

The open circuit voltage (OCV) of a cell is E^O is a quantitative measurement of maximum cell potential. Under the standard pressure and temperature (SPT) values, the following Nernst equation open circuit voltage (E^O) given in the work of Amphlett et al. [8] which involves the temperature and partial pressures of a fuel cell is

$$E^O = 1.229 - 0.85 \times 10^{-3}(T_{fc} - 298.5) + 4.3085 \times 10^{-5} T_{fc} [\ln PH_2 + 0.5 \ln PO_2] \quad (1.3)$$

Where T_{fc} is temperature of fuel cell, PH_2 and PO_2 are partial pressures of hydrogen and oxygen respectively. When no load applied across the fuel cell terminals, the practical potential is less than the theoretical value due to losses in the fuel cell. If load is applied to the fuel cell, voltage across the terminals of the fuel cell still decreases due to polarization and interconnection losses. The major polarization losses occurs in a fuel cell described as follows [2,5,9].

1.2.1.1 Activation polarization loss

Activation losses (η_{act}) are occurred in a fuel cell due to slow reaction on the surface of the electrodes. This occurrence is strongly non linear having more significant at low current densities. These losses are based on

a) temperature,
b) partial pressures,
c) catalyst used

and represented by the semi empirical equation

$$\eta_{act} = -\left[\xi_1 + \xi_2 T_{fc} + \xi_3 T_{fc} ln(C_{02}) + \xi_4 T_{fc} ln(i_{FC})\right] \quad 1.4$$

Where $\xi_{(1\text{-}4)}$ are parametric coefficients whose values are shown in the Table 1.1, cell current is i_{FC}in A, T_{fc} is fuel cell temperature and C_{O2} represents the concentration of oxygen in mol/cm^3 on the catalytic interface by the law of Henry[10]:

$$C_{O2} = \frac{P_{02}}{\left(5.08*10^6 * exp^{\left(-498/T_{fc}\right)}\right)} \quad 1.5$$

Table 1.1 Fuel Cell's parameters and its values for cell voltage.

Parameters	Values	Parameters	Values
T	343 K	**B**	0.016
A	100 cm^2	**ξ_1**	-0.948
l	50.2 μm	**ξ_2**	0.00268+0.0002 ln(A)+4.38×10^-5 ln(CH_2)
PH_2	1 atm	**ξ_3**	7.6×10^-5
PO_2	1 atm	**ξ_4**	-1.93×10^-4
R_c	0.0003	**I_L**	4 A/cm^2

1.2.1.2 Ohmic polarization loss

The ohmic polarization loss includes the variation of membrane resistance caused by membrane hydration and the resistance offered by connection wires between the electrodes and the external circuit. The following equation represents ohmic polarization loss:

$$\eta_{ohm} = i_{FC} * (R_m + R_C) \quad 1.6$$

Where R_c is the cell's constant resistance, and $R_m$gives the equivalent resistance of electron flow and R_m is given by [11,12]

$$R_m = \frac{\rho_m * l}{A} \quad (1.7)$$

Where l is thickness of membrane in cm, A is active area of cell in cm^2, ρ_m specific membrane resistance Ω.cm is used in [10,13]:

$$\rho_m = \frac{\left(181.6 * \left[1 + 0.03 * \left(\frac{i_{FC}}{A}\right) + 0.062 * \left(\frac{T_{fc}}{303}\right)^2 * \left(\frac{i_{FC}}{A}\right)^{2.5}\right]\right)}{\left(\left[\Psi - 0.634 - 3\left(\frac{i_{FC}}{A}\right)\right] * exp\left[\frac{4.18 * \left(T_{fc} - 303\right)}{T_{fc}}\right]\right)} \quad (1.8)$$

The parameter Ψ represents hydration level of membrane.

Value of Ψ is = 14: if the membrane is fully hydrated

= 23: if the membrane is over saturated.

1.2.1.3 Concentration polarization loss

There is a limit for rate of supply of the reactants to produce more current density for a fuel cell. Beyond the limit of rate of supply of reactants, it can't used properly, it leads to a concentration polarization loss. So, the limit is obtained maximum current density (i_L) of the fuel cell. The concentration loss represented by [14]

$$\eta_{conc} = -B.ln\left(1 - \frac{i}{i_L}\right) \quad (1.9)$$

i the current density fuel cell mA/cm^2.

Hence, the fuel cell voltage of a single cell will calculate as:

$$V_{FC} = E^O - \eta_{act} - \eta_{ohm} - \eta_{conc} \quad (1.10)$$

The stack voltage of 'n' number of fuel cell scan determined as:

$$V_{stack} = n * V_{fc} \quad (1.11)$$

Where n is number of fuel cells and V_{fc} is a single cell potential.

Figure 1.3 shows the typical power density and polarization curves representing the responses of power density (W/cm^2) and cell voltage (V) and with respect to changing current density (A/cm^2) of fuel cell under partial pressures of $P_{H2}$and $P_{O2}$are equals to 1atm and cell temperature T_{fc} is 343K. Using Equation 1.10 and Table 1.1 obtained the cell voltage and power density curves.

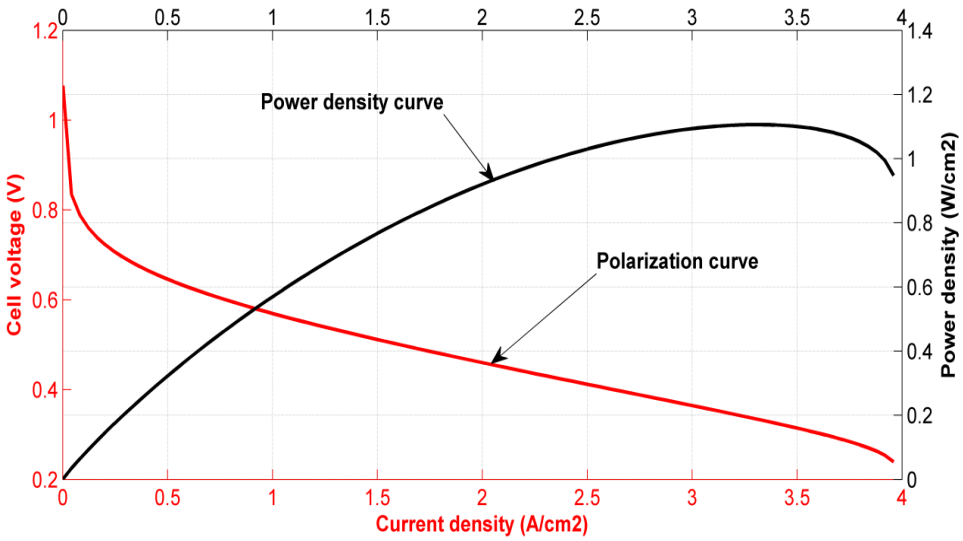

Figure 1.3 Polarization curve of a fuel cell representing the responses of cell voltage and power density with respect to current density.

1.2.2 Subsystems of fuel cell power generation

To generate the electrical energy from a fuel cell stack, it required to incorporate the fuel cell stack with subsystems to develop a fuel cell power generation system. Figure 1.4 shows interconnection between the different components with the fuel cell stack. The following section describes the important subsystems.

1.2.2.1Reactant flow subsystem

The reactant flow subsystem contains hydrogen and oxygen /air supplying units to feed the stack. In PEM fuel stack system, air-supply compressor supplies pressurized air to the cathode of stack. Usually, part of the power generated from the stack is supplied to operate the air-supply compressor due to this there is reduction in the quantity of power available for external loads. It results in decrease in overall performance of the fuel cell stack system. From the Figure 1.4, the pure hydrogen is supplied to anode of the stack from a pressurized tank through pressure reduction and control valves.

1.2.2.2 Temperature management subsystem

The performance of the fuel cell strongly depends on temperature, so thermal management is highly important for the fuel cell power generation system. Temperature

management subsystem consists of a stack cooling and reactant heating systems. A fan or a water refrigeration system can used to control the stack temperature.

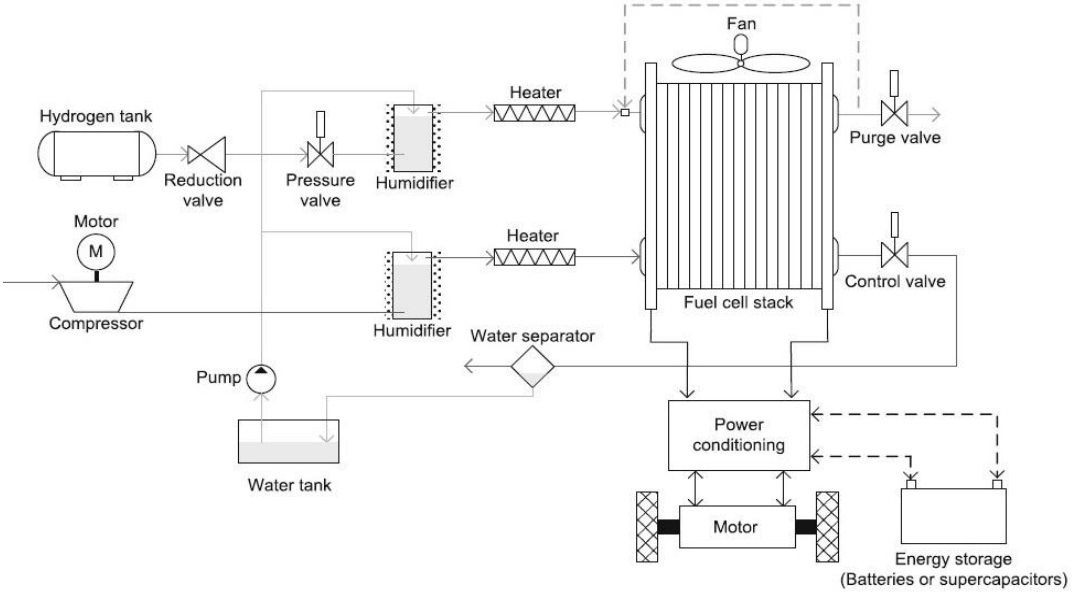

Figure 1.4 Schematic diagram of PEM fuel cell stack system connections with subsystems for automobile application.

1.2.2.3 Water management subsystem

Membrane hydration is one of the important issue which influences the performance of the PEM fuel cell system. To maintain an efficient hydration of a membrane, there is a need of water management subsystem. To keep membrane hydrated, the air and hydrogen are moistened using humidifier before going into fuel cell stack. The water comes from outlet of the cathode is feed back to the water separator and used for the humidification.

1.2.2.4 Power conditioning subsystem

Generally, the generated output voltage from the PEM fuel cell stack terminals is unregulated DC voltage and it drops when there is increase in the current load variations due to polarization curve. The power conditioning subsystem necessary to make unregulated output voltage into regulated voltage and to supply the load properly. For these actions, there is need of DC/DC boost converters and Inverters to convert the DC/AC voltage conversion.

1.2.2.5 Power management system

If there is no energy storage device is connected, then there is no necessity of the power management system as the total produced voltage is supplied to the load. In case of any storage devices such as batteries or super capacitors, there is need of the power management system between stack and devices.

1.2.3 Need of control system for the PEM fuel cell system

The major limitations of a fuel cell are high cost, moderate reliability and decreased life time. In order to accomplish the reduction in cost, improvement in performance and increase the efficiency of fuel cell there is need of incorporation of advanced control strategies. The design of control systems must be take into the consideration of sensing devices, actuators for each subsystem, supervisory and fault tolerant approach for effective energy management of a fuel cell system. A fuel cell system involves highly complex systems. For proper function of fuel cell system supply pressure, humidity levels and temperature parameters are required to maintain at their desired levels. To produce reliable and efficient power output and to avoid the membrane damage, and oxygen starvation, it is necessary to design a closed loop control system to achieve optimal values of above parameters based on the current utilization [9, 16]. A reliable control system should be handle the following such that external perturbations, model uncertainties as well as ensuring stability and better performance of the fuel cell system.

1.3 Motivation & Problem Definition

A single PEMFC will produce a cell voltage of 0.7V at minimal current density of 1A/cm^2. By connecting number of fuel cells in series forms a fuel cell stack which generates the stack voltage of desired value. If partial pressure of oxygen drops down to a certain value, oxygen starvation occurs. This causes sudden drop in stack voltage and causes hot spot on the membrane. Sudden drop in the stack voltage leads to short circuit and causes hot spot on the surface of membrane. There is formation of regions with higher IR drop due to number of cells present in cell which causes the drop in stack voltage leads to hotspots. In fact the drop in voltage is also related to the deficiency of reactants/uneven distribution of reacting gases on polyelectrolyte membrane assembly. This leads to damage of the membrane. To prevent oxygen starvation, it is necessary to maintain the supply manifold pressure (P_{sm}) at desired value. To control the supply manifold

pressure, it is essential to design a suitable control structure for desired flow rates at cathode channel.

The present work discusses about the design of controllers for the control of supply manifold pressure on cathode side of PEM fuel cell. For this purpose, classical and fractional order controllers are designed and verified their robustness for the uncertainties in the model.

1.4 Aim and Objectives of work

To improve the performance of PEM fuel cell system, develop systematic control strategies and analysis to control of supply manifold pressure and oxygen excess ratio.

The objectives are set as follows:

1. Uncertainty analysis and control of supply manifold pressure of PEM fuel cell stack.
2. Design of fractional order PID controllers based on maximum sensitivity and minimization of IAE
3. Optimal design of fractional order PID controllers using Genetic Algorithm.
4. Design of Fuzzy self-tuning PID controller for control of oxygen excess ratio of PEM fuel cell stack.

1.5 Organization of Thesis

The thesis is organized as follows

Chapter 1 presents the introduction covering all aspects of the present work

Chapter 2 presents the literature review for the design of Feed forward and feedback controllers, Sliding mode controllers, model predictive controllers, Fuzzy logic and Neural network based controllers and fractional order controllers for the PEM fuel cell systems.

Chapter 3 provides the considered fuel cell model equations, steady state response for the supply manifold pressure, design of FOPTD model from the steady state response and generally used performance indices.

Chapter 4 presents uncertainty analysis of transfer function for the FOPTD model and design of classical controllers for the supply manifold pressure control of PEM fuel cell. Design of Smith predictor and compared with other tuning methods like: ZN-PI, Skogestad- Internal Model Control (SIMC)-PI, Improved SIMC-PID. Design of MPC controller and design of decentralized

controllers using decoupler method for the MIMO of PEM fuel cell system. This chapter highlights the first objective.

Chapter 5 provides details of different fractional order PI/PID controller tuning methods and applied these tuning methods to the FOPTD model which is developed for the control of supply manifold pressure of PEM fuel cell system in chapter 3. It presents the comparative analysis of fractional order PI/PID controllers. The robustness of fractional order controller verified on original non linear PEM fuel cell by integrating the model parametric uncertainties under load disturbances

Chapter 6 proposes design of a fractional order controller based on minimization of Integral Absolute Error (IAE) with pre specified maximum sensitivity (M_s) as a constraint to regulate the supply manifold pressure of PEM fuel cell system.Uncertainty and measurement noise analysis was carried out to verify the robustness of the designed controller and simulation results are compared with AMIGO PID controller designing method. This chapter focused on the second objective

Chapter 7 proposes optimal tuning of fractional order PID (FOPID) controllers using Genetic algorithm for the control of supply manifold pressure of PEM fuel cell air feed system. In order to obtain the best controller performance, Genetic Algorithm (GA) was employed. The response of proposed objective function was compared with response of objective functions involving performance indices such as ISE, IAE, and ITAE. This chapter deals with the third objective

Chapter 8 presents the application of Fuzzy self tuning PID controller for the control of oxygen excess ratio of PEM fuel cell system. The response of oxygen excess ratio was obtained by the stack current variation and compared with classical PID controller.This chapter deals with the fourth objective.

Chapter 9 gives the overall conclusions and future scope of the present work.

Appendix A shows the model parameters and constants used in simulation.

Appendix B shows different simulink block diagrams are used for simulation work.

Chapter 2
Literature Review

In this chapter, the literature are reviewed the design of different control strategies for Proton Exchange Membrane (PEM) fuel cell systems. The control methods available for the design controllers for the PEM fuel cell system are presented. The review is given on control and design of Feed forward and feedback control, Sliding mode control, Model predictive control, Fuzzy logic and Neural Network based control, Fractional order control strategies for PEM fuel cell system

Design of Feed forward and feedback controllers

This section gives the overview of the literature on Feed forward and feedback controllers for PEM fuel cell system. In the literature, number of linear and nonlinear control strategies has been proposed for control of air flow of PEM fuel cell system. Feed forward and Linear Quadratic Regulator (LQR) methods using linearization of 9^{th} order nonlinear model of PEM fuel cell has been explained in [15,22].

Pukrushpan et al. [15] have described a 9^{th} order dynamic control-oriented model to analyse the dyanamic behavior of PEM fuel cell. They have proposed three control configurations such as static feed forward (sFF), dynamic feed forward+ PI (dFF+PI) and static feed forward + Observar based control (sFF+ObsFB) controllers are applied to control the oxygen excess ratio of PEM FC stack system. Out of these sFF+ObsFB configuration is superior in terms of robustness.

Grujicic et al. [16] implemented Static feed forward and observer based integral feedback controllers to analyze the transient response of stack current system to maintain optimum level of the O_2 excess ratio. They linearized the 9^{th} order control oriented model [15] around a nominal operating point with the maximum net power. By applying feed forward control strategy to analyze the transient behavior of PEM fuel cell system [15] leads to existence of steady state errors in the performance variables such as net power and oxygen excess ratio. Kalman- Filter based state observer is formed and used in feed back control of air-supply compressor motor voltage. For the observer based integral feedback controller, the air-supply compressor motor voltage has better transient behavior when compare to static feed forward control to effectively

reject the oxygen excess ratio (λ_{O2}) disturbance following an sudden change in stack current. The designed feedback controllers decreases the rise time and settling time for the O_2 excess ratio under stack current abrupt changes. This is accomplished by compromise the net power. Therefore, it needs a separate power management system such as electric battery.

Bao et al. [17] Considering the coupling among air-side performance, a two-freedom linear state-feedback controller based on a Kalman estimator was designed for the set point tracking. LQG algorithm was adapted for state feedback control for setpoint tracking and implemented a non linear adaptive controller having model predictive controller (MPC) with an on line neural network (NN) identifier to improve the robustness for the flow rate and pressures of PEM fuel cell system. Also compared with decentralized PI controllers, the multivariable controllers improve the transient response and shows better disturbance rejection capability.

Wang et al. [19] applied system identification techniques to PEMFC model to obtain MIMO system to control the output voltage and further reduced to SISO system. A robust H_∞ controller was applied to SISO model only. Weighting functions are included to improve the overall performance of the system. The simulation results of designed controller was verified with experimental results. From the experimental results, the designed controller will achieve good system performance and stability.

Wang et al. [20]applied multivariable LQG control techniques to control output voltage by controlling air and hydrogen flow rates. They obtained the MIMO model from the dynamic model of PEMFC system. By fixing the output resistance, MIMO model was converted into MISO model and applied the multivariable LQG controller to get steady output voltage by regulating the hydrogen and air flow rates. The experimental results show that the proposed controller provides the steady output voltage even operating conditions are varying and improves the reduction of hydrogen consumption.

Wang et al. [21]designed a multivariable H_∞ robust controller for output voltage control and to deal system uncertainty. The performance of the MIMO system robust controller is compared with SISO system robust controller. The proposed controller provides the steady output voltage and significantly reduces consumption of hydrogen.

Niknezhadi et al. [22] was proposed design of LQR/LQG control law strategies for the 7^{th} order linearized PEM fuel cell model to keep away from the oxygen starvation problem and to

maximize the output net power i.e the difference between the power of the fuel cell and the air-supply compressor consumption. For this objective they first linearized the non linear model of 7^{th} order using Taylor series. For theoretical analysis and experimental results show that the proposed LQR/LQG control strategies allows the maximizing the energy conversion efficiency and avoids the oxygen starvation problem.

Wang et al. [23] Time delay control (TDC) algorithm was implemented for the control of oxygen excess ratio and experimentally implemented.

Ozbek et al.[24] developed Gain scheduling controller for control of anode pressure and compared with static feed forward and state feedback controller. Gain scheduling controller shows better results than other two controllers.

Al-Durra et al. [25] proposed a gain scheduling control for the PEM fuel cell.**Da et al. [26]** designed a non linear controller based on differential flatness control theory for the control of oxygen excess ratio.

Rios et al. [27]was designed linear quadratic state feedback regulator and a Kalman filter to avoid oxygen starvation and to minimize the fuel consumption.

Na et al. [28] applied a non linear control method based on feedback linearization to reduce the deviations between hydrogen and oxygen partial pressures.

Liu et al. [83] combined the model of air supply system with the humidification process model and validated with simulation study results. A feed forward control was designed to regulate the humidification process without effecting the regulation of the oxygen excess ratio.

Zhao et al. [86] adopted a semi-physical modeling method to analyze the operating property of a centrifugal compressor. The modeled compressor map has good agreement with the experimental data. A dynamic feed forward controller was proposed based on load torque to control the air mass flow, eliminating the disturbance produced by the compressor load in transient.

Li et al. [90] proposed a combined controller with feedback control based on LQR method and feed forward control to the third-order model for the control of oxygen excess ratio. Simulation results are verified for the proposed controller to track the oxygen excess ratio under different working conditions.

Chavan et al. [91] first time proposed the system identification black box approach to developea number of simple and more realistic mathematical model structures for the

polarization curve of a PEM fuel cell. The performance of each model structure is compared with the data from a 25 cm^2 active area practical PEM fuel cell for result validation.

Ma et al. [92] proposed a novel observer-based nonlinear triple-step controller for the air supply system of polymer electrolyte membrane (PEM) fuel cell to regulate the oxygen excess ratio to its reference value under fast current transitions. The proposed triple-step method consists of design a steady-state control, to design a reference variation-based feed forward control, and error feedback control to handle the final tracking offset. The final control rate is derived by the triple-step method with an additive process. The simulation results indicate that the proposed controller is capable of better tracking performance in adjusting the oxygen excess ratio for different load variations and parametric uncertainties.

Design of Sliding mode controllers for PEM fuel cell system

The sliding mode control techniques for the control of oxygen excess ratio of PEM fuel cell has been carried out in [29-35,1].

Kunusch et al. [29] Proposed a second-order sliding mode controller using a super twisting algorithm for solving control problem of power optimization and oxygen starvation for 9^{th} order PEM fuel cell model.

Kunusch et al. [30] implemented second order sliding mode controller using super twisting algorithm to optimize the energy conversion of fuel cell in a laboratory test station and verified the performance with extensive computer simulations.

Baroud et al. [31] proposed a sliding mode controller to 8^{th} order model to control the oxygen excess ratio during disturbance, uncertainties.

Matraji et al. [1] proposed a second order sliding mode controller in cased form structure to produce optimum net power response using 4^{th} order PEM fuel cell model.

Garcia-Gabin et al. [32] was identified a control model for PEM fuel cell system from experimental input/output data, further applied the sliding mode controller to control the O_2 excess ratio as well as smooth power supply under load variations.

Park et al. [33] have been applied the sliding mode control strategy for the linearized model of 5^{th} order non linear PEM fuel cell model to control the pressures of Hydrogen and oxygen at required values.

Sankar et al. [34] was proposed a sliding mode observer (SMO) based multivariable sliding mode controller (SMC) and globally linearizing controller (GLC) for PEM fuel cell.

Pilloni et al. [35] applied HOSM approach to observer-based output feedback control of a PEM fuel cell for the control of O_2 excess ratio.

Deng et al. [84] proposed a cascade adaptive sliding mode control to regulate oxygen excess ratio. The performance of the controller is implemented on a real time emulator. The proposed strategy performs better than convention constant sliding mode (CSM) control and PID method.

Sankar et al.[85] proposed reduced order sliding mode observer (SMO) based nonlinear control to regulate a reversible proton exchange membrane fuel cell integrated system. The proposed strategy is used to control compressor air flow and fuel cell body temperature at their desired values to avoid oxygen starvation on cathode side and adverse effect of the system temperature, respectively. The performance of the proposed control strategy is compared with conventional PI controller in terms of servo and regulatory responses.

Design of Model predictive controllers (MPC) for PEM fuel cell system

Golbert et al.[36] used model predictive controller for power tracking of fuel cell.

Gruber et al.[37] was developed a linear MPC uses parameter adaption to load current changes for the O_2 excess ratio. The proposed constrained MPC controller tested and validated on stand alone commercial fuel cell. The constrained MPC reacts much faster and stabilizes the oxygen excess ratio.

Gruber et al. [38] designed a nonlinear predictive controller based on a second order volterra series model to control the O_2excess ratio. The simulation results of proposed controller controls oxygen excess ratio in under load disturbances.

Vahidi et al. [39] applied MPC based load governor and Fast reference governor (FRG-based load governor) to linearized fuel cell model to preventing oxygen starvation and compressor surge.

Vahidi et al. [40] implemented a model predictive controller for optimal distribution of current sources based on current demand in a hybrid structure to avoid oxygen starvation during rapid current changes in a fuel cell.

Zhao et al. [41] proposed a parametric MPC (pMPC) controller to optimally control output voltage and operating temperature set points in PEM fuel cell.

Hahnel et al. [42] proposed constrained MPC to coordinately control output power andO_2excess ratio. The proposed controller effectively controls the partial pressures of anode and cathode.

Ziogou et al. [87] presented a development of energy management framework [EMF] and implementation of advanced MPC control strategies at a PEMFC unit based a SCADA automation system. The responses of MPC strategies is assessed through a set of comparative experimental studies shows that the fuel cell system operates economically for the varying operating conditions.

Design of Fuzzy logic and Neural Network (NN) based controllers for PEM fuel cell system

Baroud et al. [43] proposed a novel hybrid fuzzy-PID controller to control O_2 excess ratio of PEM fuel cell stack. The proposed controller produces better response in terms performance and time domain indices when compared to PID controller.

Li et al. [44] designed fuzzy sliding mode controller to regulate the air supply on cathode side.

Aliasghary [45] proposed an interval type-2 fuzzy PID (IT2FPID) controller to control oxygen excess ratio which effectively deals withload current variations. The proposed controller performs better in terms of time domain indices compare to Type-1 fuzzy PID and classical PID controllers. New fuzzy system for varying PID controller parameters and adaptive fuzzy logic controllers implemented in [46,47] to maintain steady stack voltage. Adaptive neural network control implemented in [48-49] for PEM fuel cell.

Abbaspour et al. [48] proposed a NN adaptive controller with feedback linearization to decrease deviations between partial pressures of H_2 and O_2 in PEM fuel cell. The proposed controller rejects the disturbances and improves performance output.

Rezazadeh et al. [49] designed a NN predictive controller to control stack voltage.

Methekar et al. [50] examined a linear ratio control strategy for the distributed parameter model to prevent the oxygen starvation. Proposed controller able to overcome problem of oxygen starvation but the performance is slow due to nonlinearities in the model.

Based on uncertainty and disturbance estimation (UDE) and Lyapunov method **Zhiyang Liu etal. [51]** proposed a cascade controller. The effectiveness of the controller was validated through the experimental results.

Chang et al. [52] implemented a novel constrained extremum seeking control method to regulate the O_2excess ratio at an optimum value for maximizing the net output power of the PEM fuel cell system.

Ou et al. [88] proposed a new fuzzy-PID controller based on feed forward approach to regulate the oxygen excess ratio of PEMFC. The performance of the feed forward fuzzy-PID (FFPID) control is compared with convention PID and convention fuzzy-PID. The proposed FFPID results proves thatit better controls the oxygen excess ratio and reduces the parasitic power loss.

Fan et al. [89] proposed a self-adaptive fuzzy PID (SFPID) controller to regulate oxygen excess ratio for the fourth- order model of the PEM fuel cell system, The response of proposed (SFPID) is compared with feed forward, PID, PID plus feed forward (PID-FF) control strategies under different load current disturbances. The simulation results show that the proposed controller tracked the setpoint of oxygen excess ratio with rapidly and accurately.

Design of Fractional order controllers for PEM fuel cell system

Recently, development of fractional order dynamics and controllers have been reported in [53-56]. Fractional model approximation and Fractional complex order control strategies have been implemented in [57-59] for the control of oxygen excess ratio of PEM fuel cell. Digital implementation of FOPID controllers has been implemented in [60], fractional order model and control of boost converter for stack voltage of PEM fuel cell have been reported in [61]. PEM fuel cell fractional order model identification have been carried out in [62.63].

Table 2.1 Summary of literature review on different control strategies implemented on PEM fuel cell stack system

Type of controller	**Control strategy**	**control objectives**	**Performance**	**model**	**disturbance**	**References**
Dynamic feed forward-PI feedback	static and dynamic feed forward concepts	to prevent oxygen starvation	compressor motor voltage and oxygen excess ratio	9^{th} order model	current	Pukrushpan et al. [15]
	LQR/LQG control law	to prevent oxygen starvation	compressor motor voltage and oxygen excess ratio	7^{th} order model	current	Niknezhadi et al. [22]
	Feed forward	to regulate cathode air humidity	improves the performance of the humidifier without affecting the regulation of O_2 excess ratio	new control oriented model of humidifier air supply system	current	Liu et al. [83]

	dynamic feed forward	to control the air mass flow	fuel cell and compressors works with high efficiencies	Semi-physical model	current	Zhao et al. [86]
Sliding mode control (SMC)	(SO-SMC) using a super twisting algorithm	power optimization and to prevent oxygen starvation	robustness to parameter uncertainties and external disturbances	9th order model	model uncertainties, external disturbances, and current demand	Kunusch et al. [29]
	sliding mode controller	to control the oxygen excess ratio under disturbances and uncertainties	robustness of sliding mode controller to parameters uncertainties and external disturbances.	9th order model	disturbances and uncertainties	Baroud et al. [31]
	robust nonlinear second order sliding mode controller	to maintain optimum net power output	The Hardware-In-Loop experimental results have shown that the proposed controller performs well with varying loads.	4th order model	Load current and model uncertainties	Matraji et al.[1]
	Feed-forward control of output current and sliding mode (feedback) control (SMC) of oxygen stoichiometry	To prevent Oxygen starvation as well as smooth power supply under load variations	Steady power supply under load variations	4th order model	load current	Garcia-Gabin et al. [32]
	sliding mode observer (SMO) based nonlinear multivariable sliding mode controller (SMC) and globally linearizing controller (GLC)	oxygen excess ratio control of PEM fuel cell system	compared the performance between the SMC and GLC with reference to a dual-loop PI controller.	model with methonal reformer	load current	Sankar et al. [34]
	high-order sliding-mode approach to the observer-based output feedback control	control of oxygen excess ratio.	it provides a finite-time converging and theoretically exact (in absence of noise and parameter errors) state reconstruction.	6th order model	Stack current	Pilloni et al. [35]
	cascade adaptive sliding mode control	control of oxygen excess ratio	The performance of the controller is implemented on a real time emulator	6th order model	Stack current with simultaneously uncertaintie	Deng et al. [84]

					s and noises	
	reduced order sliding mode observer (SMO) based nonlinear controller	Multivariable PEMFC integrated system	the performance of the controller is done with set point tracking and load disturbances.	Integrated MIMO PEMFC model	load current	Sankar et al.[85]
Model predictive control (MPC)	Constrained Model predictive control (MPC)	oxygen excess ratio	the constrained MPC reacts much faster and stabilises the oxygen excess ratio around the desired value approximately five times faster.	4^{th} order model	Stack current changes	Gruber et al. [37]
	MPC based on second order Volterra series model	control the oxygen excess ratio	The simulation results show that the hierarchical controller stabilizes the oxygen excess ratio in the desired value and reacts in a fast and efficient form	4^{th} order model	errors due to disturbances .	Gruber et al. [38]
	constrained MPC strategy	to coordinately control the output power and the oxygen excess ratio	effective control of partial pressures of anode and cathode	9^{th} order model	load changes	Hahnel et al. [42]
	advanced MPC control strategies	Multi objectives	. The response of the MPC strategies is assessed through a set of comparative experimental studies	Semi-empirical model	varying operating conditions	Ziogou et al. [87]
Fuzzy logic control	novel hybrid fuzzy-PID controller	to prevent oxygen starvation and damage of the PEM fuel cell.	The proposed controller performs better than the classical PID controller and the FLC in terms performance indices as well as time domain indices for the closed-loop feedback control system	4^{th} order model	Load current	Baroud et al. [43]
	interval type-2 fuzzy PID controller	to handle the effect of external disturbances and fix the O_2 excess ratio	The responses of the IT2FPID controller has a smaller settling time, less overshoot and better	4^{th} order model	Load current	Aliasghary [45]

			performance when compared with the T1FPID and ordinary PID controllers.			
	Fuzzy PID controller based on feed forward approach (FFPID)	to control oxygen excess ratio	The response of the FFPID is better than conventional PID	Model presents cathode and anode mass flow transients, membrane hydration model	Load current	Ou et al. [88]
	self-adaptive fuzzy PID (SFPID) controller	to regulate oxygen excess ratio	proposed controller has good dynamic response performance	4^{th} order model	Load current	Fan et al. [89]
Adaptive neural network control	neural network adaptive control with feedback linearization	to reduce the deviations between the partial pressure of hy drogen and ox ygen in PEM fuel cell.	Simulation results show that the proposed control can significantly enhance the output performance as well as reject the disturbances.	Model involves both hydrogen and Oxygen pressures	unknown disturbances and parameter uncertaintie s	Abbaspour et al. [48]
Ratio controller	linear ratio control strategy	to prevent the oxygen starvation.	A ratio control strategy is able to overcome the problem of oxygen starvation but the performance of the linear controllers is slow due to the presence of nonlinearities in the dynamic response of the PEMFC.	distributed parameter model	Stack Current	Methekar et al. [50]
Cascade controller	cascade controller based on uncertainty and disturbance estimation (UDE) and Lyapunov method.	Control of air supply	The effectiveness of the controller was validated through the experimental results.	4^{th} order model	Load disturbance and uncertainty	Zhiyang Liu et al. [51]
Fractional (FO) order controllers	fractional order model approximation	to control oxygen excess ratio	Reduced Fractional order model control using Heuridtic algorithm performs well in terms of reducing the negative peak and also the speed of the	9^{th} order model	Stack current	Shahiri et al. [57]

			response			
	Fractional complex order controller	to regulate oxygen excess ratio in different operating conditions	The stability and performance of the controller is verified in the presence of uncertainty by means of the frequency criteria, i.e. the phase and the gain margins, as well as the time indices.	9^{th} order model	Stack current	Shahiri et al. [58]
	Fractional complex order controller (FCOC) using standardised K-chart	To regulate oxygen excess ratio in different operating conditions	The simulation verifies validity and significance of the proposed design procedure with respect to other conventional robust controllers. i.e FO-PI and H_∞ controllers	9^{th} order model	Stack current	Shahiri et al. [59]
	Fractional order PID controller using improved Oustaloup filter algorithm	Tracking of the reference stack voltage	Hydrogen pressure is used as control variable to control the PEMFC output voltage	Stack Voltage model	Stack current	XueqinLü et al. [60]
	Hybrid optimization based approach for fractional order modelling and FO-PI controller	To regulate output voltage irrespective of variation in both load and source operating condition.	hybrid optimization based approach for fractional order modeling and control of PEMFC fed DC/DC converter is proposed and validated in real time.	Stack Voltage model	Stack current	Phani Teja Bankupalli et al. [61]

The most important control objects in air supply for fuel cell stack system are the stoichiometry of oxygen (λO2) and air pressure which are the two key parameters to maintain the fuel cell stack performance and also highly influence the fuel cell durability. To realize precise control either at steady and transient states, PID control, fuzzy logic control, neural control, sliding mode control and model predictive control etc have been implemented as the control of air supply. For such individual controls, it seems that fuzzy logic control are usually simpler and cheaper without heavy computational burden compared to PID control, model predictive control and sliding mode control. Fractional order controllers have been applied for the PEM fuel cell stack system

to analyze the uncertainties in model and to regulate the oxygen excess ratio (λ_{O2}) under sudden changes in load current. When comparing with other controllers, fractional order controllers have better control and robustness. To stabilize the stoichiometry of oxygen in a fast and efficient form with controlled errors from disturbances, hybrid or hierarchical controls are introduced including Fuzzy-PID combined, Neural-PID combined and so on in the form of parenting/supervising, parallel and hybrid.

Based on above literature survey the following important research problems are noted:

1) Design of classical controllers for the 4^{th} order model using approximated FOPTD model to control the supply manifold pressure of PEM fuel cell stack system.
2) Design of fractional order PI/PID controllers using reduced FOPTD model of 4^{th} order control oriented PEM fuel cell model to control the supply manifold pressure. Justifying the robustness of the proposed controller.
3) Design of FOPID controllers based on minimization of IAE and maximum sensitivity as a constraint for the control of supply manifold pressure of PEM fuel cell system.
4) Design of FOPID controllers using Genetic Algorithm (GA) optimization method for the FOPTD model of 4^{th} order PEM fuel cell stack system to control the supply manifold pressure.
5) Design of fuzzy logic controller for the 4^{th} order model to control the oxygen excess ratio of PEM fuel cell system.

Chapter 3
Dynamic modeling of PEM fuel cell system

3.1 Introduction

The purpose of this chapter is to explain proposed research control method and to examine the dynamic behavior of the air feed control oriented PEM fuel cell model for the control of supply manifold and oxygen excess ratio.After getting steady state response, we develop the FOPTD models for the easy control purpose.

3.2 Non linear PEMFC dynamic model

To analyze the dynamic behavior of the non linear PEMFC air feed system it is necessary to develop a mathematical model. Pukrushpan et al. [64] proposed the 9^{th} order control oriented model for the PEMFC system. It involves complex calculations and equations which are highly non linear in nature because of that a 4^{th} order control oriented model for the PEMFC system proposed by Kyung Wan Suh [65] was considered for controlling purpose. Suh [65] demonstrated that the air feed system can be separated from the complete fuel cell model while preserving the dynamic behavior of the PEMFC by following the assumptions. (i) The supply manifold pressure on anode side is well controlled and maintained at desired value (ii) the temperature and humidity at the entrance off the PEMFC stack are constant and (iii) the electrodynamics of the air-supply compressor motor is not considered. Air contains 21% of oxygen and control of oxygen reaction is very important to avoid the oxygen starvation and damage to membrane of the PEM fuel cell. To focus on air (oxygen) dynamics of the fuel cell system, we assumed that a pressurized high-purity hydrogen is supplied on anode side of the fuel cell system and control of hydrogen supply is accurate for tracking the anode pressure to the cathode pressure. The dynamics of humidity and temperature are neglected because they are slower than the air flow dynamics. To concentrate on the dynamics of the air supply, the humidity and temperature of the fuel cell stack is assumed to be controlled perfectly by dedicated hardware and controller. The fuel cell system under consideration is mainly consists of a fuel cell stack, air-supply compressor and motor arrangement, a hydrogen storage tank, supply manifold, humidifiers and temperature controllers.

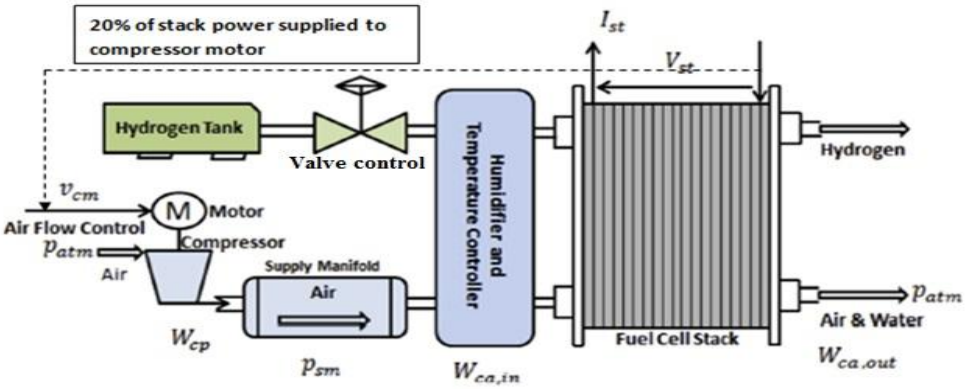

Figure 3.1 Schematic diagram of integrated PEM FC stack system.

The schematic diagram in Figure 3.1depicts the arrangement of different subsystems for the PEM fuel cell system. The following governing equations represent the dynamics of PEM fuel cell model [65]. For the details of mathematical equations the reader may refer to [64, 67].

3.2.1 Model description Air feed system of PEM fuel cell stack system

The following governing equations represent the dynamics of PEM fuel cell model [65].The PEM fuel cell is highly non linear system and involves the non linear functions in its state dynamics

(i)The oxygen and nitrogen partial pressure are calculated from the law of conservation of mass and ideal gas law [65].

$$\frac{dp_{O_2}}{dt} = \frac{RT_{fc}}{V_{ca} M_{O_2}}\left(Q_{O_2,ca,in} - Q_{O_2,ca,out} - Q_{O_2,reacted}\right), \quad 3.1$$

$$\frac{dp_{N_2}}{dt} = \frac{RT_{fc}}{V_{ca} M_{N_2}}\left(Q_{N_2,ca,in} - Q_{N_2,ca,out}\right), \quad 3.2$$

The subscript "ca" represents the fuel cell cathode, where V_{ca} is the lumped cathode volume. R is universal gas constant,T_{fc} is fuel cell stack temperature, M_{O_2} and M_{N_2} are the respective molar masses of O_2 and N_2 gases. The inlet mass flow rates of oxygen and nitrogen $Q_{O_2,ca,in}$ and $Q_{N_2,ca,in}$ are determined from the cathode inlet mass flow rate $Q_{ca,in}$

Where $Q_{ca,in} = \frac{1}{1+\Omega_{atm}} k_{ca,in}(p_{sm} - p_{ca})$ 3.3

$$Q_{O_2,ca,in} = x_{O_2,atm} Q_{ca,in} \quad 3.4$$

$$Q_{N_2,ca,in} = (1 - x_{O_2,atm}) Q_{ca,in} \quad 3.5$$

Humidity ratio $\Omega_{atm} = \frac{M_v}{M_a} \frac{\emptyset_{atm}\, p_{sat}\,(T_{atm})}{p_{atm} - \emptyset_{atm}\, p_{sat}\,(T_{atm})}$ 3.6

Where $x_{O_2,atm}$ is the oxygen mass fraction and $\emptyset_{atm}$ is the relative humidity, p_{atm} is the atmospheric pressure and $p_{sat}(T_{atm})$ is the saturation pressure at ambient temperature. $k_{ca,in}$ iscathode inlet orifice constant and p_{ca} is the cathode pressure, which is calculated using Dolton's law of partial pressures and is given by

$p_{ca} = p_{O_2} + p_{N_2} + p_{sat}$ 3.7

The outlet mass flow rates of oxygen and nitrogen $Q_{O_2,ca,out}$ and $Q_{N_2,ca,out}$ are determined from the mass fraction of O_2 and N_2 as follows

$$Q_{O_2,ca,out} = \frac{M_{O2} p_{O_2}}{M_{o2} p_{O_2} + M_{N_2} P_{N_2} + M_v P_{sat}} Q_{ca,out} \quad 3.8$$

$$Q_{N_2,ca,out} = \frac{M_{N2} p_{N_2}}{M_{o2} p_{O_2} + M_{N_2} P_{N_2} + M_v P_{sat}} Q_{ca,out} \quad 3.9$$

Where $Q_{ca,out}$ is the cathode outlet mass flow rate given as

$$Q_{ca,out} = c_{17}\, P_{ca} \left(\frac{c_{11}}{P_{ca}}\right)^{c_{18}} \left(1 - \left(\frac{c_{11}}{P_{ca}}\right)^{c_{12}}\right)^{0.5} \quad 3.10$$

The mass flow rate of O_2 consumption expressed using basic electro chemical principles, as follows

$$Q_{O_2,react} = M_{O_2} \frac{n I_{stack}}{4F}, \quad 3.11$$

whereI_{stack} is the stack current, F is the Faraday number, and nis the number of cells in the stack

.

(ii) The governing equation for the angular speed of the air-supply compressor motor is [65]

$$\frac{d\omega_{cp}}{dt} = \frac{1}{J_{cp}} (\tau_{cm} - \tau_{cp}) \quad 3.12$$

Where J_{cp} is the air-supply compressor motor inertia, τ_{cm} is the air-supply compressor motor torque, τ_{cp} is the air-supply compressor load torque.

$$\tau_{cm} = \frac{\eta_{cm} K_t (V_{comp} - K_V \omega_{cp})}{R_{cm}} \quad 3.13$$

$$\tau_{cp} = \frac{C_p T_{atm}}{\eta_{cp}\, \omega_{cp}} \left[\left(\frac{p_{sm}}{p_{atm}}\right)^{\frac{\gamma-1}{\gamma}} - 1\right] Q_{cp} \quad 3.14$$

where K_t is motor constant, η_{cp} is the air-supply compressor efficiency, η_{cm} is the motor mechanical efficiency, γ is the ratio of specific heats of air, C_p is the specific heat capacity of air and Q_{cp} is air-supply compressor air flow rate and it depends on the rotational speed of the air-supply compressor motor and the supply manifold pressure p_{sm} and Q_{cp} is approximated with the following equation:

$$Q_{cp}(x_3, x_4) = \frac{Q_{cp}^{max} x_3}{x_3^{max}} \left(1 - \exp\left(\frac{-r\left(s + \frac{x_3^2}{q} - x_4\right)}{s + \frac{x_3^2}{q} - x_4^{min}}\right)\right) \quad 3.15$$

Where $Q_{cp}^{max} = 0.0975 \frac{kg}{s}$, $r = 15$, $q = 462.25\ rad^2/(s^2 Pa)$, $x_3^{max} = 11500\ rad/sec$, $x_4^{min} = 50000\ Pa$ and $s = 100000\ Pa$. For further more details are reported by Gruberet al. and Baroud et al. [66, 67].

(iii) The dynamics of the supply manifold air pressure is defined by the following differential equation [65]

$$\frac{dp_{sm}}{dt} = \frac{RT_{cp}}{M_a V_{sm}} \left(Q_{cp} - k_{ca,in}(p_{sm} - p_{ca})\right) \quad 3.16$$

Where V_{sm} is the supply manifold volume and T_{cp} is the temperature of the air leaving the air-supply compressor and is given by

$$T_{cp} = T_{atm} + \frac{T_{atm}}{\eta_{cp}} \left[\left(\frac{p_{sm}}{p_{atm}}\right)^{\frac{\gamma-1}{\gamma}} - 1\right] \quad 3.17$$

3.2.2 Representation of state space equations of PEM fuel cell stack

The dynamic model of the PEM fuel cell based on Equations (3.1, 3.2, 3.12, and 3.16) consists of following four states, one control input and one disturbance input.

$x_{Nonlinear} = [p_{O_2}, P_{N_2}, \omega_{cp}, P_{sm}]$

$\dot{x}_{Nonlinear} = f(x_{Nonlinear}, u, w)$ State equations

$u = v_{comp}$ Control input (manipulated variable)

$w = I_{st}$ Disturbance Input

$y^T = [\omega_{cp} \quad P_{sm}]$ Outputs

Supply manifold pressure P_{sm} is controlled variable. In this model control input, u is the air-supply compressor motor voltage (v_{comp}) and the stack current (I_{stack}) is the measurable

disturbance input, w. Table 3.1 shows the four state variables of PEMFC control oriented model proposed by Suh [65]

Table 3.1 State variables of the nonlinear FEMFC model

S. No.	State variable	Process variable	Units
1	x_1	Oxygen partial pressure (P_{O2})	Pa
2	x_2	Nitrogen partial pressure (P_{N_2})	Pa
3	x_3	Air-supply compressor motor angular speed (ω_{cp})	rad/s
4	x_4	Supply manifold pressure (P_{sm})	Pa
5	V_{comp}	motor voltage supply	Volt
6	I_{stack}	stack current	Amp

3.2.3 Air feed dynamic model equations

From the above relationships the constants are developed and the complete model of the air feed system was written in the following simplified representation

$$x = \left[P_{O_2} P_{N_2} \omega_{cp} P_{sm}\right]^T = [x_1 x_2 x_3 x_4]^T \quad 3.18$$

The complete state model equations of PEM fuel cell can be written as follows [67]

$$\dot{x}_1 = (x_4 - x_1 - x_2 - c_2)\dot{c_1} - \frac{c_3 x_1 Q_{ca,out}}{c_4 x_1 + c_5 x_2 + c_6} - c_7 I_{stack} \quad 3.19$$

$$\dot{x}_2 = (x_4 - x_1 - x_2 - c_2)c_8 - \frac{c_3 x_2 Q_{ca,out}}{c_4 x_1 + c_5 x_2 + c_6} \quad 3.20$$

$$\dot{x}_3 = -c_9 x_3 - \frac{c_{10}}{x_3}\left[\left(\frac{x_4}{c_{11}}\right)^{c_{12}} - 1\right] Q_{cp} + c_{13} V_{comp} \quad 3.21$$

$$\dot{x}_4 = c_{14}\left[1 + c_{15}\left[\left(\frac{x_4}{c_{11}}\right)^{c_{12}} - 1\right]\right]\dot{}\left[Q_{cp} - c_{16}(x_4 - x_1 - x_2 - c_2)\right] \quad 3.22$$

V_{comp} is control input and I_{stack} is stack current considered as measurable input disturbance to the system. Supply manifold pressure (P_{sm}) is output of the system.The coefficients from$c_1, c_2, \ldots, c_{18}$ are constants and defined in Table II in the Appendix. The cathode inlet pressure (P_{ca}) is sum of oxygen, nitrogen partial pressures and saturation pressure, i.e $P_{ca} = x_1 + x_2 + c_2$. The

control objective in this work is to control the supply manifold pressure i.e the system output is x_4. In the next section, open loop analysis and for PEM fuel cell was presented.

3.3 Block diagram representation of PEMFC Model

Block diagram representation of the PEM Fuel Cell model is shown in Figure 3.2 in which air-supply compressor motor voltage is control input, stack current is disturbance input and supply manifold pressure is output.

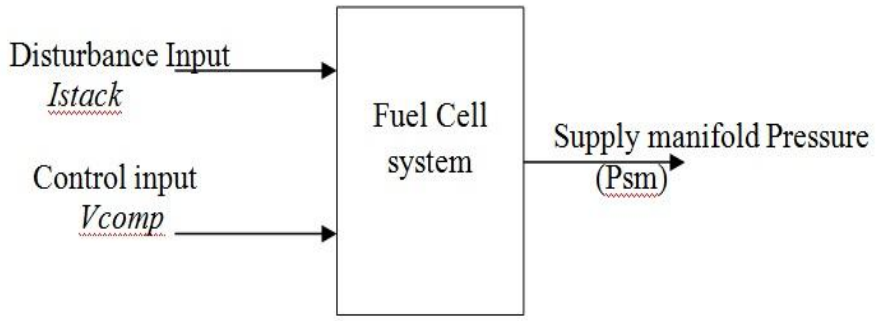

Figure 3.2 Block diagram representation of the PEM Fuel Cell system

3.4 Steady state response for the supply manifold pressure of PEM fuel cell

By considering the nonlinear dynamic model equations (3.19-3.22) of PEMFC, these are simulated in the MATLAB®/ SIMULINK environment to obtain the dynamic response. For the simulation purpose, the initial values are chosen as reported by Liu et al. [68] as shown in below Table 3.2Whilesimulation partial pressure of nitrogen is also considered because of air feed is combination of nitrogen and oxygen gasses.

Table 3.2 Initial value of state variables are considered for simulation

S.No:	Parameter	Initial values, x(0)	Steady state values
1	Oxygen partial pressure (P_{O2}), x_1	100000 Pa	24353 Pa
2	Nitrogen partial pressure (P_{N2}), x_2	66000 Pa	159075 Pa
3	Air-supply compressor motor speed (ω_{cp}), x_3	1500 rad/s	8080 rad/s
4	Supply manifold pressure(P_{sm}), x_4	130000 Pa	204396 Pa

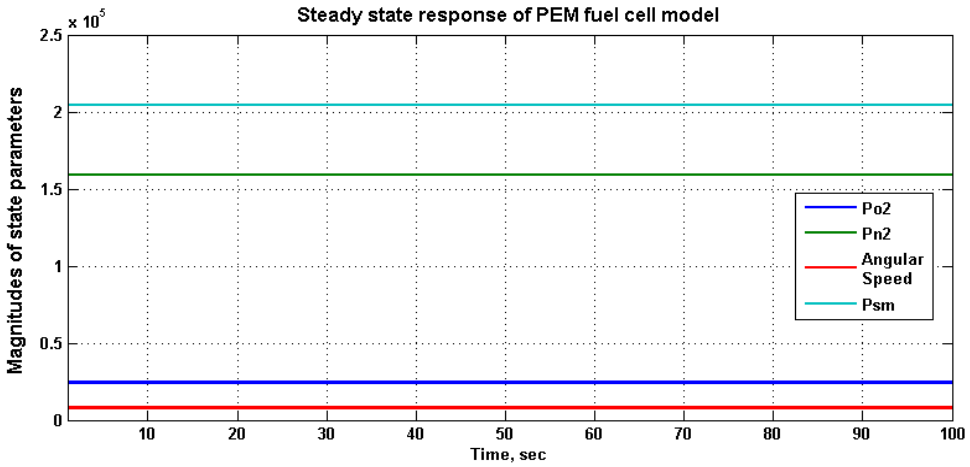

Figure 3.3 Steady state response of PEM fuel cell model

Figure 3.3 shows the steady state response of the PEM fuel cell model. The steady state values of the state variables are shown in the Table 3.2. By changing the air-supply compressor motor voltage (V_{comp}) value from 160 V to 250 V, the open loop step response was obtained and shown in Figure 3.4.

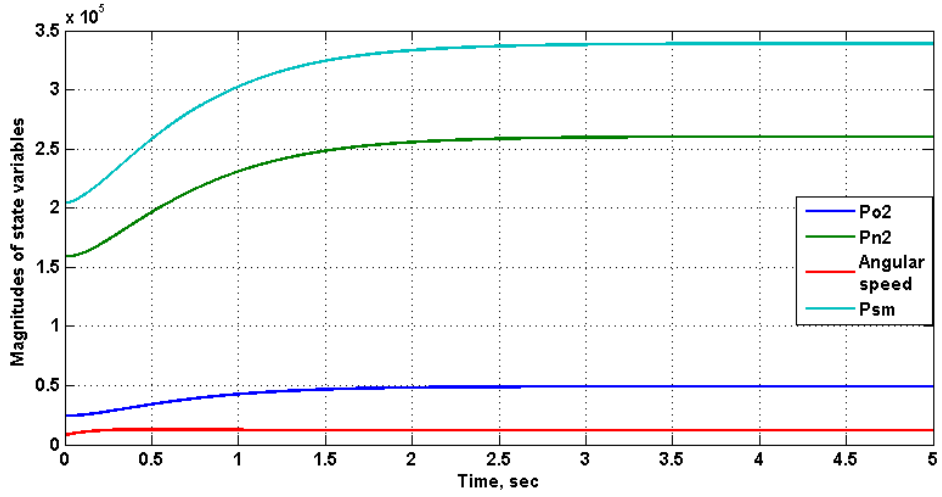

Figure 3.4 Open loop step response curves

3.5 System identification methodology from the steady state response

3.5.1 FOPTD model

The processes which are having higher order transfer function model are difficult to analyze. Generally higher order transfer function models are approximated to the FOPTD (First

Order plus Time Delay) or SOPTD (Second Order plus Time Delay) models as these are easy to analyze. The complexity of PEM Fuel cell model is very high. The Reaction curve method is preferred because of less effort is required to develop an approximated FOPTD model from highly complex system. The PEM Fuel cell control oriented model which is approximated to FOPTD model of general form is given by Seborg et al.[69]. The First Order plus Time Delay (FOPTD) model is

$$G(s) = \frac{K\, e^{-\theta s}}{\tau s + 1} \qquad 3.23$$

For FOPTD parameters, the method proposed by Sundaresan et al. [70] is used. By using this method, the FOPTD model parameters (K, θ, τ) are determined from the open loop response of the higher order model. To represent the FOPTD model, two values are required namely t_1 and t_2 from the step response curve, where t_1 and t_2 are the time when the responses are 35.3% and 85.3 % of the final value respectively. Using the following relations, parameters are calculated for FOPTD model

$$\text{Time delay, } \theta = 1.3t_1 - 0.29t_2 \qquad 3.24$$

$$\text{Time constant, } \tau = 0.67(t_2 - t_1) \qquad 3.25$$

The process gain K is found by calculating the ratio of the steady state change in output to the size of the input step change

$$K = \frac{\Delta y_\infty}{\Delta u_\infty} \qquad 3.26$$

These values of θ and τ approximately minimize the difference between the measured response and the model response, based on a correlation for many data sets. The Model parameters (K, θ, τ) of FOPTD model are depends on the operating conditions of the process, the size of the input step change and the direction of the change.

3.5.2 Determining the FOPTD model based on worse case model

Different FOPTD model parameters are derived for different percentage change of air-supply compressor motor voltage input (V_{comp}) which are shown in Table 3.3. From the Table 3.3 the extreme values are considered for the derivation FOPTD model which is shown in Equation 3.27. The FOPTD model parameters are selected from Table 3.3 as based on worse case values i.e. gain should be large, time constant should be small and time delay should be large.

Table 3.3 FOPTD parameters for percent change of input

% of change in input (V_{comp})	Gain, K_p (Large)	Time constant, τ (Small)	Delay time, θ_d (Large)
+10 %	1220	0.41138	0.14312
+20 %	**1252**	0.43483	**0.1562**
-10 %	1155	0.37185	0.10973
-20 %	1123	**0.3551**	0.09274

$$G_p(s) = \frac{P_{sm}(s)}{V_{comp}(s)} = \frac{1252}{0.3551*s+1} e^{-0.1562*s} \quad 3.27$$

Using Equation 3.27, classical controllers can be designed which is discussed in chapter 4 for the control of supply manifold pressure of PEM fuel cell system. Table 3.4 show the fit values of real and approximated responses

Table 3.4 Goodness of fit:

S.No:	Parmeter	Value
1	sum of squares due to error (SSE)	1.057e+07
2	R-square	0.9972
3	Adjusted R-square	0.9972
4	Root mean squared error (RMSE):	14.54

3.5.3 FOPTD model validation

By changing the air-supply compressor motor voltage from 160-161 V there is a change in the output supply manifold pressure (P_{sm}) response. The obtained response is in the s-shaped form and the process is approximated to the FOPTD model as shown in Equation 3.28.

$$G(s) = \frac{P_{sm}(s)}{V_{comp}(s)} = \frac{7.3913\,e^{-0.1314\,s}}{0.3832\,s+1} \quad 3.28$$

The Figure 3.5 illustrates the comparison of variation of actual process and the approximated FOPTD model responses for a unit step change in manipulated value. The actual response is obtained from the simulation results of 4th order model for supply manifold pressure. From Figure 3.5 the approximated model has the acceptable accuracy with actual process response. Equation 3.28 is used in design of fractional order controllers which are discussed in Chapters 5 and 6 for the control of supply manifold pressure of PEM fuel cell system.

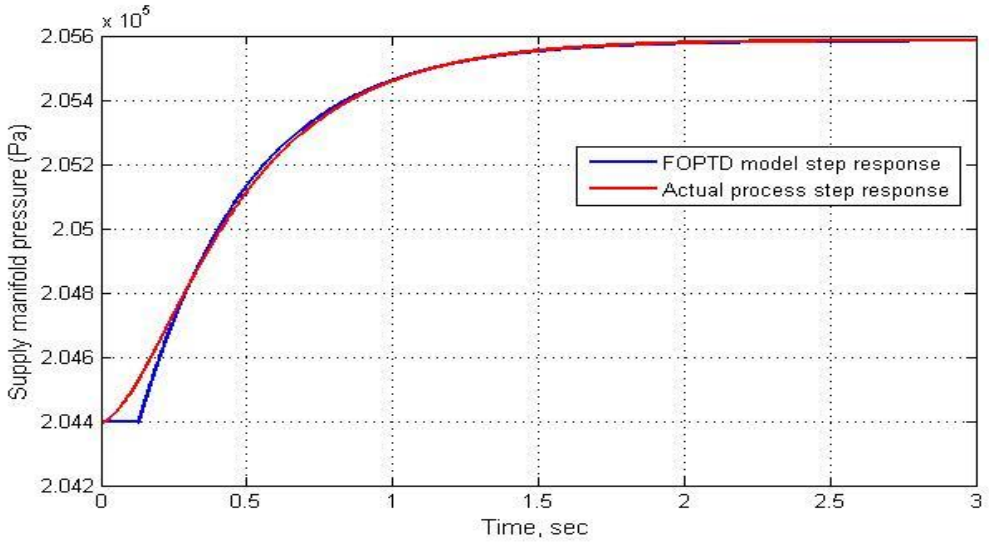

Figure 3.5 Representation of step responses of actual process and its FOPTD model for supply manifold pressure.

3.5.4 Performance metrics of the controller

The control performance and measurement analysis is performed by considering the following performance metrics and Total Variation throughout this thesis work.

1. Integral Square Error (ISE)

$$ISE = \int_0^\infty (e(t))^2 dt \quad 3.29$$

2. Integral Absolute Error (IAE)

$$IAE = \int_0^\infty |e(t)| dt \quad 3.30$$

3. Integral Time Absolute Error (ITAE)

$$ITAE = \int_0^\infty t|e(t)| dt \quad 3.31$$

Each performance Index (Equations 3.29 to 3.31) represents different aspects of the system response. Minimization of these index results in reduced peak overshoot decreased settling time and peak time.

4. Total Variance (TV)

Total Variance (TV) is another performance measure used for the closed-loop response.

$$TV = \sum_{i=1}^{\infty} |u_i - u_{i-1}| \quad 3.32$$

TV is the sum of all its moves up and down. TV value corresponds to measure of the total variation in the controller output signal, *u*. It represents the smoothness of the control action as well as robustness of the controller.

3.6 Conclusions

In this chapter described about the modeling equations of PEM fuel cell system, state space representation of the model, steady state response of the model. Approximated FOPTD models developed from the steady state model response to design the controllers. Approximated model is validated with actual response. The approximated FOPTD model used to develop control strategies in further chapters.

Chapter 4
Uncertainty analysis of Transfer Function of Proton Exchange Membrane Fuel Cell and Design of PI/PID controller for supply manifold pressure control

The main theme of this chapter is to develop different controller strategies for control of supply manifold pressure in air feed system of PEMFC system. The FOPTD approximated model is derived from the dynamic model of the PEM fuel cell. The uncertainty analysis of transfer function of PEMFC was performed based on FOPTD model. Based on FOPTD model derived the tuning parameters of various PI/PID controllers such as ZN-PI, Skogestad-Internal Model Control (SIMC)-PI, Improved SIMC-PID and compared the servo response with smith predictor response. In addition, the dynamics of the PEM fuel cell process was tested by model predictive control (MPC) controller and Design of Decentralized PI controllers for the MIMO system of PEM fuel cell based on decoupler method.

4.1 Introduction

Fuel cell is an electrochemical device in which the energy of a reaction between a fuel (e.g., hydrogen) and an oxidant (e.g., oxygen), is converted directly and continuously into electrical energy. A single fuel cell consists of an electrolyte sandwiched between two thin electrodes (a porous anode and cathode). Fuel-cell systems offers clean alternative to energy production and are currently under intensive development. Based on types of electrolytes, fuel cells are divided into Polymer Electrolyte Membrane fuel cell (PEMFC), Direct Methanol fuel cell (DMFC), Solid Oxide fuel cells (SOFC) and so on. Due to low operating temperature Proton exchange membrane fuel cell (PEMFC) is the most promising fuel cell system for both stationary and automotive applications as a substitute of traditional systems such as internal combustion engines.

It is necessary to design a controller scheme to the PEMFC system for the following such as 1) to prevent membrane damage, 2) decrease in the stack voltage and 3) Oxygen starvation. To achieve these objectives, it is required to put focus on developing the system models and corresponding controller strategies. Out of these, a very fundamental model proposed in literature is a 9^{th} order non linear dynamic model developed using lumped parameter and control volume approach's [64]. As this model involves more complexity in mathematical equations and

it made inappropriate for controller design. By separating the air feed system from the overall system [65]was proposed a 4^{th} order control oriented model for the PEMFC system.

The fuel cell has the problem of oxygen starvation, when the load changes rapidly. If the load increases, it needs more power and the load current of the fuel cell rises. The chemical reactions should accelerate to give the required power to the load, using more oxygen or air supply on cathode side, which is provided through supply manifold from air-supply compressor. So supply manifold should maintain the required air pressure to supply, when there is demand in oxygen on cathode side. Therefore, it is necessary to design a controller to maintain the pressure in the supply manifold on cathode side.

4.2 Simulation results and discussions

4.2.1 Uncertainty analysis of FOPTD model of FEMFC system

The non linear PEM Fuel cell dynamic model was approximated by the following FOPTD model as

$$G_p(s) = \frac{P_{sm}(s)}{V_{comp}(s)} = \frac{1252\ e^{-0.1562\,s}}{0.3551\ s+1} \qquad 4.1$$

Before the controller development, it is necessary to get the FOPTD plant models about some predefined operating points for supply manifold pressure (P_{sm}).The stack is a combination of 381 fuel cells connected in series with 75 kW gross power output and maximum stack current of $I_{stack,max}$ = 320A and the stack voltage varies between 220 V to 350 V. An uncertainty analysis is performed by changing the operating current range of $I_{stack,}$from 100 A to 250 A for a fixed difference.

In the PEMFC system, disturbance occurrence I_{stack} alters the operating conditions. The changes in operating conditions results in changes in the resultant linearized model of PEMFC. The discrepancy between those deviated models from the nominal plant will be regarded as system uncertainties. The different operating conditions are taken from literature reference [58].These eight operating points of air-supply compressor motor voltage (V_{comp}) and stack current (I_{stack}) are shown in Table 4.1configures eight FOPTD models. These FOPTD models are derived based on the method proposed by Sundaresan et al. [70] which is used in chapter 3.Those FOPTD models will be used during the controller design and their corresponding Bode diagrams are shown in Figure 4.2.

Table 4.1 FOPTD model transfer functions for eight different operating points of PEM fuel cell stack.

S.No	V_{comp} (V)	I_{stack} (A)	FOPTD model transfer function
1	90	90	G1= (727.14*e^(-0.0578*s))/(1+0.2739*s)
2	110	120	G2= (448.73*e^(-0.0639*s))/(1+0.3028*s)
3	130	150	G3=(239.733*e^(-0.0838*s))/(1+0.3337*s)
4	150	180	G4= (72.30*e^(-0.1136*s))/(1+0.3698*s)
5	161	198	G5= (7.3913*e^(-0.1314*s))/(1+0.3832*s)
6	170	210	G6= (68.55*e^(-0.147*s))/(1+0.4141*s)
7	190	240	G7= (191.66*e^(-0.1729*s))/(1+0.4663*s)
8	200	250	G8= (249.78*e^(-0.1493*s))/(1+0.5628*s)

Describing the derivation of FOPTD transfer function for a given operating point as follows. Consider the case of compressor voltage V_{comp} = 170 V and stack current of I_{stack} = 210 A

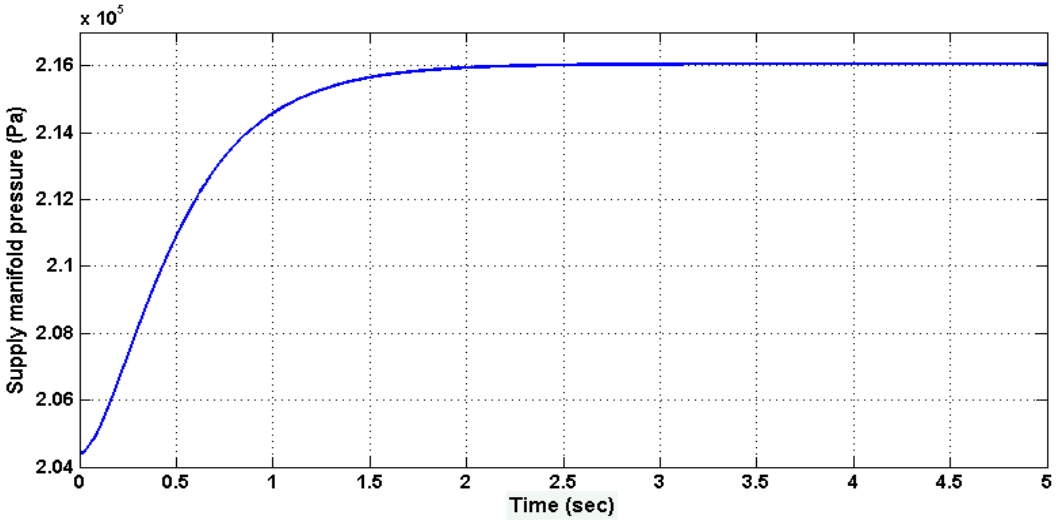

Figure 4.1 Open loop response of supply manifold pressure P_{sm} for operating point of V_{comp} = 170V and I_{stack} = 210A

From the response shown in Figure 4.1 for the given operating point, obtain the t_1 and $t_2$for the corresponding 35.3% and 85.3% of the final value of the response. In this case, t_1=

0.3230 sec and t_2= 0.9410 sec. From the method proposed by Sundaresan et. al. [70] is explained in section 3.5.1 is used to obtain FOPTD transfer function.

FOPTD parameters are calculated as follows

$$\theta = 1.3t_1 - 0.29t_2$$

=1.3*0.3230-0.29*0.9410

= 0.147

$$\tau = 0.67(t_2 - t_1)$$

= 0.67*(0.9410-0.3230)

= 0.4141

The process gain is found by calculating the ratio of the steady state change in output to the size of the input step change

$$K = \frac{\Delta y_\infty}{\Delta u_\infty}$$

= (216050-204400) / (170-0)

= 68.55

Obtained FOPTD model T/F

$$G_p(s) = \frac{68.55 * e^{-0.147*s}}{0.4141 * s + 1}$$

Similarly, we obtain the FOPTD T/F for the remaining operating points.

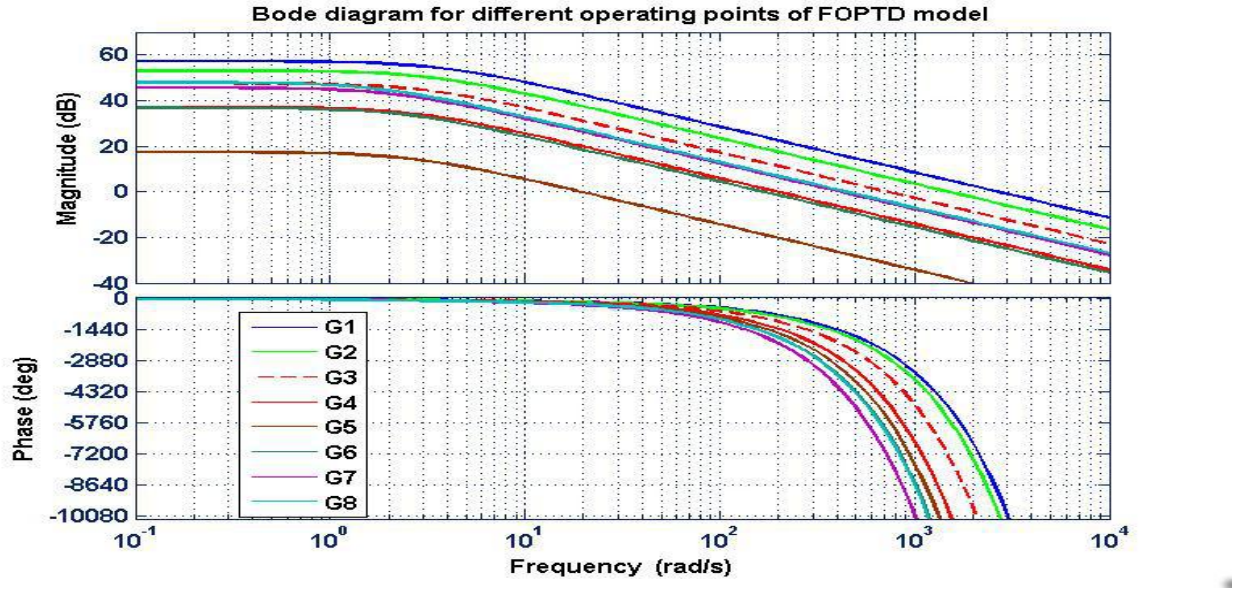

Figure 4.2 The Bode diagrams of FOPTD model of PEMFC for eight different operating points.

It was observe from Figure 4.2, that the transfer function has spreads in its gain values and in the roll-off frequency values. Thus it can conclude that the linearized model has uncertainty in its transfer function, with varying operating conditions. The fuel cell dynamic behavior is inherently nonlinear and time varying. A linearization technique is used to achieve transfer function instead of nonlinear dynamics. When the current load is suddenly changed, the voltage and the operating points will be changes. Therefore, the resultant linearized model of the PEMFC changes. The discrepancy between those deviated models from the nominal plant will be regarded as system uncertainties. In this, not included any variation in parameters of the model. The supply manifold pressure (P_{sm}) closed loop response with SIMC-PI controller for FOPTD model gain changing from 1252 to 12520 and corresponding control actions are shown in Figure 4.3.The uncertainty in the phase and the gain ruins the performance of the nominal plant of the PEMFC; since the response of the PEM fuel cell is adjusted using the nominal plant transfer function.

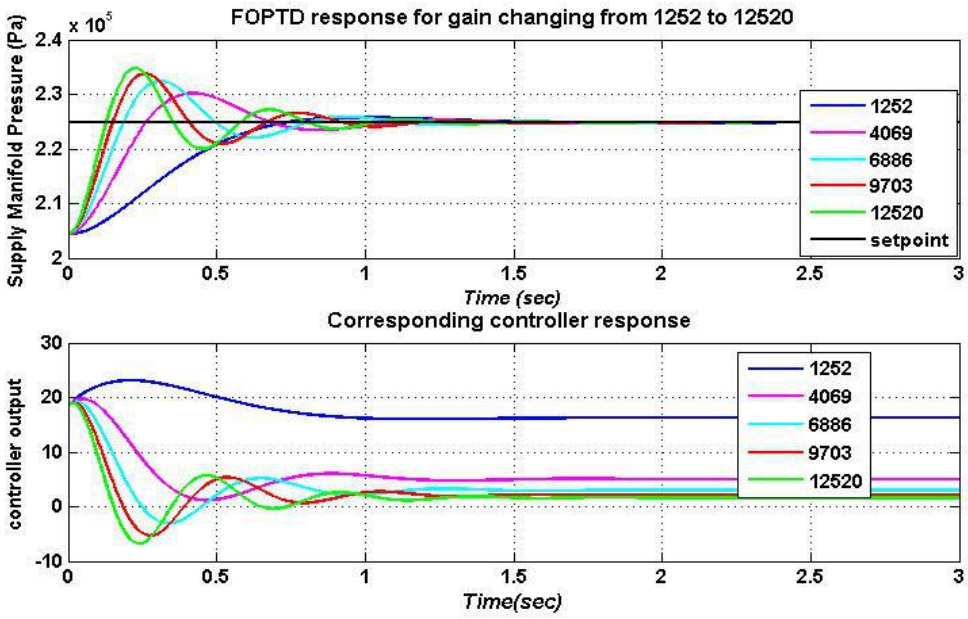

Figure 4.3 P_{sm} response and corresponding controller actions for FOPTD gain changing 1252 to 12520.

4.2.2 Closed loop Analysis using SIMC-PI controller

The tuning rules of ZN-PI, Skogestad Internal Model Control (SIMC)-PI, improved SIMC-PID and Smith predictor-PI methods are given in Table 4.2 and their corresponding values are reported in Table 4.3

Table 4.2 PI/PID controllers tuning rules [69, 93]

Process	Method	k_p	τ_I	τ_D
$\frac{Ke^{-\theta s}}{\tau s+1}$	**ZN-PI [69]**	$\frac{0.9*\tau}{K\theta}$	$3.33*\theta$	--
	SIMC-PI [93]	$\frac{\tau}{K(\lambda+\theta)}$	$min(\tau, 4(\lambda+\theta))$	--
	Improved SIMC-PID [93]	$\frac{2\tau+\theta}{3K\theta}$	$\frac{2\tau+\theta}{3K\theta}$	$\frac{\tau\theta}{2\tau+\theta}$
	Smith predictor-PI controller [69]	$\frac{1}{K}$	T	--

Table 4.3 PI/PID controller tuning values

Tuning Method	k_p	τ_I	τ_D
ZN-PI	0.001634	0.52014	--
SIMC-PI	0.0009078	0.3551	--
Improved SIMC-PID	0.001476	0.4332	0.064
Smith Predictor	0.000798722	0.3551	--

The output supply manifold pressure is connected as feedback for the nonlinear model of the PEMFC and step change of pressure from 204396 to 204396*1.1 Pa applied and the closed loop response is obtained for the designed SIMC-PI settings. Figure 4.4 (a) shows the servo controlled response of supply manifold pressure and its corresponding control action using SIMC-PI controller. From servo control response it depicts that better response, faster settling time and lesser peak overshoot. Figure 4.4(b) shows the regulatory controlled response of supply manifold pressure and its corresponding control action using SIMC-PI controller. At time t = 0sec, output disturbance with -2000 units of supply manifold pressure change was applied .

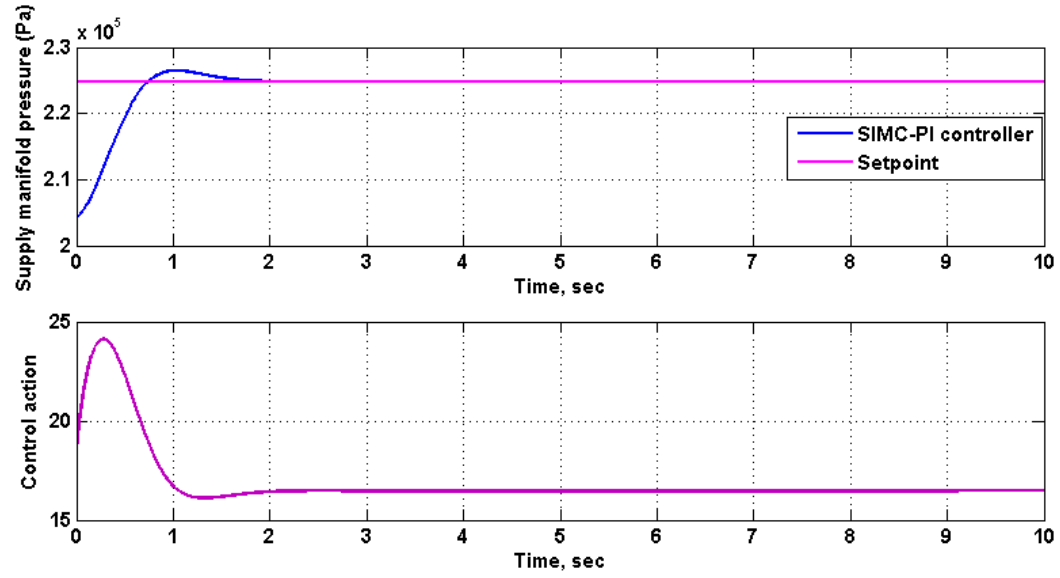

(a)

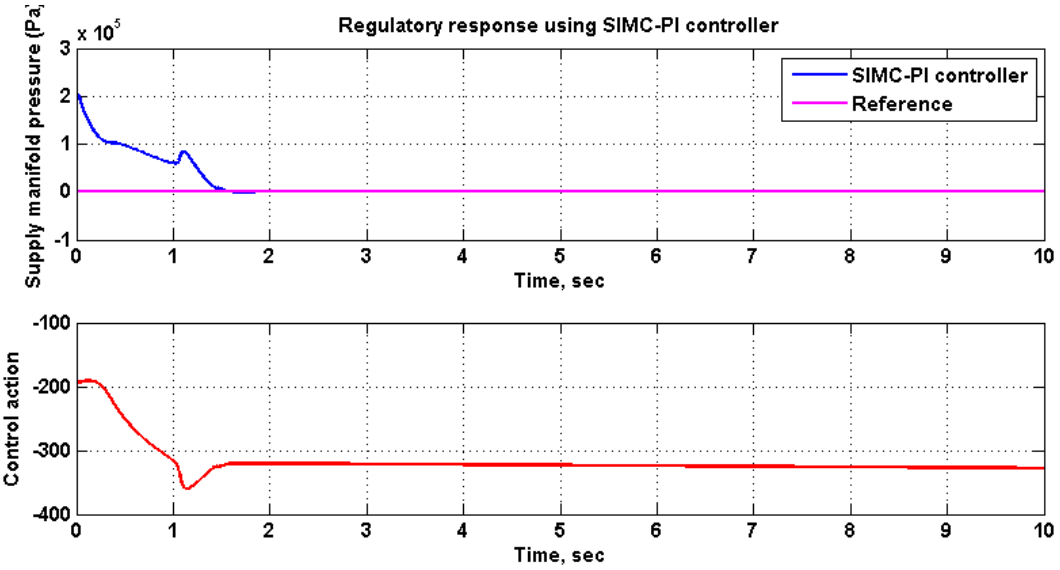

(b)

Figure 4.4 Control responses for supply manifold pressure with SIMC-PI controller. (a)Servo response and (b) Regulatory response.

4.2.3 Discussion on Bode Plots and stability issues

The performance of the improved SIMC PID controller on PEM fuel cell is studied by frequency domain analysis. To know the stability margins of the open loop system, frequency domain (Bode plot) stability analysis was performed.

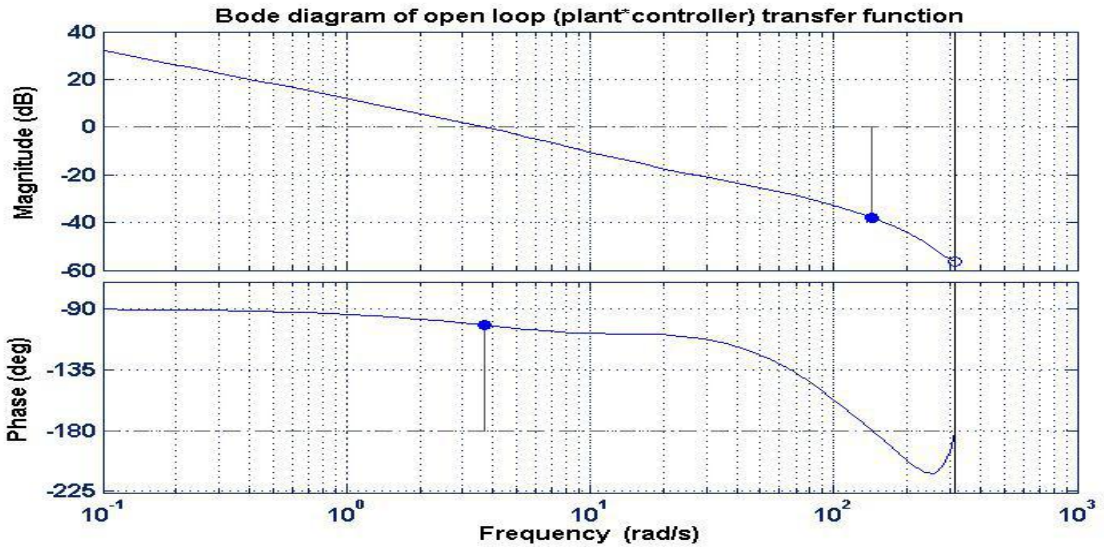

Figure 4.5 Bode plot for the product of Plant and controller (Improved SIMC PID) transfer function.

The bode plot for open loop (Plant and improved SIMC PID Controller) is shown in Figure 4.5. It shows the gain margin is 76.1(dB) and the phase margin is 78.8^{o}. This observation states that the closed loop system is stable at these points. Figure 4.6 illustrates the bode plot of closed loop improved SIMC PID controlled plant. From Figure 4.6 the Gain margin is infinity. This observation states that the closed loop system is stable at these points.

4.2.4 Discussion on uncertain plant response

The Figure 4.3 shows the response to step input of the closed loop system, with plant transfer function, whose transfer function varies with the operating conditions. Thus, the uncertain plant makes the response from too sluggish (without any overshoot) to fast response (with overshoot).

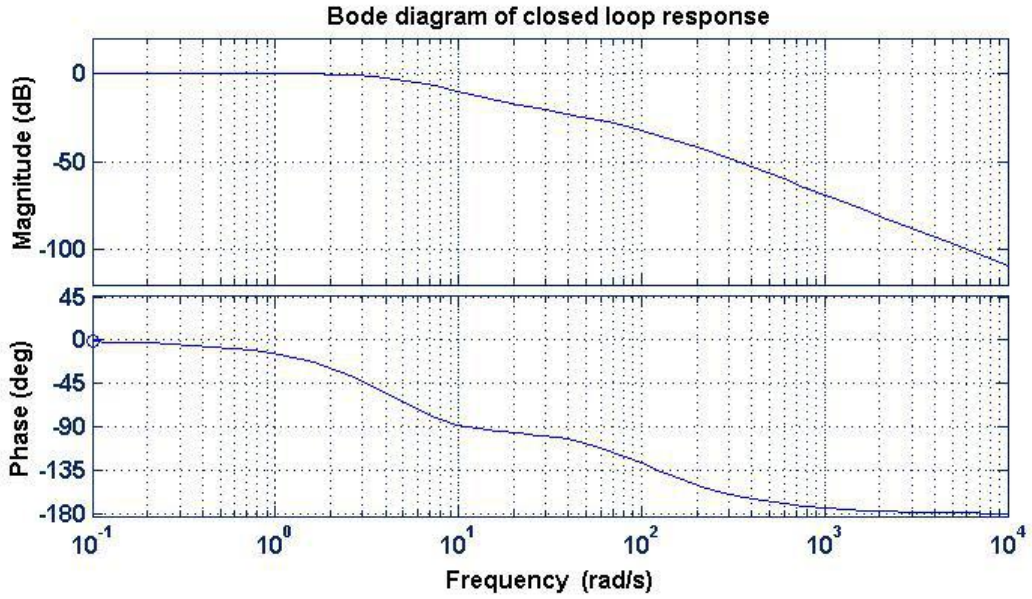

Figure 4.6 Bode plot of Improved SIMC PID controlled closed loop transfer function of the system.

Though with wide change in uncertain plant gain from 1252 to 12520, the system remains stable. In order to get "iso-damped" response, (desirable) that is having same overshoot with change in plant parameter to be implemented using Fractional Order PID (FOPID). Fractional order controller can be applied to integer order mathematical model for closed loop analysis using different fractional tuning methods.

4.2.5 Design of Smith predictor controller for PEM fuel cell system

In order to handle the time lag effects of a process, the control system should stay before response taking action. The performance of the PID controller is strictly restricted by the long dead time. The Smith predictor is the well-known control scheme to treat with time delay systems. Smith predictor is also known as dead time compensator as it compensates the dead time effects. In 1957, Smith developed the smith predictor structure to compensate systems with time delay, where it is too difficult to control processes with long time delay using PID algorithm [71, 72]. This section describes the design of a smith predictor controller to control the supply manifold pressure of PEM fuel cell to analyze the dynamics of the process. Figure 4.7 shows the smith predictor PI control response and its control action.

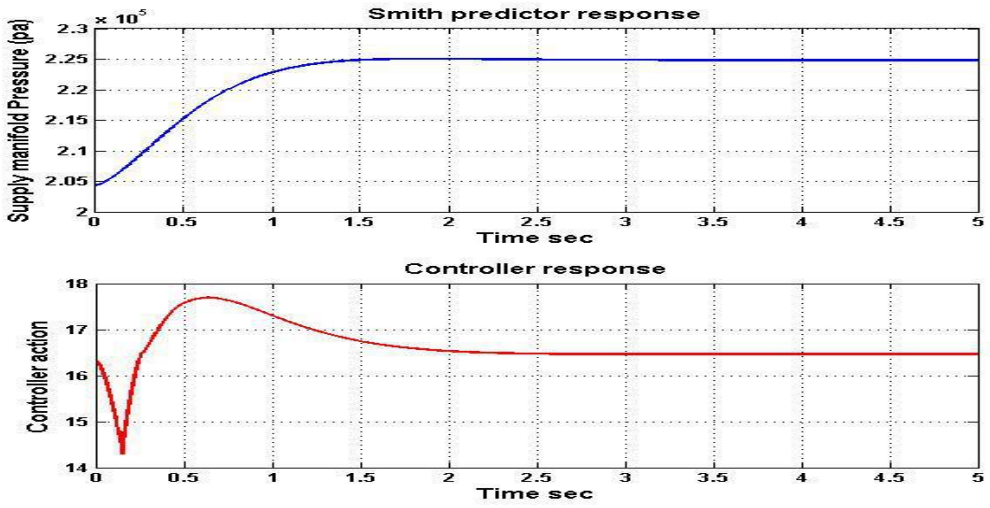

Figure 4.7 Smith predictor PI control response.

4.2.6 Control responses for the PEM Fuel Cell model

The responses are evaluated with different tuning methods such as ZN-PI, SIMC-PI, Improved SIMC PIDand Smith predictor applied to 4th order `nonlinear model of the PEMFC system. The comparative response for different control tuning methods is shown in Figure 4.8.

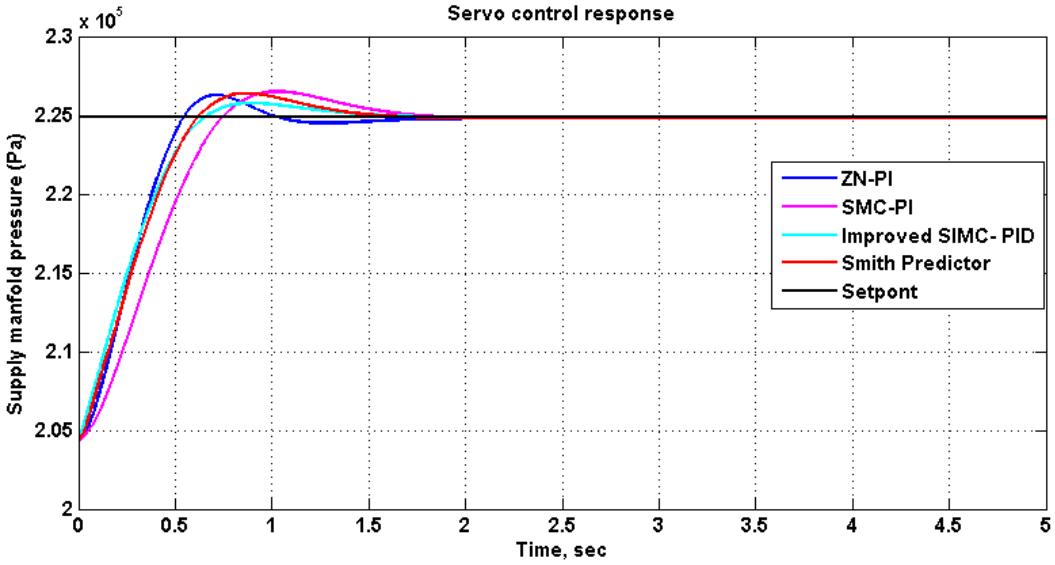

Figure 4.8 Supply manifold pressure responses for Tuning methods of ZN_PI, SIMC_PI, improved SIMC-PID and Smith predictor

Table 4.4shows the comparative performance analysis different tuning methods. From Table 4.4 and Figure 4.8, it is clear that the smith predictor PI controller controls supply manifold pressure smoothly with moderate rise time, peak times and having drastically reduced peak overshoot (%). It depicts that the smith predictor PI controller performs better than improved SIMC-PID controller in terms of peak overshoot (%).

Table 4.4 Time domain specifications of various tuning methods

Tuning Method / Parameter	ZN-PI	SIMC-PI	Improved SIMC-PID	Smith Predictor PI
Rise Time (Sec)	**0.459**	0.6269	0.5075	0.8578
Peak Time (Sec)	**0.703**	1.0084	0.8685	1.8691
Peak Overshoot (%)	64.2	74.0	41.1	**9.30**
IAE	6085	8403	**5928**	7581
ITAE	**1572**	2872	1581	2826

Due to large peak time of the smith predictor PI response, it is having more integral of absolute error (IAE) value than Improved SIMC-PID but lesser than SIMC-PI. When compared the values of integral of the time absolute error (ITAE), smith predictor PI response having lesser value than SIMC-PI controller. Smith predictor PI produces 9.3% of peak overshoot when compare with other methods. Because of lesser peak overshoot the Smith predictor PI controller well suitable for set point tracking. From the performance analysis of controller and transient response analysis, the model has very accurate regarding set point tracking and regulatory response and adaptable for any variation of supply manifold pressure. In this chapter 8 different operating conditions are considered because of the fuel cell will produce the accurate response for the operating range of current.

4.3 Design of MPC for supply manifold pressure control of PEM fuel cell

Model Predictive Control (MPC) has become the accepted standard for complex constrained multivariable control problems in the process industries. Model Predictive Control of supply manifold pressure control was implemented using MATLAB MPC Toolbox [73]. The nonlinear system of the PEM fuel cell process is simulated using SIMULINK of the MATLAB. The linear model of the fuel cell system is used to implement the MPC through a linearization at

operating point: V_{comp} = 160V in manipulated variable. I_{stack} = 198A in measured input disturbance. The supply manifold pressure measurement is controlled by implementing the MPC controller. The air-supply compressor voltage is considered as a constraint input due to physical limits.

The state space (SS) model is obtained by performing the linearization with given set points. Equations 4.2 and 4.3 represent the state space representation of the model without disturbance input.

$$x(t+1) = Ax(t) + Bu(t) \quad 4.2$$

$$y(t) = Cx(t) + Du(t) \quad 4.3$$

where y(t) is supply manifold pressure (Pa) and u(t) is the air-supply compressor voltage (V). The system matrices for SISO of PEM fuel cell are given as follows

$$A = \begin{bmatrix} -10.85 & -7.671 & 0 & 7.65 \\ -28.69 & -32.32 & 0 & 28.94 \\ 0 & 0 & -7.329 & -0.04092 \\ 19.84 & 19.84 & 89.85 & -21.47 \end{bmatrix},$$

$$B = \begin{bmatrix} 0 \\ 0 \\ 365.7 \\ 0 \end{bmatrix}, \; C = [0 \quad 0 \quad 0 \quad 1] \quad 4.4$$

Before design of MPC the state space model is validated using simulation in MATLAB/SIMULINK and it is well validated. The results of validation is shown in below Figure 4.9.

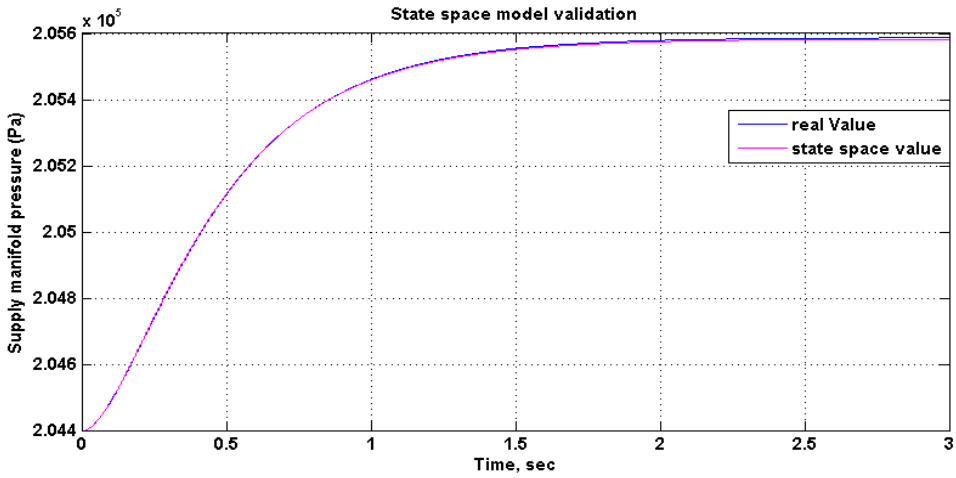

Figure 4.9 State space model validation results

Figure 4.10 shows the evolution of supply manifold pressure control using MPC for the 4th order nonlinear model. The control action computed by the MPC is shown in Figure 4.11. The output of the MPC air-supply compressor voltage is the input for the plant.

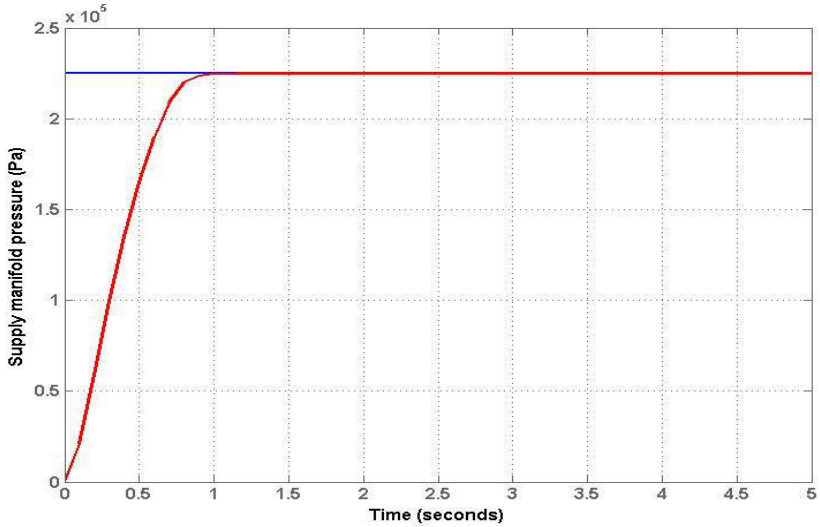

Figure 4.10 Model Predictive Controller response for supply manifold pressure control

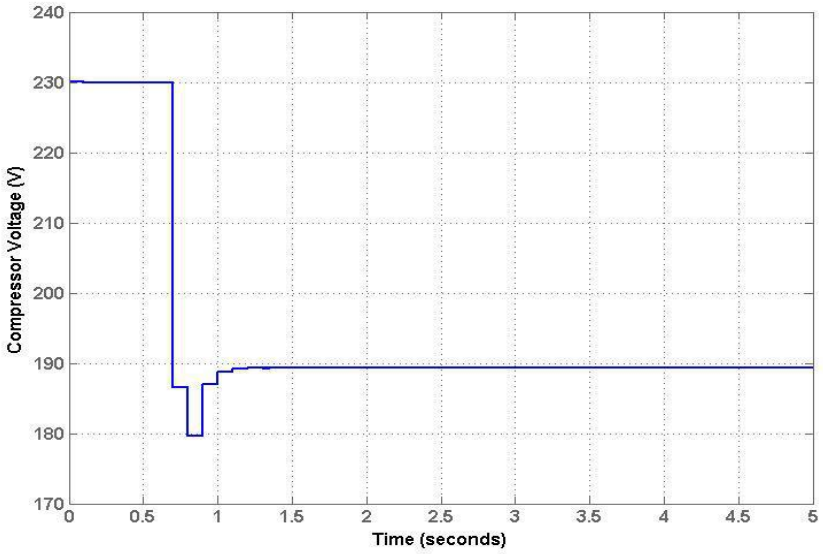

Figure 4.11 MPC control action for the control of supply manifold pressure

4.3.1 Conclusion for MPC controller

From Figure 4.10 4.9red color depicts the response of supply manifold pressure and blue line shows the reference line. Figure 4.11shows the control action of MPC. For design of the MPC, 4th order `nonlinear model of the PEMFC is used. The air-supply compressor voltage is constrained between 160-230V. The response shows no peak overshoot and also having smooth rise of control.

4.4. Design of Decoupler and decentralized controller for PEM fuel cell system

PEM FC process model is a multi-input and multi-output (MIMO) system. Control of MIMO systems is relatively complex when compared to SISO systems because of interactions in control loops. To eliminate or minimize the control loop interactions, design of decoupler is one of the popular approaches. Decoupler decomposes a MIMO process into independent single loop sub-systems.

The nonlinear model of the PEM fuel cell is linearized into MIMO system to design the decoupler and controller. The system matrices for MIMO of PEM fuel cell is given as follows

$$A = \begin{bmatrix} -10.85 & -7.671 & 0 & 7.65 \\ -28.69 & -32.32 & 0 & 28.94 \\ 0 & 0 & -7.329 & -0.04092 \\ 19.84 & 19.84 & 89.85 & -21.47 \end{bmatrix},$$

$$B = \begin{bmatrix} 0 & -289.9 \\ 0 & 0 \\ 365.7 & 0 \\ 0 & 0 \end{bmatrix}, \quad C = \begin{bmatrix} 0 & 0 & 0 & 1 \\ 0 & 0 & 1.644 * 10^{-5} & -2.988 * 10^{-7} \end{bmatrix} \qquad 4.5$$

Where the inputs for the MIMO system are air-supply compressor voltage (V) as u1 and stack current (A) is manipulated variable as u2. The outputs are supply manifold pressure (Pa) as y1 and Air-supply compressor out flow rate (kg/sec) as y2 which is another measurable output for the considered MIMO system. Air-supply compressor out flow rate is typically measured as an internal feedback to the compressor local control. The following transfer function matrix was derived for the above TITO PEM fuel cell process

$$G(s) = \begin{bmatrix} \frac{203.165 e^{-0.0085 s}}{0.3742 s+1} & \frac{0.0008724}{0.1465 s+1} \\ \frac{-35.523 e^{-0.0085 s}}{0.3742 s+1} & \frac{0.0001061 e^{-0.0085 s}}{0.3742 s+1} \end{bmatrix} \qquad 4.6$$

The decoupler and decentralized PI controller was designed based on the procedure explained in [16]. The decoupler matrix is

$$D(s) = \begin{bmatrix} 1 & -\frac{0.0000043\,(0.3742s+1)}{0.1465s+1} \\ 334806.786 & e^{-0.0085s} \end{bmatrix} \quad 4.7$$

The resultant diagonal system is:

$$q1(s) = \frac{203.165\,e^{-0.0085\,s}}{0.3742\,s+1} + \frac{292.1}{0.1465\,s+1} \quad 4.8$$

$$q2(s) = \frac{0.000152\,e^{-0.0085\,s}}{0.1465\,s+1} + \frac{0.0001061\,e^{-0.0176\,s}}{0.1465\,s+1} \quad 4.9$$

For design of decentralized PI controller $q1(s)$ and $q2(s)$ are approximated into a first order plus time delay (FOPTD) model and decoupled PI controller is tuned by using non dimensional tuning (NDT) controller method [74]. Table 4.5 gives the tuning parameters for control of supply manifold pressure and air-supply compressor out flow rate.

Table 4.5 Tuning parameters for supply manifold pressure and air-supply compressor out flow rate

	Non dimensional tuning (NDT) method	
Tuning parameters	**supply manifold pressure**	**air-supply compressor out flow rate**
K_c	0.29132	44832.92
T_i	0.008999	0.0899

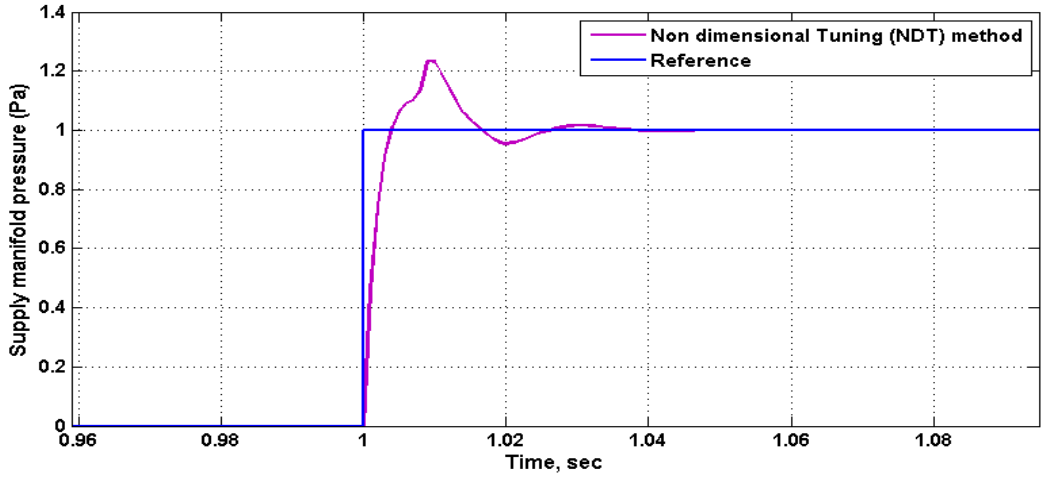

Figure 4.12 Supply manifold pressure (y1) output response of PEM fuel cell process.

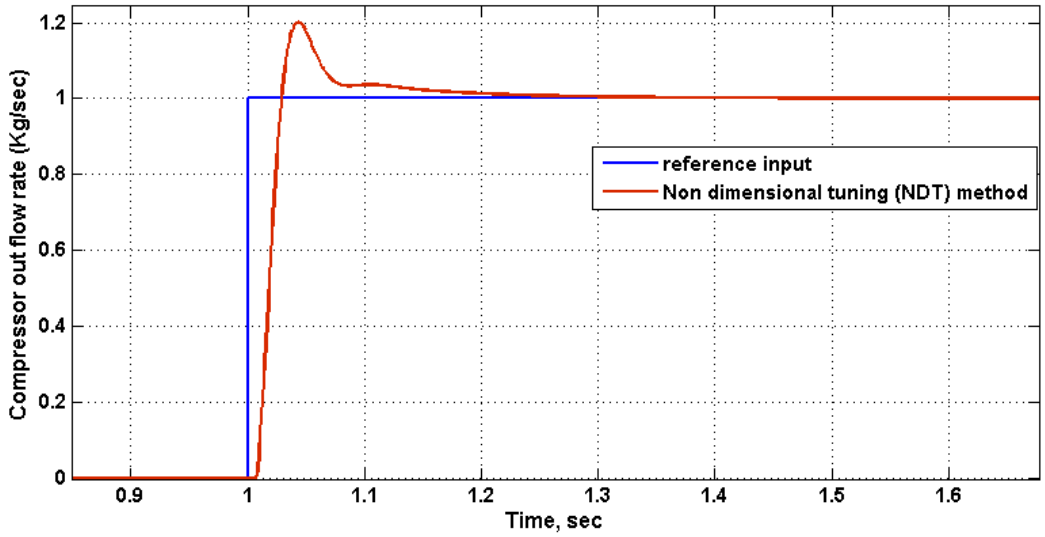

Figure 4.13 Air-supply compressor out flow rate (y2) output response of PEM fuel cell process

4.4.1 Conclusion for Decentralized controller using Decoupler method and Comparison of time scales of different controllers with time scale of open loop response

Decentralized PI controller with decoupler was designed and applied to the MIMO system for PEM fuel cell process. Figure 4.12 and Figure 4.13 shows the responses for supply manifold pressure and air-supply compressor out flow rate of PEM fuel cell process. Decentralized controller was applied for the approximated FOPTD models of the MIMO of PEM fuel cell system. Time constant for open loop model response = 0.5275 sec.

Table 4.6 Time constant values of controllers

S.No	Type of controller	Time constant of the response in sec
1	ZN-PI	0.3158
2	SIMC-PI	0.4286
3	Improved SIMC-PID	0.3110
4	Smith predictor	0.3319
5	MPC	0.4526

Table 4.6 shows the time constant values of different controllers used in this chapter. When compare the time scales of different controller responses, the time constant of different controller responses from Table 4.6 are smaller than the time constant of the open loop response of the PEM fuel cell system.

4.5 Conclusions

In this chapter, proposes a dynamic non linear model for the PEM fuel cell and presents the design of PI/PID controller by FOPTD-approximation method for controlling the supply manifold pressure in PEMFC. Uncertainty analysis of PEMFC is performed, which showed that plant transfer function varies with operating conditions. The design was implemented in MATLAB® /SIMULINK; simulation results show that Smith predictor PI controller produces better performance for servo and regulatory responses compared to other existing techniques such as ZN-PI, SIMC-PI, Improved SIMC-PID for the modeled PEMFC; and the effect on response due to uncertainty of transfer function. The frequency domain analysis of PEM fuel cell model with stability margins analyzed. The control of the supply manifold pressure was implemented using Model Predictive Control (MPC). The interactions between the control loops of the PEM fuel cell model was analyzed by designing the decoupler and Decentralized controller for the MIMO system.

Chapter 5
Design of fractional order PI/PID controllers based on robustness to control supply manifold pressure of PEM fuel cell system: A comparative study

5.1 Introduction

From the past few years, usage of motor vehicles increased drastically. Large consumption of petrochemical fuels causes more environmental pollution and limited availability of traditional fuels it is necessary to switch over to non conventional energy sources such as solar, wind, fuel cells etc. The wind and solar powers are usually depends on external environmental conditions largely which causes instability of power generation. Fuel cells produce electricity in continuous manner and it is been unaffected by external environmental conditions.

A fuel cell is an electrochemical device which converts the chemical form of energy into electrical form of energy by reaction between hydrogen and oxidants (air or oxygen) and generates water and heat as its byproducts of the reaction. A Proton Exchange Membrane (also called as Polymer Electrolyte Membrane, PEM)fuel cell is one of the most favorable type of fuel cell because of its compact size, high energy efficiency, easy start up, lower operating temperature (50^{o}-80^{o} C), high reliability.

PEM fuel cell mainly consists of cathode, anode and membrane. Hydrogen fuel is supplied to anode channel and air or oxygen to the cathode channel. The membrane separates the anode and cathode channels of fuel cell. When hydrogen gas enters into the anode channel electrons, protons will produce and electrons travel through an external load circuit finally reach the cathode. Due to the flow of electrons in the external circuit, there is generation of current and voltage at load. Protons from anode side travel through the membrane and recombines with electrons and air or oxygen from the cathode channel. This results in generation of water at cathode channel.

A single PEMFC will produce a cell voltage of 0.7V at minimal current density of1 A/cm^2. By connecting number of fuel cells in series forms a fuel cell stack and generates the stack voltage at large value. If partial pressure of oxygen on cathode side of the cell drops down to a certain value, oxygen starvation occurs. This causes sudden drop in stack voltage and causes hot spot on the membrane. This leads to burn the surface of the membrane. To prevent oxygen starvation, it is necessary to maintain the supply manifold pressure (P_{sm}) at desired value. To

control the supply manifold pressure, it is necessary to design a suitable control scheme for desired flow rates at cathode channel.

Because of having more tuning parameters and less sensitive to parameter variations fractional order controllers will produce better control response when compare with the Integer order controllers such as ZN-PI, SIMC-PI, Improved SIMC-PID and other methods presented in the chapter 4. Therefore, the fractional order controllers are recommended for the control of supply manifold pressure and presented fractional order control tuning methods in Chapter 5 and Chapter 6.

The maximum sensitivity, Ms, is defined as the maximum value of the sensitivity function among the frequency range. Maximum sensitivity, Ms, is a closed-loop design specification, which represents the inverse of the minimum distance on the Nyquist diagram between the loop transfer function and the critical point, has been shown to be effective as a robust performance tuning parameter[94]. The maximum sensitivity, Ms was proposed as a single robustness index, which can limit the gain and phase margin simultaneously [95]. The maximum sensitivity Ms can be seen as the worst-case amplification of disturbances, and a reasonable range of Ms for control design is 1.0–2.5 [96]. The maximum sensitivity Ms can also be used to instruct the controller design.

In this chapter, Suh's[65] control oriented PEMFC system model is used to control the transient behavior. An approximated FOPTD model is developed for the control of supply manifold pressure using Sundaresan – Krishnaswamy [70] technique for estimation of process parameters with acceptable accuracy. Various Fractional Order (FO) tuning rules are applied for the approximated FOPTD model of the fuel cell system to analyze the performance of the Fractional Order controllers. Primarily, FOPI tuning rules are applied and analyzed the performance of the controllers. Due to integral action in FOPI controller, there is large peakovershoot and oscillations are generated in the response. This problem was overcome by applying FOPID tuning rules to controller. Comparison of transient and performance analysis using IAE, ISE, IATE and Total Variation (TV) for the FOPI and FOPID controllers was implemented. The proposed fractional order PID controller has been implemented on non linear PEM fuel cell of four state equations model. Servo control response have been obtained. The

fractional order controller robustness was verified by applying to the nominal system and parametric uncertainties integrated system under load disturbance.

In this chapter 5 we applied different fractional order tuning methods to analyze the control response of fuel cell model. By comparing the various methods we will get better performance tuning method out of other methods. Robustness of the better controller was verified on the non linear model of the PEM fuel cell i.e 4th order model. For the first time in literature, we applied the fractional order controllers for derived FOPTD model of the 4th order model of PEM fuel cell stack system.

5.2 Fractional order PID (FOPID) controllers for the approximated FOPTD model

The most general form of a fractional order PID controller is the $PI^{\lambda}D^{\mu}$ controller which is a combination of integrator order of $\lambda$and differentiator order of $\mu$where $\lambda$and μ are any real numbers. The transfer function of the fractional order controller can be represented as form of Equation 5.1.

$$G_c(s) = \frac{U(s)}{E(s)} = k_p + k_i \frac{1}{s^{\lambda}} + k_d s^{\mu}, \qquad (\lambda, \mu > 0) \tag{5.1}$$

Where$G_c(s)$ represents the transfer function of the fractional order controller, error is $E(s)$ and $U(s)$is controller output. While representing the integrator term $\frac{1}{s^{\lambda}}$ on Bode diagram, there is a line having slope -*20*λdB/decade. The control signal *u(t)* in time domain can be expressed as

$$u(t) = k_p e(t) + k_i D^{-\lambda} e(t) + k_d D^{\mu} e(t) \tag{5.2}$$

Figure 5.1 shows the block-diagram representation of FOPID controller. All the classical types

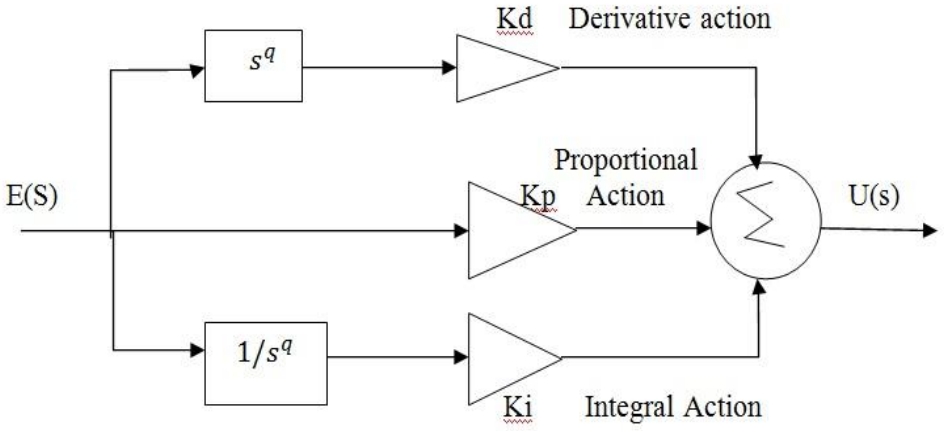

Figure 5.1 Block diagram representation of FOPID controller structure.

of PID controllers can be designed by the fractional $PI^{\lambda}D^{\mu}$ controller. Because, by selecting $\lambda = 1$ and $\mu = 1$ in Equation 5.2, a classical PID controller can be recovered. Similarly by selecting $\lambda = 1$, $\mu = 0$ and $\lambda = 0$, $\mu = 1$ respectively conventional PI & PD controllers can be developed. When compared with Integer Order PID controller (IO_PID), Fractional Order PID (FOPID) controller has two more tuning parameters for better adjustment of dynamical properties of a fractional order control system. Because of this reason, $PI^{\lambda}D^{\mu}$ controllers having the following advantages.

1.Less sensitive to parameter variations.

2. Improves the systems control functioning, and

3. Better control of dynamics of the system is possible.

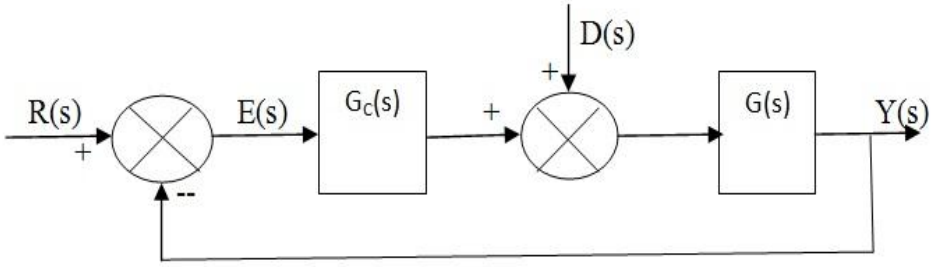

Figure 5.2 Block diagram representation of closed loop control structure.

Figure 5.2 shows the closed loop control structure for the analysis of the system. The process denoted by G(s), $G_c(s)$ represents the FOPID controller transfer function, the reference input is R(s), error is E(s), disturbance input is D(s) and Y(s) is controlled output. The following sub sections describes tuning methods of fractional order PI/PID controllers for the control of supply manifold pressure of PEM fuel cell system.

5.2.1 Design of Fractional-order Proportional-Integral (FOPI) controllers for the supply manifold pressure control of PEM fuel cell system

The transfer function of the fractional order PI controller has the following form

$$G_c(s) = \frac{U(s)}{E(s)} = k_p + k_i \frac{1}{s^{\lambda}} \qquad 5.3$$

Where k_p is proportional constant, k_i is integral constant, λ is integral fractional order. Tuning methods reported by Chen et al.[75] and Bhambhani et al.[76] are considered for design of FOPI

controller. All the tuning methods of fractional order controllers are designed for the approximated FOPTD model which derived in chapter 3 for the control of supply manifold pressure and given by the Equation as

$$G(s) = \frac{P_{sm}(s)}{V_{comp}(s)} = \frac{7.3913\,e^{-0.1314\,s}}{0.3832\,s+1} \quad 5.4$$

5.2.1.1 Chen et al. FOPI tuning method

Chen et al.[75]proposed the following rules for the fractional order PI controllers to the type of FOPTD model of the form given in Equation 5.5

$$G(s) = \frac{K\,e^{-Ls}}{Ts+1} \quad 5.5$$

$$\tau = \frac{L}{L+T} \quad 5.6$$

whereτ is the normalized dead time of the system and it represents the measure of the complexity for control of the process.

$$K_p = \frac{1}{K}\left(\frac{0.2978}{\tau+0.000307}\right) \quad 5.7$$

$$K_i = \frac{K_p(\tau^2-3.402\tau+2.405)}{0.8578\ T} \quad 5.8$$

$$\lambda = \begin{cases} 0.7 & \text{if } \tau < 0.1 \\ 0.9 & \text{if } 0.4 > \tau \geq 0.1 \\ 1.0 & \text{if } 0.6 > \tau \geq 0.4 \\ 1.1 & \text{if } \tau \geq 0.6 \end{cases} \quad 5.9$$

For the approximated FOPTD model of the PEM fuel cell dead time, L= 0.1314 sec, Time constant T= 0.3832, and open loop gain, K=7.3913. The normalized dead time of the system from Equation 5.6 is $\tau = 0.25534$. The fractional value of λ is 0.9 from Equation 5.9. The Fractional order PI controller tuning parameters obtained using Chen et al.[75]tuning method for the FOPTD model of Equation 5.4 are given in Table 5.2.

5.2.1.2 Bhambhani et al. FOPI tuning method

Bhambhanietal.[76] proposed the following rules for fractional order PI controller to the FOPTD model.

$$\lambda = \frac{L}{L+T} - 0.04 * L + 1.2399 \quad 5.10$$

$$K_p = \frac{0.2*T}{KL} + 0.16 \quad 5.11$$

$$K_i = \frac{0.25K}{TL} + \frac{0.19833}{L} + 0.09 \quad 5.12$$

For the FOPTD model of the PEM fuel cell of Equation 5.4, the Fractional order PI controller tuning parameters obtained using Bhambhani et al. [76] tuning method are given in Table 5.2.

5.2.1.3 Gude et al. FOPI tuning method

Gude et al.[77] was proposed fractional order PI controller tuning rules for FOPTD process plants. These rules were obtained by minimizing the performance criteria in the frequency domain considering the maximum sensitivity as a constraint. The formulated performance criteria is given in Equation 5.13

$$J_v = \left\| \frac{1}{s} G(s)S(s) \right\|_\infty = \max_\omega \left| \frac{1}{j\omega} \frac{G(j\omega)}{1+L(j\omega)} \right| \quad 5.13$$

The performance criterion is a measure of the system ability to handle the load disturbance inputs having low-frequency.Table5.1 shows the FOPI controller parameters in terms of normalized dead time (τ) and the Equation5.14 represents the approximated function form:

$$f(\tau) = a\tau^b + c \quad 5.14$$

Tuning parameters of FO-PI controller using Gude et al. tuning method for the FOPTD model of the PEM fuel cell of Equation 5.4 are shown in Table 5.2

Table 5.1 FO-PI controller rules using Gude et al. [77] tuning method

$f(\tau)$	a	b	c	τ
KKp	0.2154	–1.169	–0.1592	$0 < \tau < 1$
aKp	–0.4645	0.3182	0.5795	$0 < \tau < 0.25$
	3.271	5.75	0.28	$0.25 < \tau < 1$
Ti/L	9.242	–0.1966	–9.171	$0 < \tau < 1$
Ti/T	5.479	0.8154	–0.03853	$0 < \tau < 0.3$
	6.06	7.066	1.18	$0.3 < \tau < 1$
λ	λ= 1.12			$0 < \tau < 1$

Table 5.2 Summary of FO-PI controller tuning parameters for Chen et al.[75], Bhambhani et al. [76] and Gude et al. [77] methods .

FO-PI controller parameters	Chen et al. [75] method	Bhambhani et al. [76] method	Gude et al. [77] method
$\mathbf{K_p}$	0.15760	0.7432	0.0857
$\mathbf{K_i}$	0.76785	6.5643	0.2236
$\boldsymbol{\lambda}$	0.9	1.49	1.12

5.2.2 Design of Fractional order PID (FOPID) controllers for the supply manifold pressure control of PEM fuel cell system.

Tuning methods reported by Valerio & Costa[56], Bayat[78] and Padula & Visioli [79] are considered for design of FOPID controllers.

5.2.2.1 Valerio & Costa method

For tuning of FOPID controller Ziegler-Nichols type tuning rules are used. For the tuning of FOPID controller parameters, Valerio and Costa [56] was established Ziegler-Nichols (ZN) type of tuning rules. These rules valid only for the plants whose unit step response is in S shaped form. Generally plants whose transfer function represented in FOPTD model given in Equation 5.15 generates S-shaped step response.

$$G(s) = \frac{K\, e^{-Ls}}{Ts+1} \qquad 5.15$$

Valerio and Costa[56] used the minimization tuning method for the plants represented by Equation 5.15 for numerous values of time delay, Land time constant, T with K = 1.Valerio and Costa[56] proposed two sets of tuning rules for various ranges of L and T.

First set of FOPID tuning rules

First set of Z-N FOPID tuning rules are shown in Table 5.3(a) and Table 5.3(b). From these tables controller tuning parameters are obtained. Equation 5.16 shows an example how to derive the integral constant K_i.

$$K_i = 0.3254 + 0.2478 * L + 0.1429 * T - 0.133 * L^2 + 0.0258 * T^2 - 0.0171 * T * L \qquad 5.16$$

Similarly, remaining parameters of FOPID controller was calculated to get controller tuning parameters. When the parameters are in the following range of$0.1 \leq T \leq 50, L \leq 2$then first set of tuning rules may be used.

Table 5.3 (a) FOPID controller parameters for the first set of tuning rules when $0.1 \leq T \leq 5$.

	K_p	K_i	λ	K_d	μ
1	-0.0048	0.3254	1.5766	0.0662	0.8736
L	0.2664	0.2478	-0.2098	-0.2528	0.2746
T	0.4982	0.1429	-0.1313	0.1081	0.1489
L^2	0.0232	-0.1330	0.0713	0.0702	-0.1557
T^2	-0.0720	0.0258	0.0016	0.0328	-0.0250
LT	-0.0348	-0.0171	0.0114	0.2202	-0.0323

Table 5.3 (b) FOPID controller parameters for the first set of tuning rules when $5 \leq T \leq 50$

	K_p	K_i	λ	K_d	μ
1	2.1187	-0.5201	1.0645	1.1421	1.2902
L	-3.5207	2.6643	-0.3268	-1.3707	-0.5371
T	-0.1563	0.3453	-0.0229	0.0357	-0.0381
L^2	1.58271	-1.0944	0.2018	0.5552	0.2208
T^2	0.0025	0.0002	0.0003	-0.0002	0.0007
LT	0.1824	-0.1054	0.0028	0.2630	-0.0014

Second set of tuning rules:

Table 5.3 (c) represents second set of tuning rules derived for Z-N FOPID controller. These rules may be applied for the range of$0.1 \leq T \leq 50$ and $L \leq 0.5$.

Table 5.3(c) FOPID controller parameters for the second set of tuning rules when $0.1 \leq T \leq 50$ and $L \leq 0.5$

	K_p	K_i	λ	K_d	μ
1	-1.0574	0.6014	1.1851	0.8793	0.2778
L	24.5420	0.4025	-0.3464	-15.0846	-2.1522

T	0.3544	0.7921	-0.0492	-0.0771	0.0675
L^2	-46.7325	-0.4508	1.7317	28.0388	2.4387
T^2	-0.0021	0.0018	0.0006	-0.0000	-0.0013
LT	-0.3106	-1.2050	0.0380	1.6711	0.0021

The approximated FOPTD model of the PEM Fuel cell is given by Equation (5.17)

$$G_{FOPTD}(s) = \frac{P_{sm}(s)}{V_{comp}(s)} = \frac{7.3913\,e^{-0.1314\,s}}{0.3832\,s+1} \qquad 5.17$$

As $L(0.1314) \leq 0.5$ and $0.1 \leq T(0.3832) \leq 50$ from the approximated FOPTD model, the second set of tuning rules were chosen for tuning of the ZN-FOPID controller

5.2.2.2 Bayat method

The main purpose of Bayat [78] method is to compute FOPID controller tuning parameters such as *K*p, *T*i, *T*d, λ and μ for the known FOPTD process model parameters (*K*, *L* and *T*) in order to minimize either ISE or ISTE performance index. This method can be applied to all FOPTD processes having the normalized dead time (τ) in between 0.1 and 3.5.Table 5.4 shows tuning rules of FOPID controller for set point and load disturbance control to minimize the ISE performance index.

Table 5.4 Tuning rules of the FOPID controller to minimize the ISE performance index

FOPID parameters	**Set point control (0.1<τ<3.5)**	**Load disturbance (0.2<τ<3.5)**
K_p	$\frac{1}{K}\left[\frac{0.3663\tau + 0.8856}{\tau + 0.000792}\right]$	$\frac{1}{K}\left[\frac{0.2709\tau + 0.566}{\tau - 0.0364}\right]$
T_i	$T(0.3827\tau + 0.9354)$	$T(1.252\tau^{0.5555} - 0.05696)$
T_d	$T(0.5036\tau^{0.7152} - 0.07974)$	$T(0.3425\tau + 0.02753)$
μ	$-0.03625\tau + 1.095$	$-1.368\tau^{0.04705} + 2.503$
λ	1	1

5.2.2.3 The Padula & Visioli method

In Padula & Visioli [79] set of tuning rules for FOPID controller was developed. These rules are structured based on to minimize the Integral of Absolute Error (IAE) performance index through a constraint of the maximum sensitivity (M_s).

Tuning rules

These rules can be applied for the FOPTD process model of the normalized dead time (τ) in the range of$0.05 \leq \tau \leq 0.8$. These rules are formulated to achieve maximum sensitivity M_s of 1.4 and 2.0. The following equations give the structure of tuning parameters of FOPID controller

$$K_p = \frac{1}{K}(a\tau^b + c) \quad 5.18$$

$$T_i = T^{\lambda}\left(a\left(\frac{L}{T}\right)^b + c\right) \quad 5.19$$

$$T_d = T^{\mu}\left(a\left(\frac{L}{T}\right)^b + c\right) \quad 5.20$$

Table 5.5(a) shows the values of a, b and c constants in Equations (5.18-5.20) for setpoint control and regulatory control when M_s=1.4.

Table 5.5(a) Tuning rules for set point control response when M_s=1.4.

	Set point control when M_s=1.4.			**Regulatory control when M_s=1.4**		
Constants	**a**	**b**	**c**	**a**	**b**	**c**
K_p	0.6503	-0.9166	-0.6741	0.2776	−1.095	−0.1426
T_i	0.04701	-0.2611	0.9276	0.6241	0.5573	0.0442
T_d	0.3563	1.2	0.0003108	0.4793	0.7469	−0.02393

Table 5.5(b) gives the values of λ and μ in Equations (5.18-5.20) for set point control and regulatory control response when M_s= 1.4.

Table 5.5(b) Tuning rules for λ and μ when M_s=1.4

set point control when M_s=1.4	
λ	**μ**
1	1.1 if $\tau < 0.1$
	1.2 if$0.1 \leq \tau$
Regulatory control when M_s=1.4.	
λ	**μ**
1	1.0if $\tau < 0.1$
	1.1if $0.1 \leq \tau < 0.4$
	1.2 if $0.4 \leq \tau$

5.3 Results and Discussion

An approximated FOPTD model was developed for control of supply manifold pressure of the Suh [65] proposed dynamic model of the PEM fuel cell.The approximated FOPTD model of PEM fuel cell system is

$$G(s) = \frac{P_{sm}(s)}{V_{comp}(s)} = \frac{7.3913\,e^{-0.1314\,s}}{0.3832\,s+1} \quad 5.21$$

For the above FOPTD model, fractional order PI/PID controller tuning methods are applied in the SIMULINK environment using FOMCON tool box to generate servo and regulatory control responses. For the better performance of a controller response, the values of IAE, ISE, ITAE, TV and time indices are required to be minimum. It is easy for the tuning of the controllers to the approximated FOPTD models of higher order systems. In this simulation studies, fractional order controllers are tuned for the FOPTD model as well as tested the effective performance of the better response produced FOPID controller on the original four state model of the PEM fuel cell system. In this process, it is possible to check the guarantee or robustness of the controller to produce the same performance under the non linear situation. To analyze the robustness of the FOPID controller, disturbance input i.e stack current (I_{stack}) was changed at $\pm$ 10A and $\pm$ 20A. Similarly, uncertainty analysis is performed by changing the limits of some of the parameters in the original model using FOPID controller.

5.3.1 FO-PI controller methods

First of all, various FOPI tuning rules are applied to fuel cell approximated FOPTD model and compared the performance of the response. Using Chen et al.[75] tuning method, FOPI controller settings are obtained as: K_p = 0.15760, K_i = 0.76785 and λ = 0.9. Similarly, using Bhambhani et al. [76] FOPI method, the controller settings are as: K_p = 0.7432, K_i = 6.5643 and λ = 1.49. The following controller settings K_p = 0.0857, K_i = 0.2236 and λ = 1.12 are obtained by Gude et al. [77] proposed FOPI tuning method. The servo responses for a unit step change in the set point as well as its controller actions are shown in Figure 5.3.

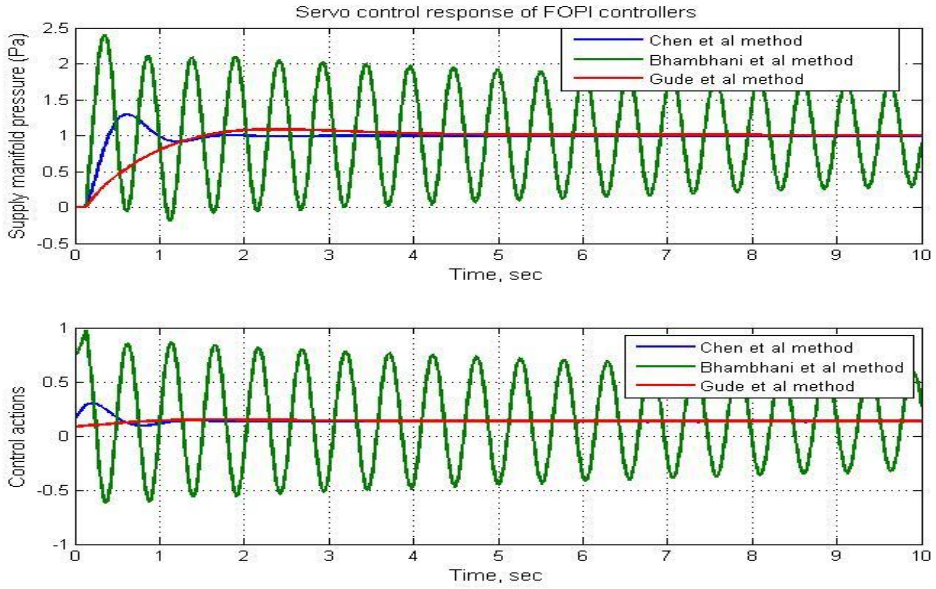

Figure 5.3 Closed loop servo control response of FOPI controllers

The regulatory control response is evaluated for a unit step disturbance in the closed loop and corresponding controller actions are shown in the Figure 5.4.

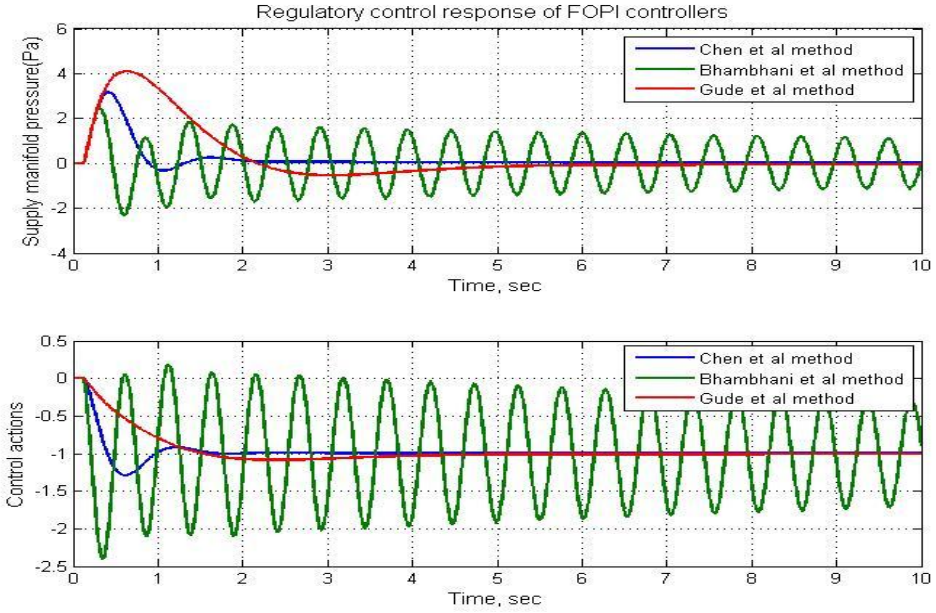

Figure 5.4 Regulatory control responses of FOPI controllers.

Table 5.6 shows peak overshoot, rise time, peak time and settling times of servo response and ISE, IAE, ITAE, TV values for servo and regulatory responses.

Table 5.6 Summary of performance of Fractional Order PI controllers.

Performance Parameters	**Gude et al. [77] method**		**Bhambhani et al. [76] method**		**Chen et al. [75] method**	
Rise Time(sec)	1.0309		0.0601		0.2059	
Peak time(sec)	2.38		0.348		0.6130	
Settling time(sec)	4.164		9.9770		1.5483	
Peak overshoot (%)	8.0268		131.65		29.5717	
	Servo	**Regulatory**	**Servo**	**Regulatory**	**Servo**	**Regulatory**
ISE	0.4395	14.333	4.4837	11.129	0.2530	3.3379
IAE	0.8513	5.8895	5.9577	9.2256	0.4460	1.8914
ITAE	1.0544	9.9684	27.0273	42.094	0.3433	2.4958
TV	0.0773	1.1670	45.8078	71.2071	0.4836	1.8700

From the Figure 5.3 and Table 5.6, tuning method reported by Bhambhani et al. [76] generates oscillatory response with peak overshoot of 131.65%, peak time of 0.348 sec. and higher values of performance indices it is the least preferable for tuning of FOPI controller. Tuning method reported by Chen et al. [75] generates the response with peak overshoot of 29.57%, settling time of 1.5483 sec, peak time of 0.613 sec. Gude et al. [77] FOPI controlled response gives peak overshoot of 8.0%, it is less than the Chen et al. [75] method but the settling time (4.164 sec), peak time (0.37 sec.) and rise time (1.03 sec) are more than the Chen et al. method. It is evident from Figures 5.3-5.4 and Table 5.6 that the Chen et al. [75] method gives minimum values of performance indices for servo and regulatory control applications. But Gude et al. [77] method has the least controller effort in terms of total variation among FOPI tuning methods. Gude et al. FOPI method is better suitable when peak overshoot is important consideration for control as it produces least value of peak overshoot among FOPI controllers. Chen et al. [75] method also

suitable for tuning of FOPI controller, which produces faster response, having lower values of time and performance indices with acceptable peak overshoot.

5.3.2 FO-PID controller methods

FOPID tuning method reported by Valerio and Costa [56], the controller settings are as follows: K_p = 1.4804, K_i = 0.8896, K_d = -0.5641, λ = 1.1526, μ = 0.0629. FOPID tuning method reported by Bayat [78], the set point control settings are as follows: K_p = 0.51719, K_i = 1.30639, K_d = 0.00179, λ = 1, and μ = 1.08. FOPID tuning method reported by Padula & Visioli [79], the set point control settings are as follows: K_p = 0.2160, K_i = 0.5702, K_d = 0.0068, λ = 1, and μ = 1.2. Figure 5.5 illustrates servo controlled responses for unit step change in the set point and their corresponding controller actions.

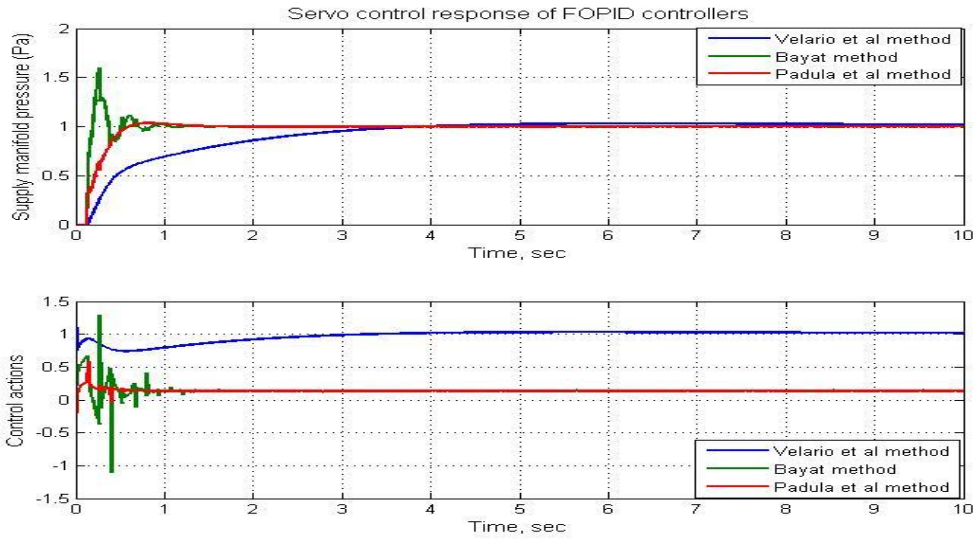

Figure 5.5 Servo control response of FOPID controllers for controlling the supply manifold pressure.

The regulatory response is evaluated for a unit step disturbance in the closed loop and corresponding controller actions are shown in the Figure 5.6. Time and performance indices are calculated for comparison of the methods and results are shown in Table 5.7. From the Figure 5.5 and Table 5.7, FOPID method reported by Valerio and Costa [56] produces peak overshoot of 1.2081%, but larger settling time of 8.6961 sec, peak time of 6.35 sec and rise time of 2.357 sec. This method produces the smaller peak overshoot but having larger settling time. Because of large settling time the controller generates slower response.

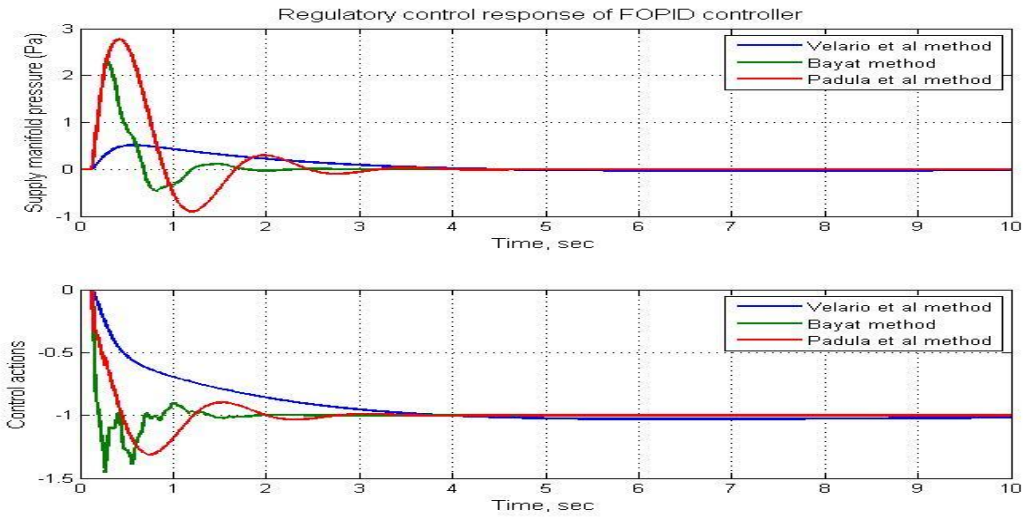

Figure 5.6 Regulatory control response of FOPID controllers.

Table 5.7 Summary of performance of FOPID controllers

Performance Parameters	**Valerio & Costa[56]method**		**Bayat[78]method**		**Padula & Visioli[79]method**	
Rise time (sec)	2.3576		0.0446		0.3211	
Peak time(sec)	6.35		0.2630		0.8200	
Settling time(sec)	3.8786		0.9783		1.1155	
Peak Overshoot (%)	1.2081		60.2080		3.559	
	Servo	**Regulatory**	**Servo**	**Regulatory**	**Servo**	**Regulatory**
ISE	0.4528	0.3030	0.1615	1.0479	0.1930	3.2336
IAE	1.05	1.028	0.2330	0.8391	0.2802	1.9676
ITAE	1.8590	2.258	0.0486	0.4513	0.0607	1.6641
TV	1.4176	1.0435	14.728	3.2258	3.8219	2.1336

When the process gain value is other than 1, it does not produce satisfactory response. FOPID controller tuning method reported by Bayat [78] gives the peak overshoot of 60.20%, settling time of 0.9783 sec, peak time of 0.2631 sec. The closed loop response gives higher peak overshoot and higher controller effort in terms of Total Variation (TV) for servo control and regulatory control problems. Bayat [78] FOPID tuning method gives lower values of time and

performance indices when compared with Padula &Visioli [79] tuning method. Because of higher peak overshoot and TV values, Bayat [78] tuning method is not a choice for tuning FOPID controllers. FOPID tuning method reported by Padula & Visioli [79], generates peak overshoot of 3.559%, settling time of 1.11 sec, peak time of 0.82 sec for servo control response and smaller values of performance indices. From Figures 5.5-5.6 and Table 5.7, the Padula & Visioli [79] FOPID tuning method produces least peak overshoot and produces lower value of controller effort in terms of total variation when compared to Bayat [78] method. Because of less peak overshoot, Padula & Visioli [79] FOPID tuning method is the highly suitable for servo control problems.

5.3.2.1 Comparison of time scales of different controllers with time scale of open loop response

Time constant for open loop model response = 0.5275 sec

Table 5.8 Time constant values of controllers

S.No	Type of controller	Time constant of the response in sec
1	Chen et al. FO-PI	0.297
2	Bhambhani et al. FO-PI	0.468
3	Gude et al.FO-PI	0.733
4	Valerio and Coast FOPID	0.733
5	Bayat FO-PID	0.135
6	Padula et al. FOPID	0.228

Table 5.8 shows the time constant values of different controllers used in this chapter. When compare the time scales of different controller responses, the time constant of Gude et al. FO-PI and Valerio and Coast FOPID controller responses from Table 5.8 are higher than the time constant of the open loop response of the PEM fuel cell system.

5.3.3 Testing of FOPID controller for the original model

In sections 5.1 and 5.2 performed the comparative analysis of various FOPI/FOPID controller applied for an approximated FOPTD model of PEM fuel cell dynamic model. In this analysis an approximated FOPTD model has considered in order to simplify the control design. But the effectiveness of the controller has to be tested on original 4^{th} order nonlinear PEM fuel cell

model in action. Figure 5.7 shows the set point control response of Padula & Visioli FOPID controller tuning method and its corresponding control actions.

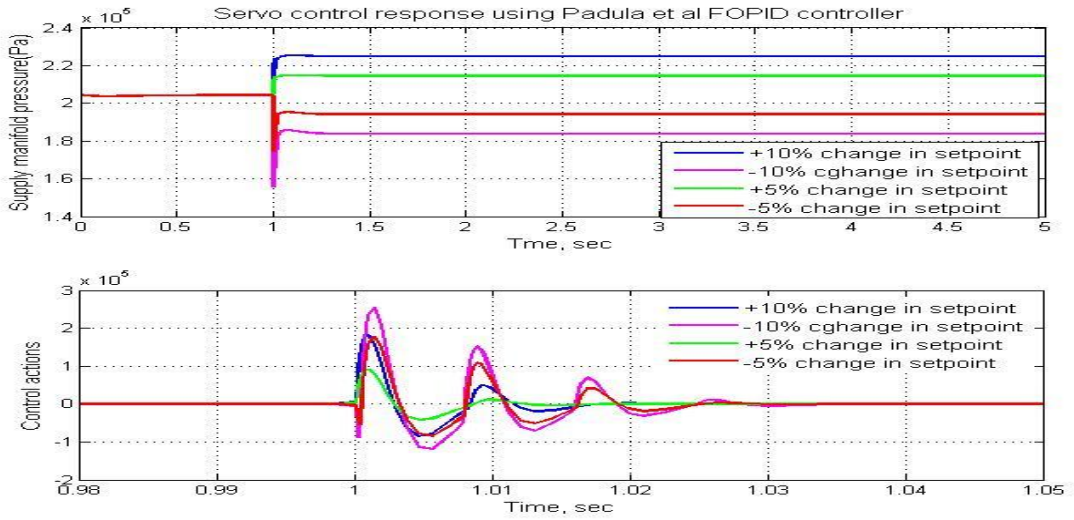

Figure 5.7 Servo control response of Padula & Visioli FOPID controller tuning method applied for original model.

The set point was changed at ±5% and ±10% of supply manifold pressure. The nominal value of supply manifold pressure (P_{sm}) is 204396 Pa. It can be noted that from Figure 5.7 Padula & Visioli FOPID controller produces better servo control response for various set point changes.

5.3.4 Robust control analysis

A controller said to be having the robustness when it is counteract against any modeling parametric uncertainty. To check the guaranteed robustness of the controller, modeling parametric uncertainty is included into the model. Table 5.9 shows the system parameters and amount of variation included in the model to study the robustness of the FOPID controller.

Table 5.9 System parameters and its variation

Parameter	Variation
Fuel cell stack temperature (T_{fc})	+10% change in ^{o}C
Supply manifold volume (V_{sm})	-10%
Cathode volume (V_{ca})	+5%
Atmospheric temperature (T_{atm})	+10% change in ^{o}C

In order to simulate the fuel cell, stack current (I_{stack}) varying between 100 and 350A has to be applied as disturbance load input. Figure 5.8 shows the variation of stack current as disturbance load input.

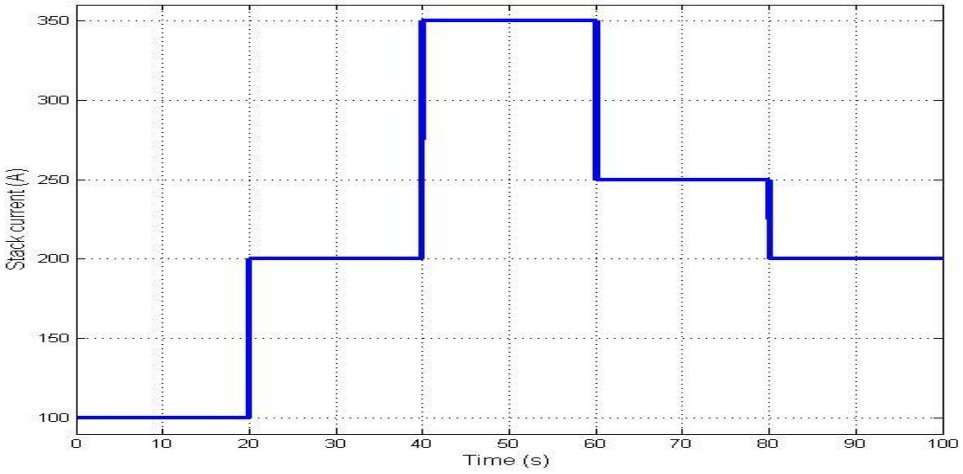

Figure 5.8 Stack current (I_{stack}) variation applied as load disturbance.

Padula & Visioli [79] FOPID tuned controller is connected in series with non linear PEM fuel cell model as closed loop control and variation stack current is applied as load disturbance. To analysis the control of supply manifold pressure (P_{sa}), x_4 state output of the fuel cell model is connected as feedback input and selected the value of reference input as 210000Pa. Figure 5.9 shows the servo control response of the supply manifold pressure (Psm) for different variations of stack current as load disturbance input. From Figure 5.9 at time t = 20 sec stack current increases from 100 to 200 A, it leads to decrease in supply manifold pressure and reaches its setpoint by the applied controller similarly at t = 60 sec stack current decreases from 350 to 250 A and due to that there is an excess of supply manifold pressure and it will be effectively controlled by the proposed controller.

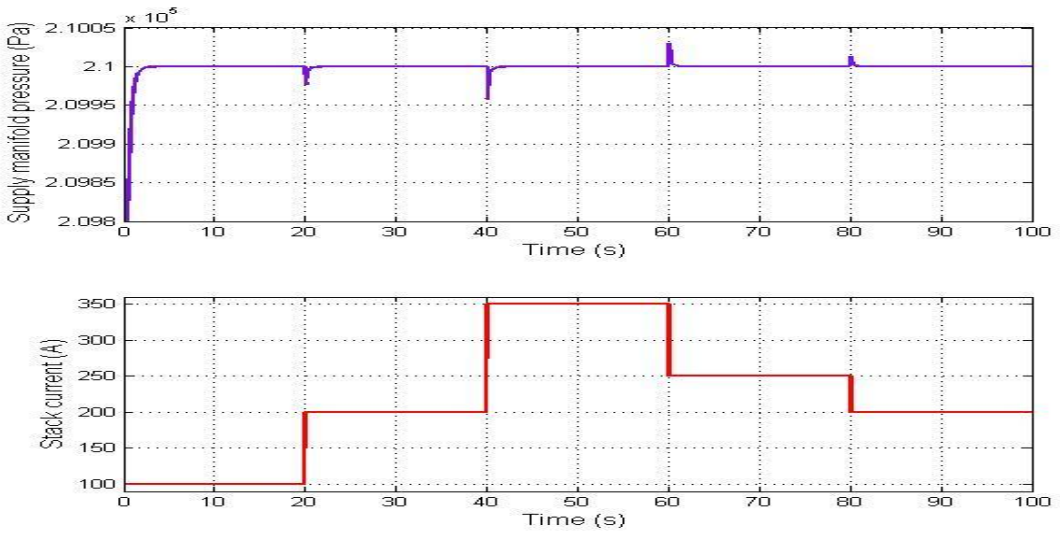

Figure 5.9 Supply manifold pressure (P_{sm}) control using Padula & Visioli FOPID tuning method.

The supply manifold pressure which is controlled by the closed loop to track the reference input. The resulted output is compared with reference input of 210000 Pa. It is depicted that the controller responds within 1-2 sec without overshoot. Figure 5.10 shows the magnified plot of Figure 5.9 at t = 40 s. At this instant of time, stack current increased from 200A to 350A causes drop in the supply manifold pressure. As shown in Figure 5.9, supply manifold pressure overshoots at t = 60 s because of stack current decreases from 350A to 250A.

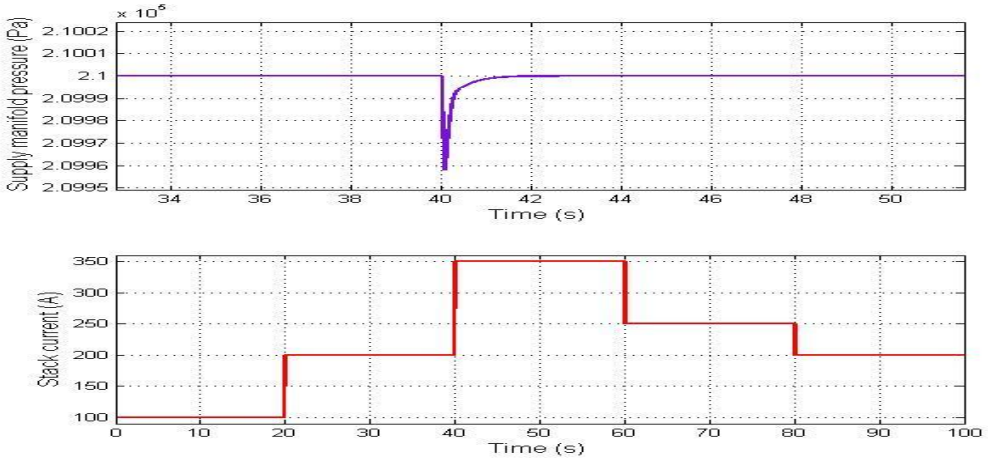

Figure 5.10 Magnified plot of Figure 5.9 representing the controlled output at time t=40 s.

Figure 5.11 shows the variation of the Padula & Visioli FOPID tuned controller output to track the supply manifold pressure with reference input under the load disturbance variations.

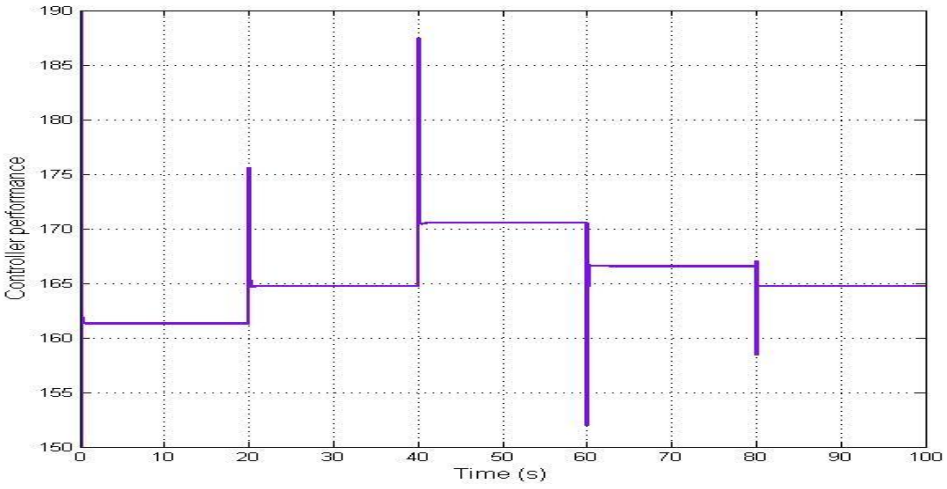

Figure 5.11 Padula & Visioli FOPID tuned controller output variation.

Controller output is manipulated variable and here it is the air-supply compressor motor voltage. Motor voltage varies in between 160V and 190V. When motor voltage changes it results in change of air-supply compressor speed, it corresponds to variation in air-supply compressor air flow rate. There is direct proportion between air-supply compressor air flow rate and air-supply compressor speed. All these variations are depicted in Figure 5.12.

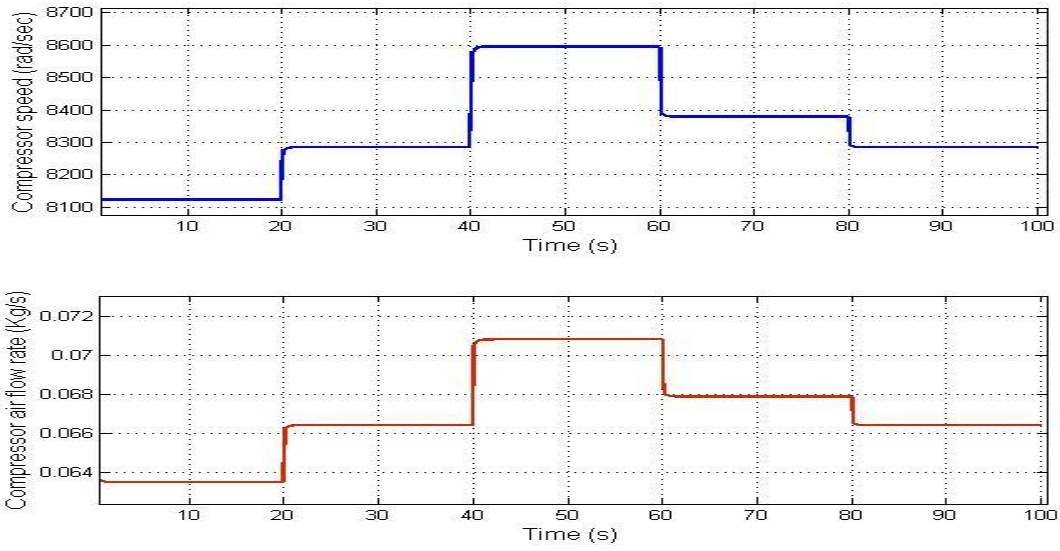

Figure 5.12 Variation of air-supply compressor angular speed and corresponding air flow rate

In order to validate the robust performance of the designed controller, some parameters of PEM fuel cell were changed under the given limits as shown in Table 5.9. Figure 5.13 shows the

response of supply manifold pressure under load disturbance variations and model parametric uncertainties.

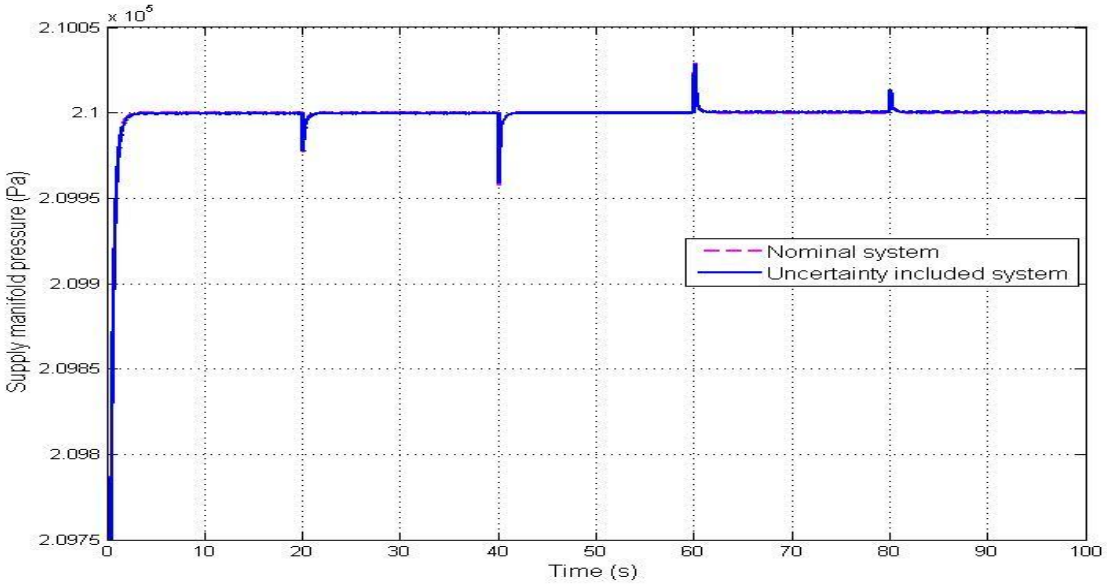

Figure 5.13 Comparison of supply manifold pressure under uncertainty variations and supply manifold pressure with the nominal system under the same FOPID controller settings.

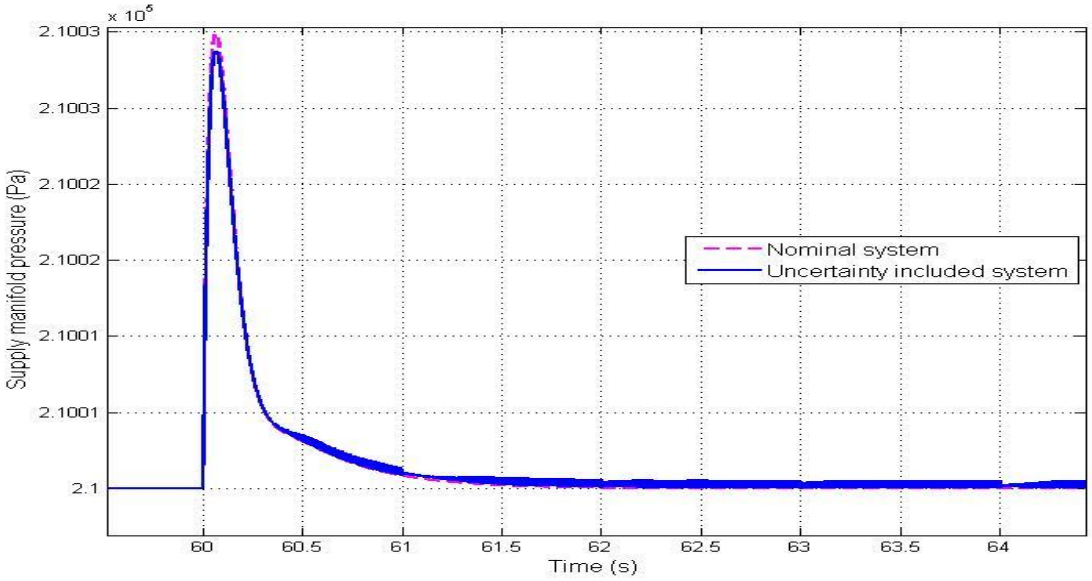

Figure 5.14 Magnified plot of Figure 5.13 at time t = 60 s representing the behavior of the supply manifold pressure

The performance of the uncertainties included PEM fuel cell system under load variations is compared with the nominal PEM fuel cell system under the same controller settings. Figure 5.14 shows the magnified plot of supply manifold pressure response at time t = 60 s. It can depict from Figure 5.14 that supply manifold pressure meets its set point value below 2 sec. Figure 5.15 shows the variation of the controller output for comparison between the uncertainties included system and the nominal system under the same controller settings.

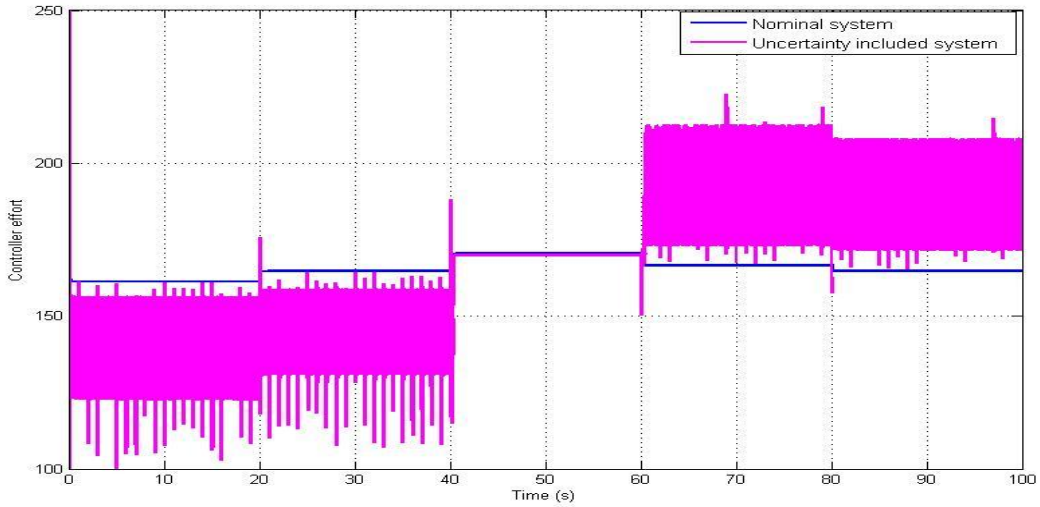

Figure 5.15 Comparison of controller performance between uncertainties included system and nominal plant under the same FOPID controller settings.

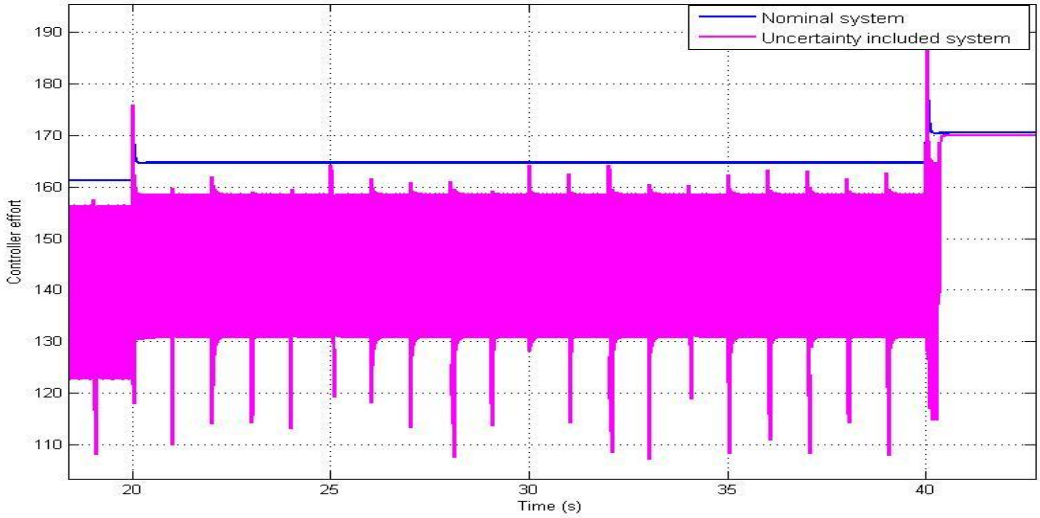

Figure 5.16 Magnified plot of Figure 5.15 representing the variation of controller output from time t =18 s to t = 42 s.

Figure 5.16 shows the magnified plot of Figure 5.15 from time t = 18 s to t = 41 s. For the uncertainties included system the controller output changes rapidly in order to compensate the parametric uncertainties of the PEM fuel cell model. In Figure 5.16 pink color represents the controller effort for uncertainties included system and blue color represents the controller effort for the nominal system. It can be concluded from these results that the Padula & Visioli FOPID controller produces response under load disturbances and parametric uncertainty variations without any change in the controller settings.

5.4 Conclusions

In this chapter, different methods of fractional order controllers were tuned and analyzed the performance for better improvement in the servo and regulatory responses of supply manifold pressure control of PEM fuel cell. Different fractional order PI and PID controller tuning methods are implemented for the approximated FOPTD model. Servo and regulatory control response analysis was carried out. Comparative performance analysis carried out using performance indices IAE, ISE, ITAE and TV as well as time indices. Padula & Visioli tuning method produces better response from FO PID tuning methods.

The robustness of the Padula & Visioli FOPID controller was verified by applying to the original PEM fuel cell model based on four state equations. Parametric uncertainties included in the dynamic model and tested the performance of the controller for the uncertainties included system and the nominal system under load disturbance. The proposed controller performed well for the both uncertainties included system and the nominal system under load disturbance for the same controller settings. Hence the robustness and insensitivity to the disturbance of the proposed controller was proved. In this simulation study, comparative analysis of fractional order controllers was carried out and verified the robustness of the proposed controller for the control of supply manifold pressure of PEM fuel cell.

Chapter 6
Fractional order PID controller design for supply manifold pressure control of PEM fuel cell based on Maximum sensitivity

6.1 Introduction

A fuel cell is an electrochemical device, which converts the chemical form of energy into electrical form of energy by reaction between hydrogen and oxidants (air or oxygen) and generates water and heat as byproduct of the reaction. A Proton Exchange Membrane (also called as Polymer Electrolyte Membrane, PEM) fuel cell is one of the most possible energy solution because of its compact size, high energy efficiency, easy start up, lower operating temperature (50 – 80 ^{o}C), and high reliability. If the partial pressure of oxygen on cathode side of the cell drops down to a certain crucial level, a complicated phenomenon called oxygen starvation occurs. To prevent oxygen starvation, it is necessary to maintain the supply manifold pressure (P_{sm}) at desired value and design a suitable control scheme to control it by considering air-supply compressor voltage as manipulated variable in the air feed system of PEM fuel cell.

The main advantage of fractional order PID controller over conventional PID controller is it's additional two degrees of freedom for tuning of the controller parameters that results in better improvement in the control performance & robustness of the response.

In this chapter, the proposed fractional order $PI^{\lambda}D^{\mu}$ controller method is applied to first order plus time delay (FOPTD) model which is approximated from the fourth order Suh's[65]proposed control oriented model of PEM fuel cell for the control of supply manifold pressure. The Padula and Visioli[79] proposed a method for design of fractional order PID (FOPID) controllers based on minimization of integrated absolute error, subject to a constraint on the maximum sensitivity which can be applied to first order plus time delay (FOPTD) models. A comparison has been performed with other methods such as the tuning rules proposed in [56] for fractional-order controllers and the AMIGO (approximate M-constrained integral gain optimization) tuning rules for integer order controllers in [80] (both Ms = 1.4 and Ms = 2.0). To verify the robustness of the proposed controller, uncertainty and measurement noise analysis have been implemented.

6.2 Fractional-order $PI^{\lambda}D^{\mu}$ Controller design

The most common form of a fractional order $PI^{\lambda}D^{\mu}$ controller [28], having an integrator order of λ and a derivative order of μ where λ and μ are any real numbers. The fractional order $PI^{\lambda}D^{\mu}$ controller transfer function is given in Equation 6.1.

$$C(s) = k_p + k_i \frac{1}{s^{\lambda}} + k_d s^{\mu}, \qquad (0 < \lambda, \mu < 2) \tag{6.1}$$

Where k_p, k_i, k_d are the proportional gain, the integral gain and the derivative gain respectively, and λ, μ are the integral order and derivative order respectively. By selecting λ =1 and μ=1 from Equation 6.1, integer order PID (IOPID) controller can be formed. Similarly by selecting λ =1, μ=0 conventional PI controller and λ =0, μ=1 conventional PD controller can be developed. When compared with Integer Order PID controller (IOPID), Fractional Order PID (FOPID) controller has two more tuning parameters; it enhances the flexibility of tuning parameters to achieve better system performance.

6.2.1 Design method

The feedback control structure shown in Figure 6.1which is considered for analyzing the dynamics of FOPTD model given in Equation 6.2 as a plant.

$$\mathrm{P(s)} = \frac{P_{sm}(s)}{V_{comp}(s)} = \frac{7.3913\,\mathrm{e}^{-0.1314\,\mathrm{s}}}{0.3832\,\mathrm{s}+1} \tag{6.2}$$

The dynamics of the process is described by normalized dead time τ and defined as $\tau = \frac{\mathrm{L}}{\mathrm{L+T}}$, where L is time delay and T is time constant of process or plant. The normalized dead time gives a measure of difficulty in controlling the process. In general, the values of the normalized dead time in the range of $0.05 \leq \tau \leq 0.8$ have been considered. The value of τ for the above said process model is 0.2553.

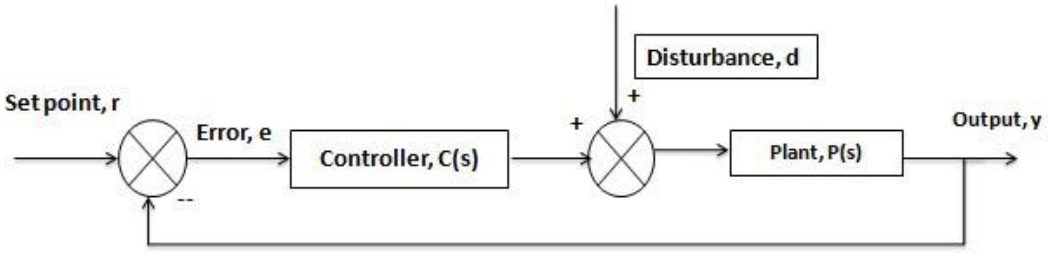

Figure 6.1 The considered control structure

The structure of the standard PID controller in series and the fractional order PID controller are considered from [79] for the design of controllers as shown in Equations 6.3 and 6.4 respectively.

$$C(s) = K_p \frac{(T_i s+1)}{T_i s} \frac{(T_d s+1)}{\left(\frac{T_d}{N} s+1\right)} \quad 6.3$$

$$C(s) = K_p \frac{(T_i s^{\lambda}+1)}{T_i s^{\lambda}} \frac{(T_d s^{\mu}+1)}{\left(\frac{T_d}{N} s+1\right)} \quad 6.4$$

WhereK_p is proportional gain, T_i and T_d are integral and derivative time constants respectively.λ and μ are fractional orders of integral and derivative time constants respectively and the value of N is typically 10. If $\lambda=\mu=1$, a standard PID controller can be obtained. It can be noted that first order filter have been applied in Equation 6.4 to make the controller proper. The main control requirement is to minimize the integrated absolute error (IAE)

$$IAE = \int_0^{\infty} |e(t)| dt = \int_0^{\infty} |r(t) - y(t)| dt \quad 6.5$$

Minimization of IAE results in reduction of overshoot and lower settling time at the same time in load disturbance or set point control responses. A controller said to be having robustness when it is not sensitive to any parameter variations or uncertainties. To improve the robustness of the supply manifold pressure controller, the controller has been designed by minimizing the IAE and maximum sensitivity as a constraint. The maximum sensitivity $M_s$is represented [79] as

$$M_s = \max_{\omega \in [0,\infty]} \left| \frac{1}{1+C(j\omega)P(j\omega)} \right| \quad 6.6$$

Where $C(j\omega)$ controller transfer function and $P(j\omega)$ plant transfer function. Maximum sensitivity represents the inverse of the shortest distance from the Nyquist curve of the loop transfer function to the critical point (-1, $j0$). Typical values of M_s are in the range of 1.2 to 2.0. If the value of M_s is lower, the system is more robust to the modeling or parameter uncertainties.

6.2.2 Tuning of optimal controller

In order to find the tuning rules of controller for the control of supply manifold pressure using an approach in Padula and Visioli[79] has been considered. The set point control and disturbance rejection tasks have been performed separately to minimize the IAE with two values of maximum sensitivity such as Ms=1.4 and Ms=2.0.For Ms=1.4, system having more robustness and for Ms=2, the aggressiveness is more important. The following structure was considered to obtain the values of the controller parameters of the IOPID and FOPID controllers.

$$K_p = \frac{1}{K}(a\tau^b + c) \quad 6.7$$

$$T_i = T^\lambda \left(a\left(\frac{L}{T}\right)^b + c\right) \quad 6.8$$

$$T_d = T^\mu \left(a\left(\frac{L}{T}\right)^b + c\right) \quad 6.9$$

The constant values of a, b and c for set point tracking and load disturbance rejection is obtained from [79].

6.2.3 Robustness analysis

The closed loop stability of system should be verified in the presence of model uncertainties for robustness of the designed controller which is derived under nominal process conditions. The designed FOPID controllers should be able to provide better closed loop performance (good servo response and regulatory response) irrespective of the perturbations in process parameters which are common in practice. Perturbed model was obtained from the normal FOPTD model by changing gain and time delay by +10%. The designed controllers were applied to the parameter uncertainty model and analyzed the robustness of the controllers. The robustness of the closed loop system can be determined by considering following two specifications.

1) Disturbance rejection at low frequency range.
2) Measurement noise rejection at high frequency range.

Let S denotes the transfer function is a ratio of the output y to the disturbance input d in the closed loop system shown in Figure 6.1 and it is termed as sensitivity function. It is given by

$$S(s) = \frac{1}{1+C(s)P(s)} \quad 6.10$$

if the magnitude of loop gain is large at low frequency range then the sensitivity S will be small, it means that the effect of the disturbance on the output was attenuated.

Let T denotes the transfer function is a ratio of the output y to measurement noise, n in the closed loop system shown in Figure 6.2 and it is termed as complementary sensitivity function.

$$T(s) = \frac{C(s)P(s)}{1+C(s)P(s)} \quad 6.11$$

if the magnitude of loop gain is small at high frequency range then the complementary sensitivity T will be small, so the effect of the noise on the output was attenuated.

From sensitivity and complementary sensitivity functions,

$$S(s) + T(s) = 1 \quad 6.12$$

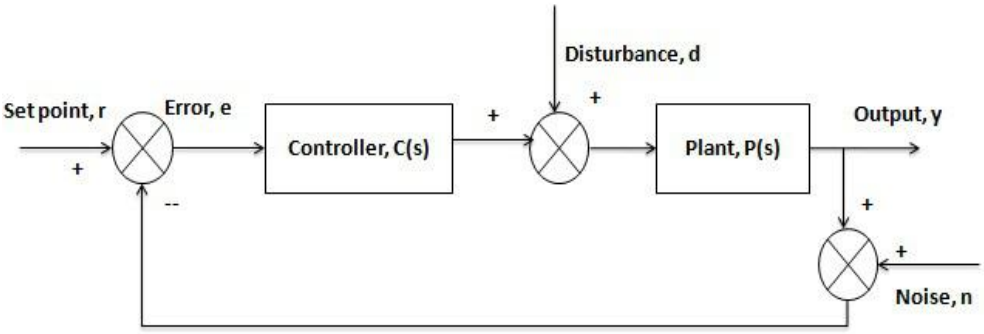

Figure 6.2 Simulation structure for measurement noise analysis.

In addition to above conditions for robust stability of the closed loop system, the following inequality constraint must be hold good to get robust closed loop performance.

$$\|l_m(s)T(s) + w_m(s)S(s)\| < 1 \qquad 6.13$$

Where $l_m(s)$ and $w_m(s)$ are bounds on multiplicative uncertainty for complementary sensitivity and sensitivity functions respectively.

6.2.4 Measurement noise analysis

Measurement noise analysis was performed to check the quality of closed loop response by introducing a white noise in the output. The considered simulation structure for measurement noise analysis is shown in Figure 6.2. The control performance of measurement noise analysis is performed by considering the performance metrics such as ISE, IAE, ITAE and Total Variation.In simulation, the designed FOPID controller is approximated using Oustaloup method. The frequency range considered for approximation is 0.001-1000 rad/sec with approximation order of 5. It is to be noted that the tuning rule applied is described as SP or LD which means that setpoint tracking or load disturbance rejection task respectively and followed by target maximum sensitivity.

6.3 Simulation results and discussion

The tuning rules proposed by Padula and Visioli[79] have been applied to the approximated FOPTD model to find the control dynamics of PEM fuel cell supply manifold pressure.The considered FOPTD model is

$$G(s) = \frac{P_{sm}(s)}{V_{comp}(s)} = \frac{1}{0.3832\,s+1} e^{-0.1314\,s},\ \tau = 0.2553 \qquad 6.14$$

The tuning rules for integer order PID (IOPID) and fractional order PID (FOPID) controllers with target values of maximum sensitivity Ms=1.4 and Ms=2 in both set point tracking and load disturbance rejection tasks have been applied to the FOPTD model given in Equation 6.14.Similarly AMIGO 1.4, AMIGO 2.0 PID [80] controllers based on maximum sensitivity (Ms) and also ZN based FOPID [56] controllers have been applied to the FOPTD model. The simulated control performance of FOPID controller is analyzed and compared with control performance of IOPID, AMIGO 1.4, AMIGO 2.0 PID and ZN based FOPID controllers. The closed loop analysis was performed by applying set-point unit step change in input and disturbance rejection task was performed by applying unit step change in disturbance signal between controller and the FOPTD model. Time domain characteristics and Integral Absolute Error (IAE) of FOPID controller was compared with IOPID AMIGO 1.4, AMIGO 2.0 PID and ZN based FOPID controller.

6.3.1 Performance assessment with Ms=1.4

Figure 6.3(a) shows the set point and load disturbance responses of FOPTD model of Equation 6.14 for FOPID, IOPID, AMIGO 1.4 PID and ZN FOPID controllers and shows their corresponding controller output responses.

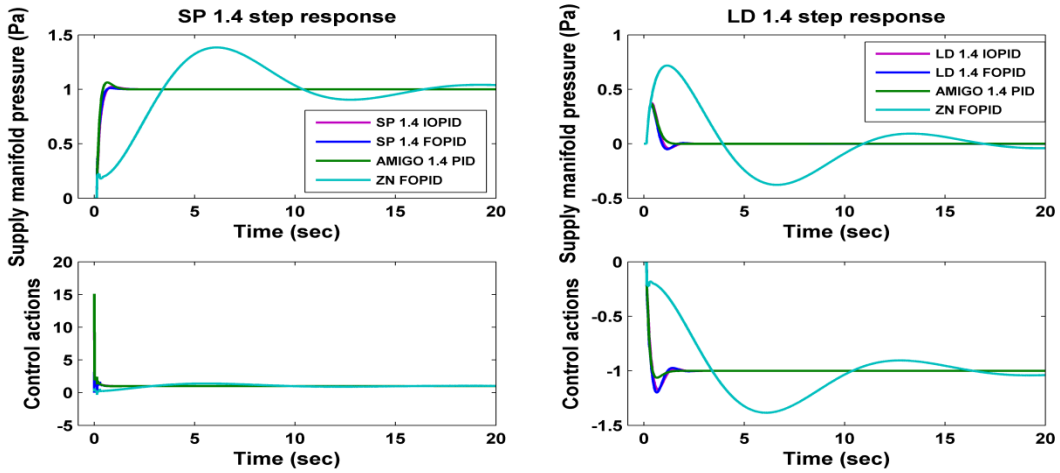

Figure 6.3(a) Closed loop response for supply manifold pressure control process with Ms 1.4 with set-point and load disturbance rejection control

Figure 6.3(b) shows the magnified plot of Figure 6.3(a) which clearly describes the response of the controllers. Left side of Figure 6.3(b) shows set point responses of SP 1.4 IOPID, SP 1.4

FOPID, AMIGO 1.4 and ZN FOPID controllers and right side of the Figure 6.3(b) shows load disturbance responses of LD 1.4 IOPID, LD 1.4 FOPID, AMIGO 1.4 and ZN FOPID controllers for closed loop system for Ms 1.4 control.

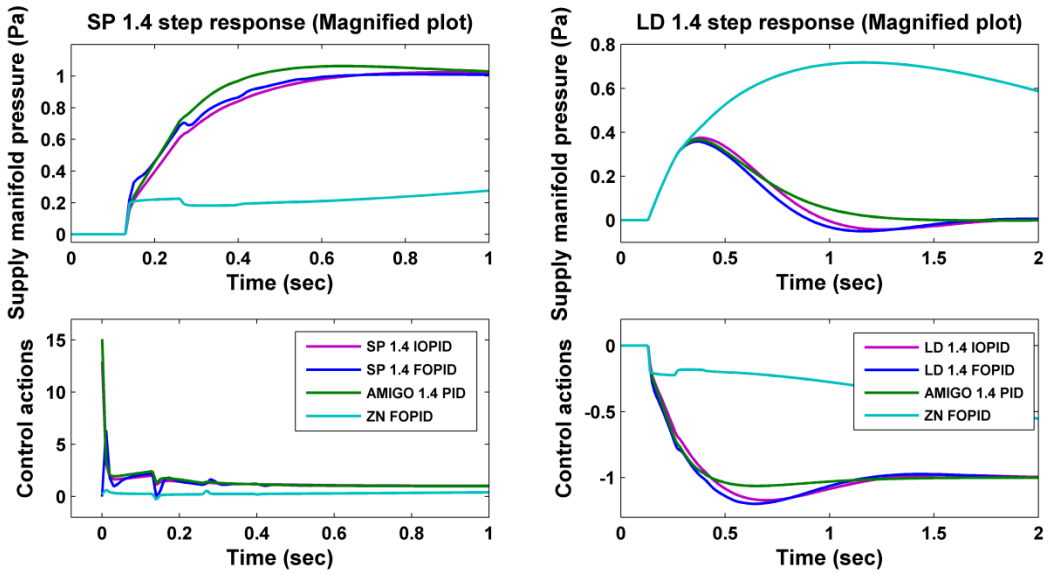

Figure 6.3(b) Magnified plot for the Figure 6.3(a) clearly shows the response for Ms 1.4 control.

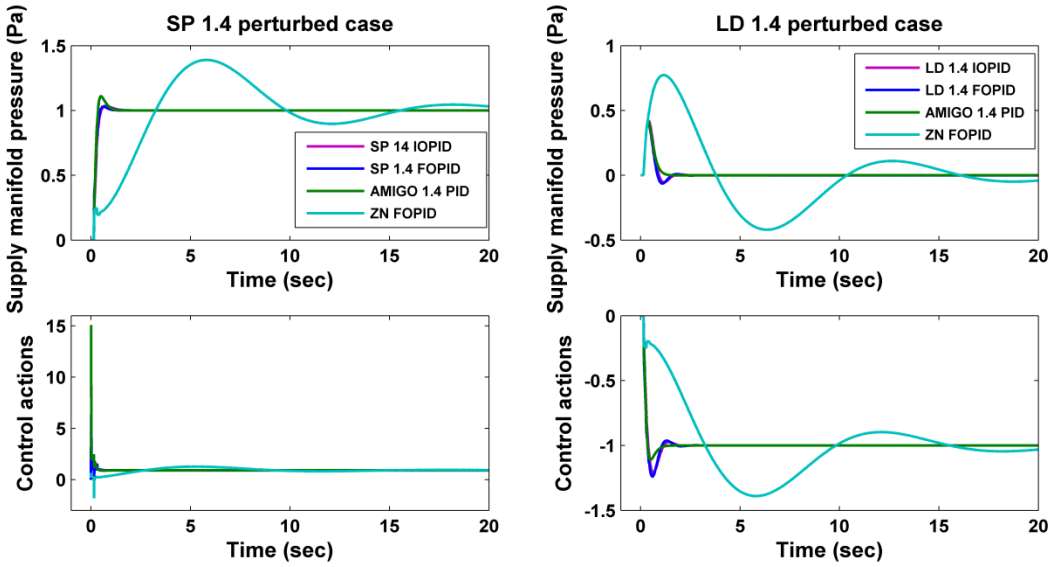

Figure 6.4(a) Closed loop responses for perturbed process with Ms 1.4 setpoint (SP) and load disturbance (LD) rejection control.

Figure 6.4(a) shows responses of perturbed system (with +10% variation in process gain and time delay of FOPTD model) to changes in setpoint and load disturbances. Figure 6.4(b)

shows magnified plot of Figure 6.4(a) which clearly shows the responses of controllers for perturbed system. Left side of Figure 6.4(b) shows set point responses of SP 1.4 IOPID, SP 1.4 FOPID, AMIGO 1.4 and ZN FOPIDcontrollers. Right side of the Figure 6.4(b) shows load disturbance responses of LD 1.4 IOPID, LD 1.4 FOPID, AMIGO 1.4 and ZN FOPID controllers for perturbed system.

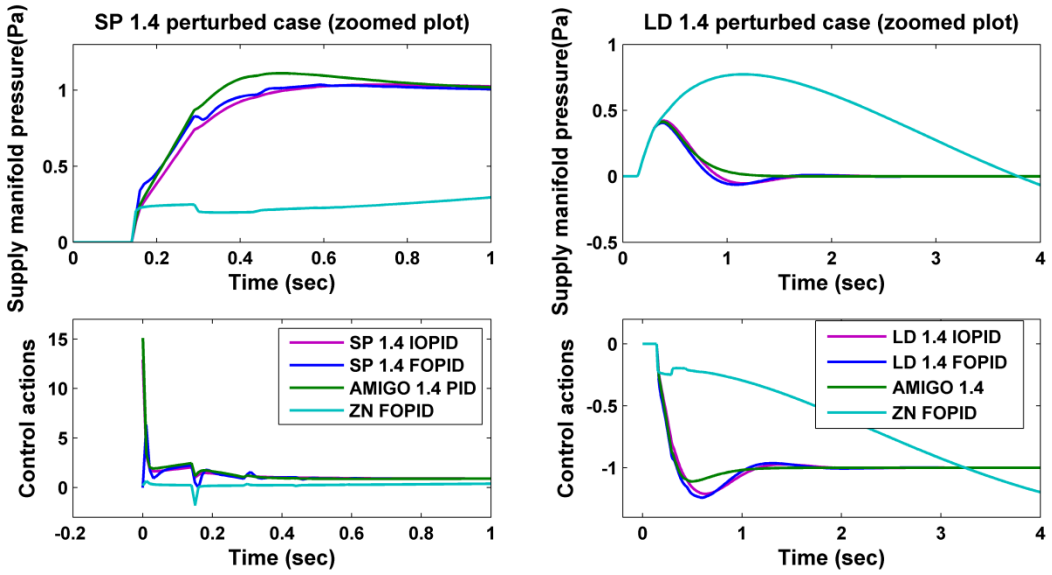

Figure 6.4(b) Magnified plot for the Figure 6.4(a) clearly shows the perturbed response for Ms 1.4 control.

Table 6.1 gives the designed optimal parameter values of integer order PID (IOPID), fractional order PID (FOPID),AMIGO PID and ZN FOPID controllers for set-point and load disturbance rejection tasks with maximum sensitivity Ms = 1.4. It also presents the obtained Integrated Absolute Error (IAE) as well as obtained maximum sensitivity (Ms) values for perfect and perturbed cases. Table 6.2 gives the time domain characteristic values for SP 1.4 IOPID, SP 1.4 FOPID, AMIGO 1.4 and ZN FOPID controllers for a unit step change in input applied to perfect and perturbed cases. From Figure 6.3(b) and Table 6.2, it can be observed that the SP 1.4 FOPID controller provides better closed loop response with faster settling time and considerably lower peak overshoot than the other three methods such as SP 1.4 IOPID, AMIGO 1.4 PID and ZN FOPID controllers. The SP 1.4 IOPID controller also provides good closed loop response nearly same as the SP 1.4 FOPID controller but have the higher values of settling time and peak overshoot. The AMIGO 1.4 PID controller produces good response with faster rise time but higher settling time and peak overshoot than SP 1.4 IOPID, SP 1.4 FOPID controllers. While ZN

FOPID controller method produces oscillation response with higher values of rise time, settling time and maximum peak overshoot.

Table 6.1 Comparison of tuning rules for IOPID, FOPID AMIGO controllers with desired maximum sensitivity, M_s=1.4 and ZN FOPID controllers

	Controller parameters					Perfect case					Perturbed case				
Tuning rules	**Kp**	**Ti**	**λ**	**Td**	**μ**	**IAE_{sp}**	**IAE_{ld}**	**M_s**	**TV_{sp}**	**TV_{ld}**	**IAE_{sp}**	**IAE_{ld}**	**M_s**	**TV_{sp}**	**TV_{ld}**
SP 1.4 IOPID	1.290	0.320	1	0.052	1	0.285	0.248	1.4	13.65	1.05	0.273	0.248	1.5	13.98	1.07
SP 1.4 FOPID	1.599	0.379	1	0.031	1.2	0.255	0.238	1.4	20.06	1.09	0.246	0.237	1.5	20.69	1.14
AMIGO 1.4	1.51	0.288	1	0.0474	1	0.263	19.82	1.5	16.27	1.13	0.269	19.82	1.6	16.82	1.22
ZN FOPID	0.21	0.506	1.5	0.4374	0.96	3.817	19.66	1.25	8.52	2.18	3.706	19.69	1.23	13.32	2.24
LD 1.4 IOPID	0.911	0.146	1	0.089	1	0.336	0.202	1.4	9.97	1.39	0.345	0.210	1.5	10.32	1.48
LD 1.4 FOPID	1.095	0.149	1	0.067	1.1	0.326	0.184	1.4	14.71	1.49	0.338	0.192	1.5	15.21	1.60

Table 6.2 Time domain indices comparison for IOPID, FOPID, AMIGO with desired M_s=1.4 and ZN FOPID controllers.

	Perfect case				Perturbed case			
Performance Parameters	**SP 1.4 IOPID**	**SP 1.4 FOPID**	**AMIGO 1.4**	**ZN FOPID**	**SP 1.4 IOPID**	**SP 1.4 FOPID**	**AMIGO 1.4**	**ZN FOPID**
Rise time (sec)	0.3230	0.331	0.2079	2.9378	0.2332	0.2860	0.1612	2.78
Settling time (sec)	1.1042	0.692	1.1052	21.765	1.0695	0.5482	0.9852	20.73
Peak overshoot (%)	2.3831	0.797	6.3064	38.188	3.5447	1.4935	11.06	38.76

From the responses shown in Figure 6.3(b), for the load disturbance case, the LD 1.4 FOPID controller produces the response with less peak value and reaches the final value with small

amount of time when compared with LD 1.4 IOPID, AMIGO 1.4 and ZN FOPID controllers. LD 1.4 FOPID controller effectively rejects the load disturbances when compare to LD 1.4 IOPID, AMIGO 1.4 and ZN FOPID controller. From the responses shown in the Figure 6.4(b), the SP 1.4 FOPID controller performs well compared to SP 1.4 IOPID, AMIGO 1.4 and ZN FOPID controllers for perturbed model. The effectiveness of the SP 1.4 FOPID controller for perturbed model can be evaluated from the Table 6.2 by considering the time domain performance indices. From the response of the SP 1.4 FOPID controller, it produces faster settling time and considerably small peak overshoot for +10% uncertainty model.

Similarly, from Figure 6.4(b) it can be noticed that LD 1.4 FOPID controller produces the better load disturbance rejection response over LD 1.4 IOPID, AMIGO 1.4 and ZN FOPID controllers for the perturbed model. From Table 6.1 it should be observed that the IAE values of SP 1.4 FOPID controller for set-point tracking are lower than the SP 1.4 IOPID, AMIGO 1.4 PID and ZN FOPID controllers in both the perfect and perturbed cases. The IAE values of LD 1.4 FOPID controller for load disturbance rejection task are lower than the LD 1.4 IOPID, AMIGO 1.4 PID and ZN FOPID controllers in both the perfect and perturbed cases. It also observed that the measured maximum sensitivity Ms value is exactly 1.4 for SP 1.4 FOPID, SP 1.4 IOPID, LD 1.4 FOPID and LD 1.4 IOPID controllers i.e the designed controllers have more robustness where as AMIGO 1.4 PID obtained measured maximum sensitivity Ms value of 1.5 and for ZN FOPID controller the Ms value is 1.25.

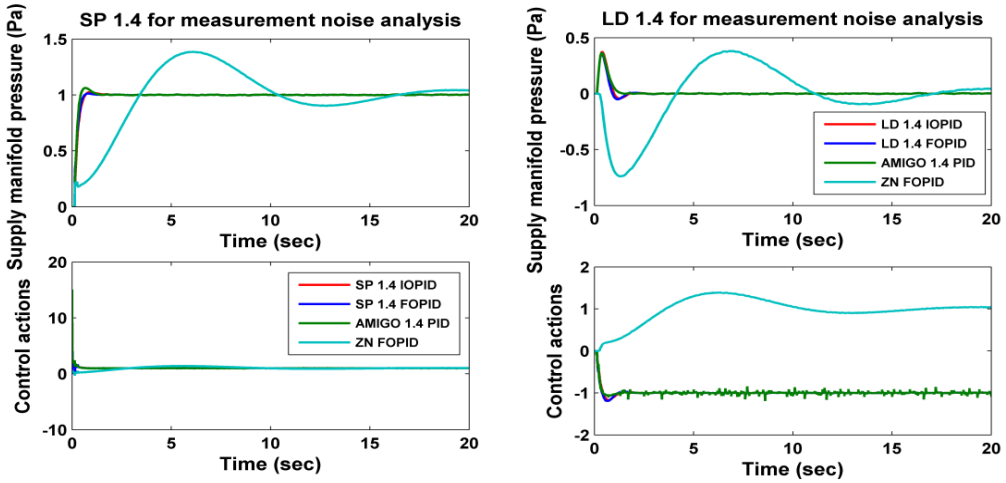

Figure 6.5(a) Closed loop response involving measurement noise with 1.4 set-point and load disturbance rejection control tasks.

From Table 6.2, the maximum peak overshoot values for SP 1.4 FOPID controller in both perfect and perturbed cases are comparatively lower than SP 1.4 IOPID, AMIGO 1.4 PID and ZN FOPID controllers. From Tables 6.1 and 6.2, it can be observed that SP 1.4 FOPID controller well performs than SP 1.4 IOPID, AMIGO 1.4 PID and ZN FOPID controllers.

The effect of measurement noise on the control response can be studied by introducing the white noise signal of power 0.00001. The closed loop responses for SP 1.4 FOPID and SP 1.4 IOPID controllers with measurement noise rejection and their corresponding controller output are illustrated in Figure 6.5(a). Figure 6.5(b) shows the magnified plot of Figure 6.5(a) which describes the set point and load disturbance responses of controllers for measurement noise analysis

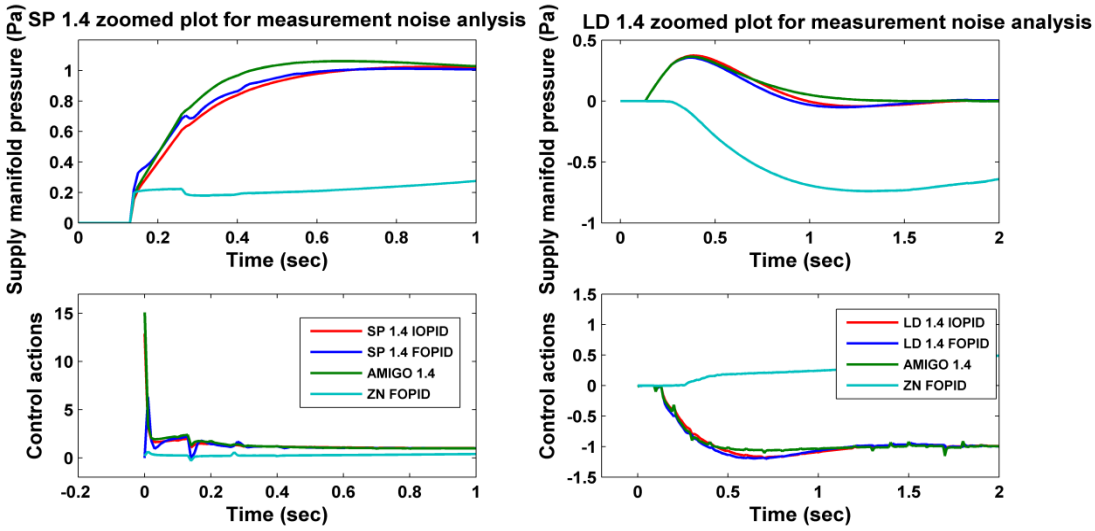

Figure 6.5(b) Magnified plot for Figure 6.5(a) with Ms 1.4 measurement noise control responses.

Left side of Figure 6.5(b) shows set point responses of SP 1.4 IOPID, SP 1.4 FOPID, AMIGO 1.4 and ZN FOPID controllers. Right side of the Figure 6.5(b) shows load disturbance responses of LD 1.4 IOPID, LD 1.4 FOPID, AMIGO 1.4 and ZN FOPID controllers for measurement noise analysis. The performance indices for measurement noise rejection control with SP 1.4 FOPID, SP 1.4 IOPID, AMIGO 1.4 PID controllers are given in Table 6.3 and improved performance can be observed for SP 1.4 FOPID controller when compared with SP 1.4 IOPID, AMIGO 1.4 and ZN FOPID controllers.

Table 6.3 Performance comparisons with measurement noise

Type of controller	Performance Index			
	ISE	IAE	ITAE	TV
SP 1.4 IOPID	0.2015	0.2895	0.0740	17.4191
SP 1.4 FOPID	0.1869	0.2600	0.0572	21.9189
AMIGO 1.4 PID	0.1871	0.2926	0.3868	37.6429
SP 2.0 IOPID	0.159	0.2013	0.0462	33.7433
SP 2.0 FOPID	0.1554	0.1949	0.0449	33.6593
AMIGO 2.0 PID	0.2072	0.3723	0.7515	79.1729
ZN FOPID	1.6392	3.9912	24.259	9.0839

Lower values of ISE, IAE, ITAE can be observed for SP 1.4 FOPID controller from Table 6.3. Similarly, SP 2.0 FOPID controller produces better performance indices values when compared to SP 2 IOPID, AMIGO 2.0 PID controllers as shown in Table 6.3.

Figure 6.6 shows the complementary sensitivity Bode magnitude plot response for SP 1.4 IOPID controller in both perfect and perturbed cases.

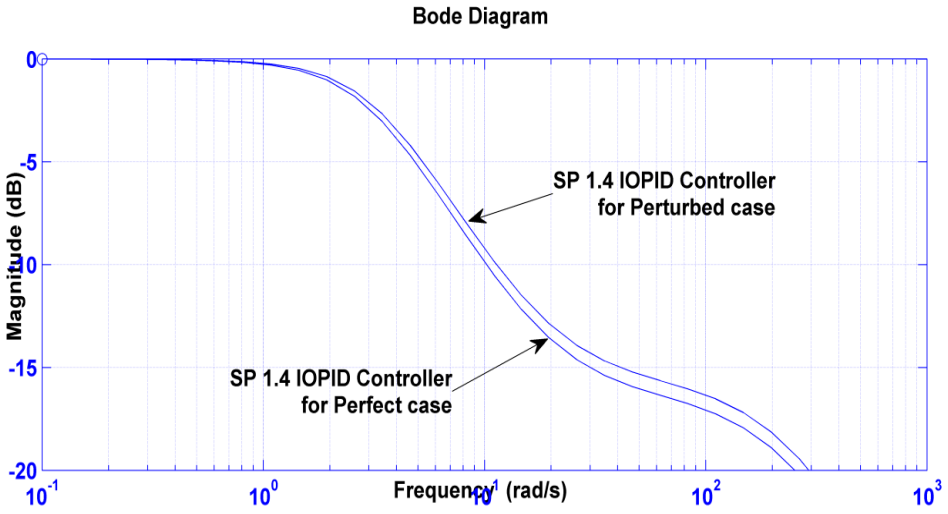

Figure 6.6 Bode magnitude plot for complementary sensitivity function: SP 1.4 IOPID controller's perfect and perturbed cases.

Figure 6.7 shows the complementary sensitivity Bode magnitude plot response for SP 1.4 FOPID controller in both perfect and perturbed cases. Figure6.8 shows the complementary sensitivity Bode magnitude plot response for AMIGO 1.4 PID controller in both perfect and perturbed cases.

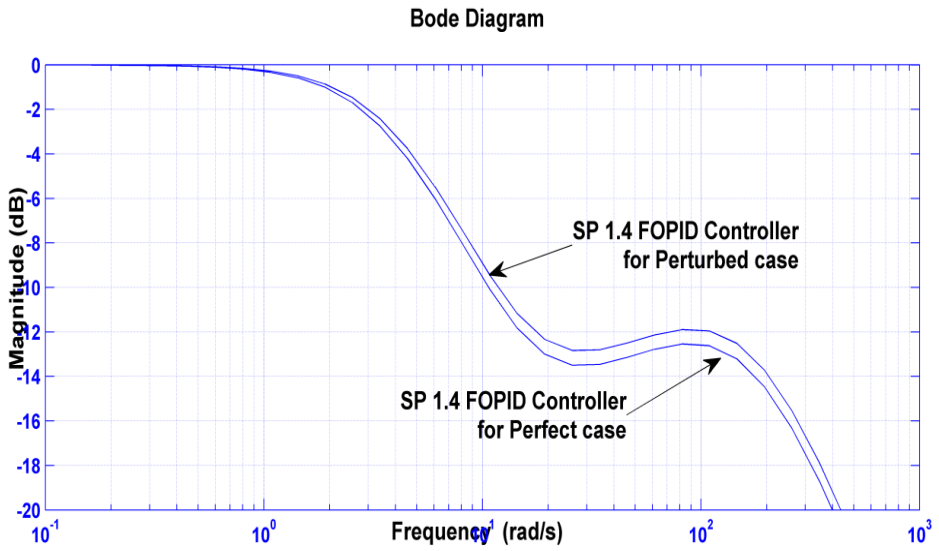

Figure 6.7 Bode magnitude plot for complementary sensitivity function: SP 1.4 FOPID controller's perfect and perturbed cases.

From Figures.6.6, 6.7 and 6.8, it is clear that the closed loop responses with SP 1.4 IOPID, SP 1.4 FOPID and AMIGO 1.4 PID are stable for parametric uncertainties.

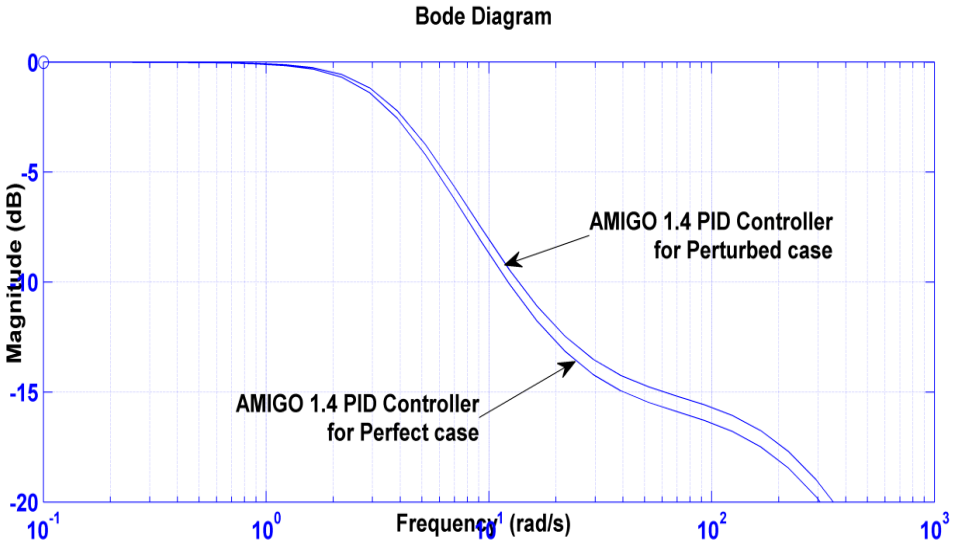

Figure 6.8 Bode magnitude plot for complementary sensitivity function: AMIGO 1.4 controller's perfect and perturbed cases.

6.3.2 Performance assessment with Ms=2

Figure 6.9(a) shows the set point and load disturbance responses of FOPTD model of Equation 6.14 for FOPID, IOPID, AMIGO 2.0 PID and ZN FOPID controllers and shows their corresponding controller output responses.

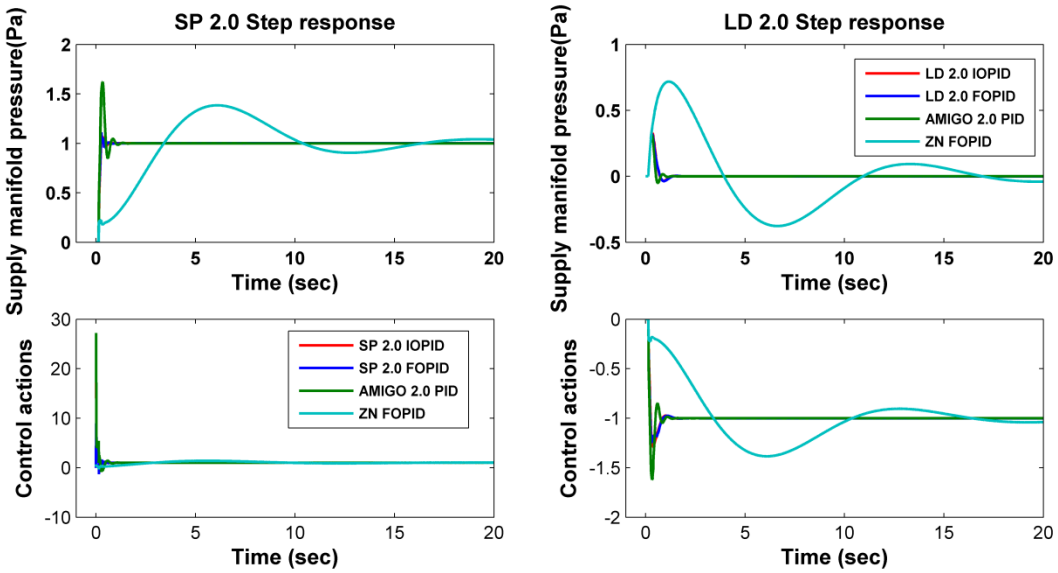

Figure 6.9(a) Closed loop response for supply manifold pressure control process with Ms 2.0 with set-point and load disturbance rejection control

Figure 6.9(b) shows the magnified plot of Figure 6.9(a) which clearly describes the response of the controllers. Left side of Figure 6.9(b) shows the setpoint step response with Ms=2.0 and right side of the Figure 6.9(b) shows the load disturbance step responses with Ms = 2.0.

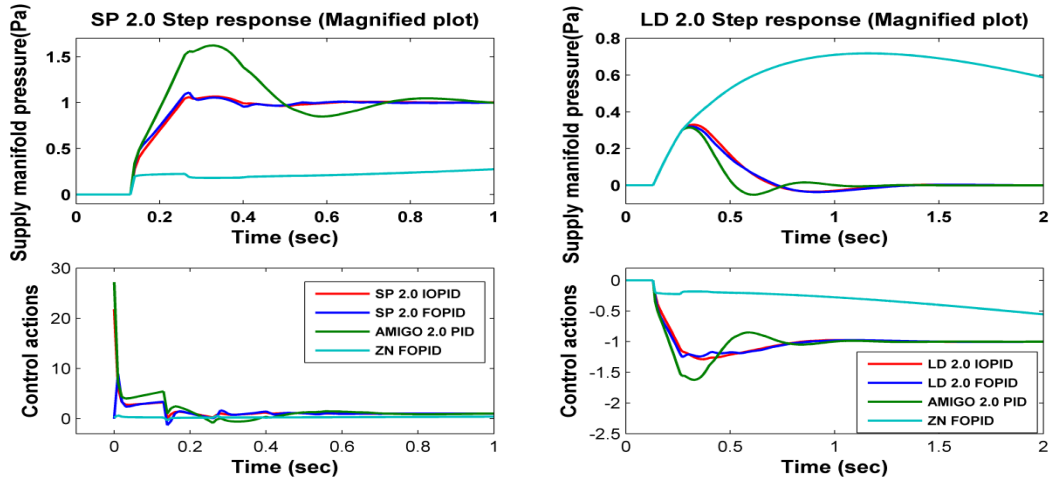

Figure 6.9(b) Magnified plot for the Figure 6.9(a) clearly shows the response for Ms 2.0 control.

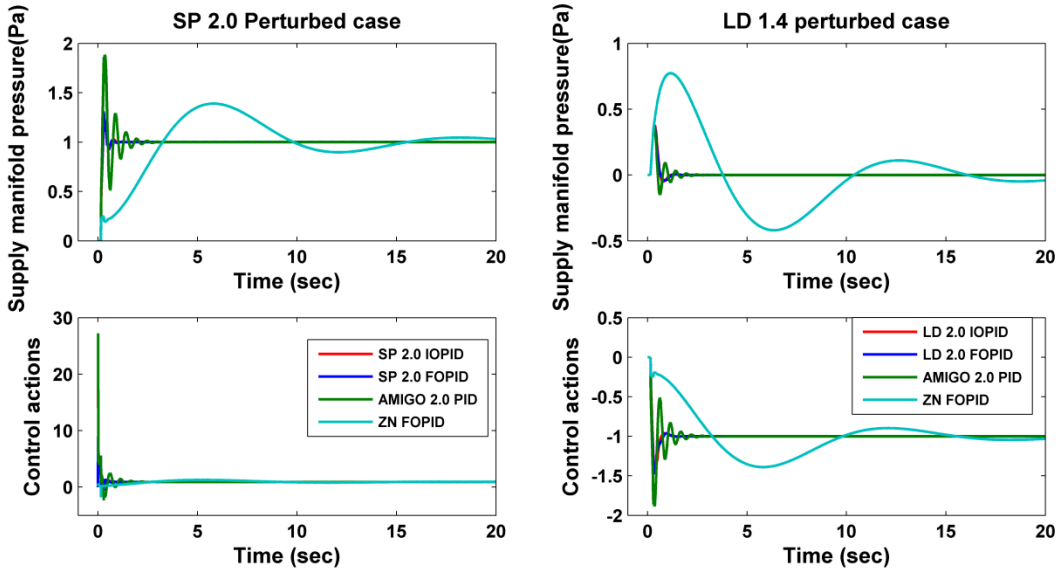

Figure 6.10(a) Closed loop response for perturbed process case with Ms 2.0 setpoint (SP) and load disturbance (LD) rejection control.

Figure 6.10(a) shows responses of perturbed system (with +10% in process gain and time delay in FOPTD model) to changes in set point and load disturbances. Figure 6.10(b) shows magnified plot of Figure 6.10(a) which clearly shows the responses of controllers for perturbed system. Left side of Figure 6.10(b) shows set point responses of SP 2.0 IOPID, SP 2.0 FOPID, AMIGO 2.0 and ZN FOPID controllers. Right side of the Figure 6.10(b) shows load disturbance responses of LD 2.0 IOPID, LD 2.0 FOPID, AMIGO 2.0 and ZN FOPID controllers for perturbed system.

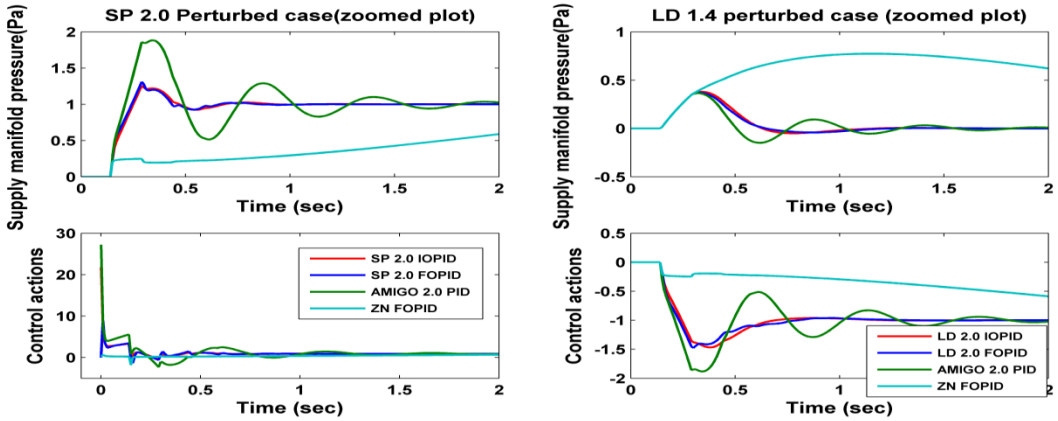

Figure 6.10(b) Magnified plot for Figure 6.10(a) with Ms 2.0 control of perturbed process case.

Table 6.4 gives the designed optimal parameter values of IOPID, FOPID, AMIGO PID with maximum sensitivity Ms=2 and ZN FOPID controllers for set-point tracking and load disturbance rejection tasks.

Table 6.4 Comparison of tuning rules for IOPID, FOPID AMIGO controllers with desired maximum sensitivity, M_s=2.0 and ZN FOPID controllers

	Controller parameters					**Perfect case**					**Perturbed case**				
Tuning rules	**Kp**	**Ti**	**λ**	**Td**	**μ**	**IAE_{sp}**	**IAE_{ld}**	**M_s**	**TV_{SP}**	**TV_{LD}**	**IAE_{sp}**	**IAE_{ld}**	**M_s**	**TV_{SP}**	**TV_{LD}**
SP 2.0 IOPID	2.18	0.37	1	0.06	1	0.194	0.169	1.9	27.11	1.26	0.233	0.169	2.3	28.64	1.74
SP 2.0 FOPID	2.40	0.40	1	0.046	1.1	0.187	0.167	1.9	31.13	1.46	0.225	0.167	2.2	33.20	1.92
AMIGO 2.0	2.72	0.179	1	0.054	1	0.308	19.94	2.9	38.66	2.69	0.529	19.94	4.9	48.22	5.17
ZN FOPID	0.21	0.506	1.5	0.4374	0.96	3.817	19.66	1.25	8.52	2.18	3.706	19.69	1.23	13.32	2.24
LD 2.0 IOPID	1.44	0.13	1	0.095	1	0.283	0.114	1.9	17.35	1.63	0.311	0.121	2.3	18.90	2.02
LD 2.0 FOPID	1.54	0.13	1	0.081	1.1	0.271	0.112	1.9	26.70	1.74	0.297	0.114	2.2	29.35	2.12

It also presents the obtained Integrated Absolute Error (IAE) as well as obtained maximum sensitivity (Ms) values for perfect and perturbed cases. Table 6.4 depicts that the IAE values of SP 2.0 FOPID controller for set-point tracking are lower than the SP 2.0 IOPID, AMIGO 2.0 and ZN FOPID controllers in both the perfect and perturbed cases. It means that the SP 2.0 FOPID controller is more effective for set-point tracking than SP 2.0 IOPID, AMIGO 2.0 and ZN FOPID controllers. Also, the IAE values of LD 2.0 FOPID controller for load disturbance rejection task are lower than the LD 2.0 IOPID, AMIGO 2.0 and ZN FOPID controllers in both the perfect and perturbed cases. It means that the LD 2.0 FOPID controller acts faster to react for load disturbances. It is also observed that the measured maximum sensitivity Ms is 1.9 for SP 2.0 IOPID, SP 2.0 FOPID, LD 2.0 FOPID and LD 2.0 IOPID controllers for perfect case, it means that the controllers have less robustness and more

aggressiveness. The AMIGO 2.0 PID controller have the measured maximum sensitivity Ms 2.9 for perfect case and 4.9 for perturbed case. It means that AMIGO 2.0 PID produces oscillations in perfect and perturbed cases, and also less robustness based on Ms values.

Table 6.5 Time domain indices comparison for IOPID, FOPID, AMIGO with desired M_s=2.0 and ZN FOPID controllers.

Performance Parameters	Perfect case				Perturbed case			
	SP 2.0 IOPID	SP 2.0 FOPID	AMIGO 2.0	ZN FOPID	SP 2.0 IOPID	SP 2.0 FOPID	AMIGO 2.0	ZN FOPID
Rise time (sec)	0.10	0.09	0.0632	2.9378	0.0894	0.0821	0.0569	2.78
Settling time (sec)	0.54	0.52	0.9388	21.765	0.8322	0.7203	2.2107	20.73
Peak overshoot (%)	6.65	11.15	62.2019	38.188	25.53	30.97	88.3147	38.76

Table 6.5 gives the time domain indices for SP 2.0 IOPID, SP 2.0 FOPID, AMIGO 2.0 PID and ZN FOPID controllers for a unit step change in input in both perfect and perturbed cases. From Figures. 6.9(b), 6.10 (b) and Table 6.5, it was observed that, the SP 2.0 FOPID controller provides better response with considerably faster rise and settling times with respect to SP 2.0 IOPID, AMIGO 2.0 PID and ZN FOPID controllers. Similarly, the maximum peak overshoot value of SP 2.0 FOPID controller is considerably smaller with respect to the other two methods such as AMIGO 2.0 PID and ZN FOPID controllers.

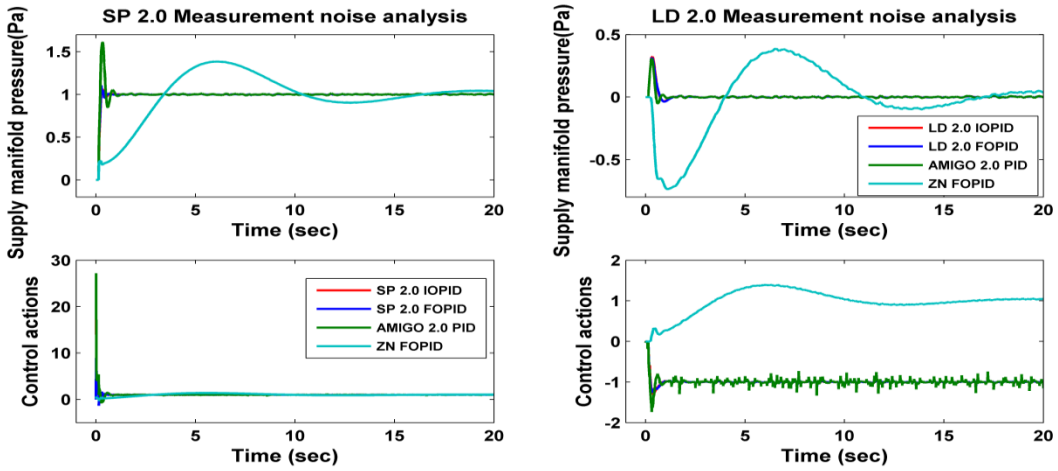

Figure 6.11(a) Closed loop response involving measurement noise with Ms 2.0 set-point and load disturbance rejection control tasks.

Figure 6.11(a) shows responses of measurement noise rejection control in set point and load disturbance with maximum sensitivity 2.0 controllers. Figure 6.11(b) shows magnified plot of Figure 6.11(a) which clearly shows the responses of controllers for measurement noise rejection control system.

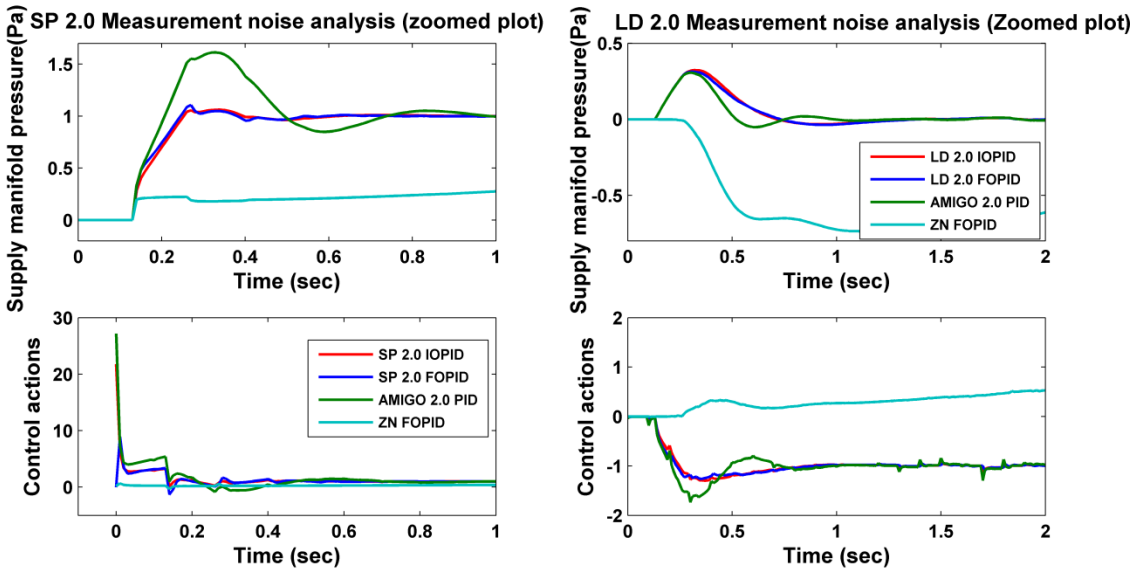

Figure 6.11(b) Magnified plot for Figure 6.11 (a) with Ms 2.0 measurement noise control.

Left side of Figure 6.11(b) shows set point responses of SP 2.0 IOPID, SP 2.0 FOPID, AMIGO 2.0 PID and ZN FOPID controllers. Right side of the Figure 6.11(b) shows load disturbance responses of LD 2.0 IOPID, LD 2.0 FOPID, AMIGO 2.0 PID and ZN FOPID controllers for measurement noise rejection control system. Table 6.6 shows the time domain indices comparison for IOPID, FOPID, AMIGO PID with desired Ms = 2.0 and ZN FOPID controllers for measurement noise rejection control analysis.

Table 6.6 Time domain indices comparison for IOPID, FOPID, AMIGO with desired Ms=2.0 and ZN FOPID controllers for measurement noise analysis.

Time domain indices	SP 2.0 IOPID	SP 2.0 FOPID	AMIGO 2.0 PID	ZN FOPID
Rise time (sec)	0.1015	0.0944	0.0632	3.0499
settling time (sec)	0.5464	0.5195	0.9419	17.1448
Peak overshoot (%)	6.1035	10.6768	61.5219	33.1117

From Figure 6.11(b) and Table 6.6, it was observed that for measurement noise rejection control analysis, the SP 2.0 FOPID controller provides better response with faster rise and settling times and considerably lower peak overshoot than the other three methods such as SP 2.0 IOPID, AMIGO 2.0 PID and ZN FOPID controllers. From Figure 6.11(b), it can be observed that both the LD 2.0 FOPID and LD 2.0 IOPID controller responses smoothly reaches the final value with less amount of oscillations for load disturbance rejection task in measurement noise control analysis with respect to AMIGO 2.0 PID and ZN FOPID controllers.

The performance indices for measurement noise rejection control with SP 2.0 IOPID, SP 2.0 FOPID, AMIGO 2.0 PID and ZN FOPID controllers are given in Table 6.3 and improved performance can be observed for SP 2.0 FOPID controller when compared with SP 2.0 IOPID, AMIGO 2.0 PID and ZN FOPID controllers. Lower values of ISE, IAE and ITAE can be observed from Table 6.3 for SP 2.0 FOPID controller.

Figure 6.12 shows the complementary sensitivity Bode magnitude plot response for SP 2.0 IOPID controller in both perfect and perturbed cases.

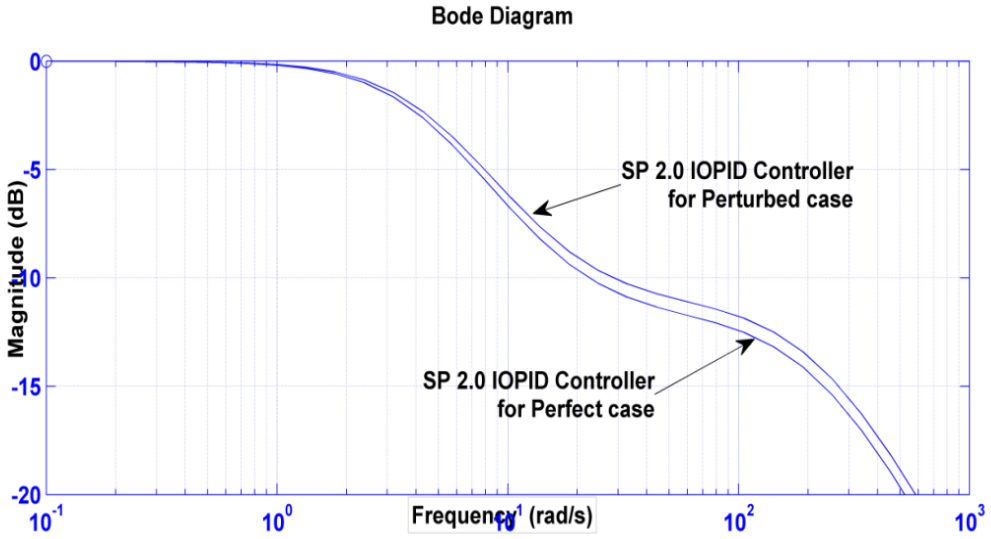

Figure 6.12 Bode magnitude plot for complementary sensitivity function: SP 2.0 IOPID controller's perfect and perturbed cases.

The magnitude plot in Figure 6.13 shows the complementary sensitivity function for SP 2.0 FOPID controller with perfect and +10% perturbations in gain and time delay cases. Figure 6.14 shows the complementary sensitivity Bode magnitude plot response for AMIGO 2.0 PID controller in both perfect and perturbed cases. From Figure 6.12 it is clear that the SP 1.4 IOPID

controlled response with +10% uncertainties in gain and time delay obeys the robust stability condition. From Figure 6.13 shows the closed loop response with SP 2.0 FOPID controller complementary sensitivity function for parametric uncertainties are stable. A better closed loop response is obtained for both SP 2.0 IOPID and SP 2.0 FOPID controllers among SP 2.0 controllers with uncertainty in gain and time delay which shows that the closed loop system gives robust stability for uncertainties.

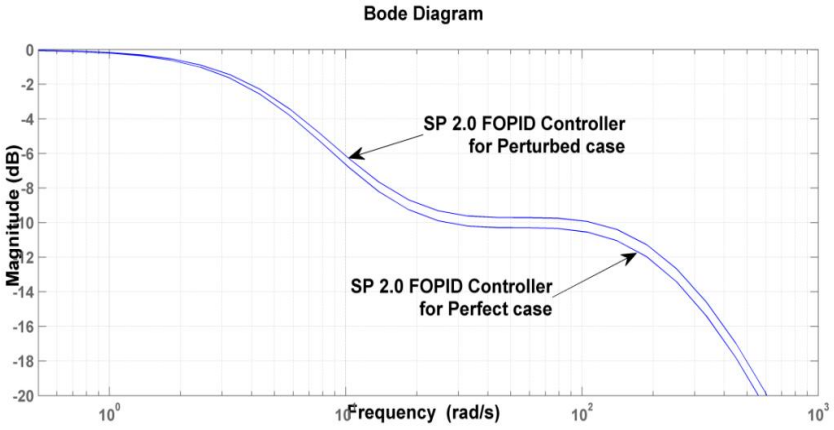

Figure 6.13 Bode magnitude plot for complementary sensitivity function: SP 2.0 FOPID controller's perfect and perturbed cases.

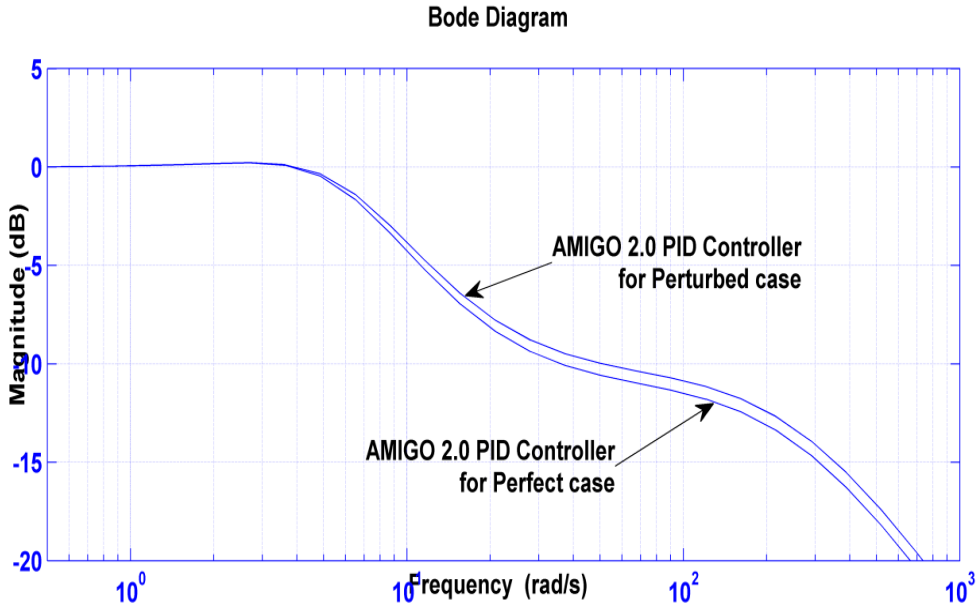

Figure 6.14 Bode magnitude plot for complementary sensitivity function: AMIGO 2.0 controller's perfect and perturbed cases.

6.3.3 Comparison of time scales of different controllers with time scale of open loop response

Time constant for open loop model response = 0.5275 sec

Table 6.7 Time constant values of controllers from this Chapter

S.No	Type of controller	Time constant of the response in sec
1	SP 1.4 IOPID	0.266
2	SP 1.4 FOPID	0.246
3	ZN based FOPID	2.233
4	AMIGO 1.4 IOPID	0.241
5	SP 2.0 IOPID	0.188
6	SP 2.0 FOPID	0.178
7	AMIGO 2.0	0.167

Table 6.7 shows the time constant values of different controllers used in this chapter. When compare the time scales of different controller responses, the time constant of different controller responses from Table 6.7 are smaller than the time constant of the open loop response of the PEM fuel cell system.

6.4 Conclusions

A fractional order $PI^{\lambda}D^{\mu}$ (FOPID) controller is designed for control supply manifold pressure of Proton Exchange Membrane (PEM) fuel cell to enhance the dynamic performance. The proposed controller is designed based on minimization of Integrated Absolute Error (IAE) and maximum sensitivity as a constraint at the same time. An approximated FOPTD model for the control of supply manifold pressure is derived from the fourth order PEM fuel cell model. The proposed tuning rules have been compared with respect to other tuning rules given in introduction section. The tuning rules of controllers discussed in this chapter are designed for application of FOPTD model. So the approximated FOPTD model was considered for design of controllers. Based on minimization of Integral Absolute Error (IAE) and desired maximum sensitivity of Ms 1.4 the performance of SP 1.4 FOPID controller is better than other related controller methods for the selected model. The SP 1.4 FOPID controller gives better results for a set point response with less overshoot and faster settling time and also better IAE value with maximum sensitivity of 1.4. Based on maximum sensitivity, the SP 1.4 FOPID controller is more robust controller. The LD 1.4 FOPID is better for load disturbance suppression. The SP 2.0

FOPID and SP 2.0 IOPID controllers produce considerable peak overshoot when comparing with SP 1.4 FOPID controller. Time domain and comparative performance analysis carried out for set point tracking and load disturbance rejection tasks using performance index IAE with Ms = 1.4 and Ms = 2. By applying the perturbation of +10% in gain and time delay also the controller still has good performance. Adding measurement noise at output of closed loop also results in better response using FOPID controller.

Chapter 7
Optimal Tuning of Fractional order PID controllers for the supply manifold Pressure control of PEM fuel cell using Genetic Algorithm

7.1 Introduction

In this chapter, a novel tuning method for FOPID controller parameters based supply manifold pressure control of PEM fuel cell using Genetic Algorithm (GA) technique is proposed. The objective function of the proposed GA is designed based on the required control characteristics of the system under study. The system is modeled using MATLAB/SIMULINK and the simulation results are obtained and compared with GA based integral absolute of the error (IAE) index, GA based integral time absolute of the error (ITAE) index, GA based integral square of error (ISE) index and proposed methods. The comparison indicates the effectiveness of the proposed tuning method as it gives a better performance and satisfies the specified control characteristics.

7.2 Genetic Algorithm tuning method

GA is an optimization search method that mimics the mechanism of natural evolution. It has been successively used to optimize many different complex problems.

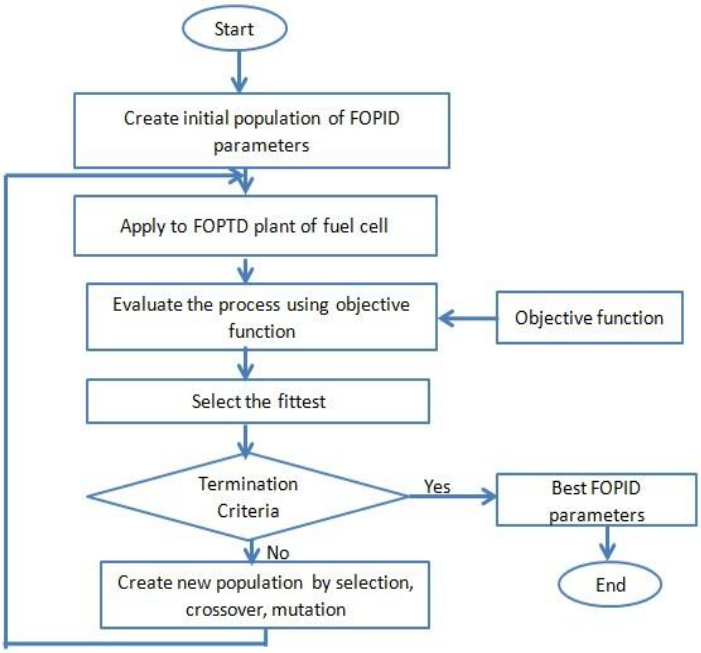

(a)

(b)

Figure 7.1 The flow chart of GA optimization for FOPID controllers: **(a)** Flow chart of GA based tuning of FOPID controller parameters. **(b)** its chromosome structure.

In this analysis, GA is used to determine the optimum values of the FOPID controller parameters that satisfy the required dynamic performance characteristics of the supply manifold pressure control system. Figure 7.1(a) shows the flowchart of GA based tuning of PID controller parameters. In the first, GA is initialized. Then, it creates an initial population of PID controller parameters. The population is generated randomly, covering the entire range of possible solutions. The population is composed of chromosomes. Each chromosome is a candidate solution to the problem. Figure 7.1(b) shows the chromosome structure, in which the five parameters (Kp, Ki,Kd, λ and μ) are included. The chromosomes are applied in the FOPTD plant of fuel cell and the dynamic performance characteristics of the plant are determined for each chromosome. Then, the fitness value for each chromosome is evaluated using the objective function. Based on the fitness values of the first generation, a group of best chromosomes is selected to create the next population. After selection, crossover and mutation are applied to this surviving population in order to improve the next generation. The process continues until the termination criterion is achieved or the number of generations is reached to its maximum value.

7.3 Proposed GA Method

The most important step in applying GA tuning method is to choose the objective function that is used to evaluate the fitness value of each chromosome. In this chapter, four objective functions are used and their performances are compared. The first is based on integral of the absolute error (IAE) index, the second is based on integral of the square error (ISE) index, the third is based on integral time absolute of the error (ITAE) index and the fourth is proposed objective function (F_{obj}) which is designed according to the required control characteristics. The four objective functions can be given as:

1) Integral Absolute Error (IAE)

$$J = \int_0^\infty |e(t)| dt \qquad 7.1$$

2) Integral Square Error (ISE)

$$J = \int_0^\infty e(t)^2 dt \quad 7.2$$

3) Integral Time Absolute Error (ITAE)

$$J = \int_0^\infty t|e(t)|dt \quad 7.3$$

4) Proposed multi-objective function

$$F_{obj} = \int_0^\infty (0.999 * |e(t)| + 0.001 * e(t)^2) * dt \quad 7.4$$

The proposed objective function for equation 7.4 is selected based on the literature. The coefficients are selected 0.999 and 0.001 as reported in literature[97].

7.4 Simulation results and discussions

Simulation using genetic algorithm for PEM fuel cell system based on different performance indices such as IAE, ISE and ITAE and weighted combination of IAE and ISE functions are carried out for servo and regulatory control responses. In simulation runs, approximated FOPTD model of PEM fuel cell to control the supply manifold pressure is used as a plant. The ranges of FOPID controller parameters are considered for the simulation and other parameters of GA optimization process are shown in Table 7.1.

Table 7.1 Settings of GA parameter values

Parameter	Value
Populations	20
Generations	50
Ranges of PID parameters	0 ~ 1000
Ranges of λ and μ	[0-2]
Crossover fraction	0.8
Mutation rate	0.01
Elite count	5

The considered FOPTD model is given in Equation 7.5

$$G(s) = \frac{P_{sm}(s)}{V_{comp}(s)} = \frac{7.3913\,e^{-0.1314\,s}}{0.3832\,s+1} \quad 7.5$$

GA optimization process based on minimization of IAE index, ISE index, ITAE index and proposed objective functions are applied for the Equation 7.5 and for each case the FOPID parameters such as K_p, K_i, K_d, λ and μ are determined. Figure 7.2 shows the servo control

response of FOPID controllers designed by Genetic algorithm based on given objective functions. Table 7.2 gives the time domain characteristics of responses for different controllers designed by Genetic algorithm with given performance indices and proposed index as objective functions.

From the servo control responses shown in Figure 7.2, it is observed that all the controllers are able to track the variation when the setpoint is changed from 0 to 1. The proposed GA based

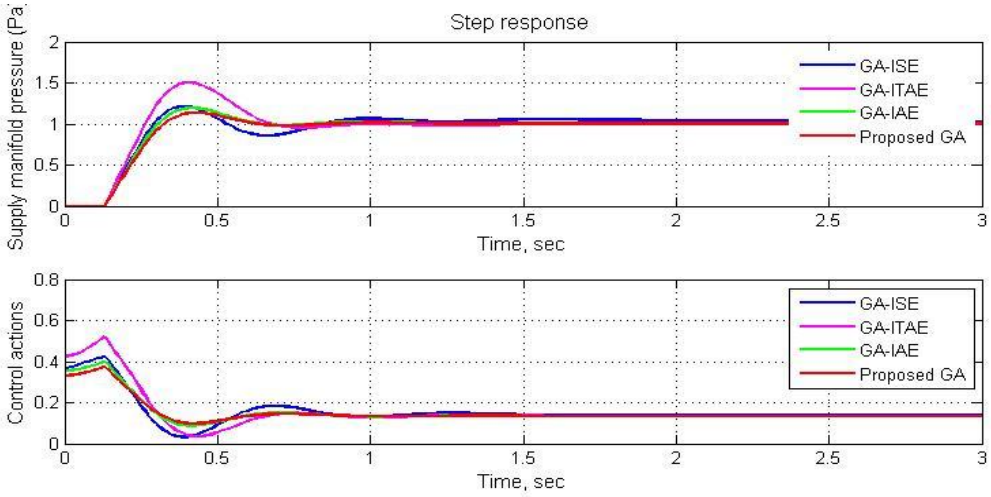

Figure 7.2 Servo control response of FOPID controllers designed by Genetic algorithm

FOPID controller response settles faster than other given GA based FOPID controller responses. The variation of controller outputs is also shown in Figure 7.2. The performance measures like settling time, percentage of peak overshoot are calculated for different cost functions as shown in Table 7.2. It also presents the simulated FOPID controller parameters under various objective functions using GA. Further, from Figure 7.2, in all the controller responses, the control action (controller output) is found to be smooth.

Table 7.2 Summary of performance measures comparison under various cost functions.

GA based method	K_p	K_i	K_d	λ	μ	Settling time, sec	% Peak overshoot
IAE	0.354	0.756	0.041	0.114	1.230	1.100	19.26
ITAE	0.425	1.534	0.006	0.134	1.000	0.889	50.35
ISE	0.362	0.756	0.041	0.114	1.23	2.854	21.22
Proposed	0.331	0.707	0.002	0.314	1.001	0.743	13.31

From Table 7.2 it can be observed that the proposed cost function FOPID controller response gives better reduction in percentage peak overshoot and settling time when compared to using ISE, IAE and ITAE separately. Figure 7.3 (a), (b) shows the servo and regulatory control responses of supply manifold pressure controllers with ISE, IAE and ITAE separately and proposed objective function. Simulation studies are carried out to explore the disturbance rejection capability of the controllers in the presence of the change in disturbance input which is applied between controller and plant.

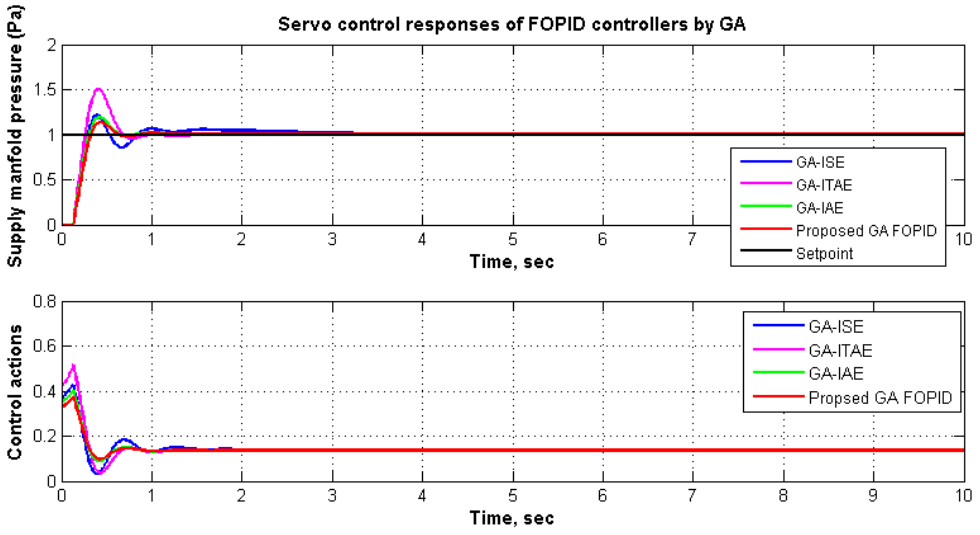

(a)

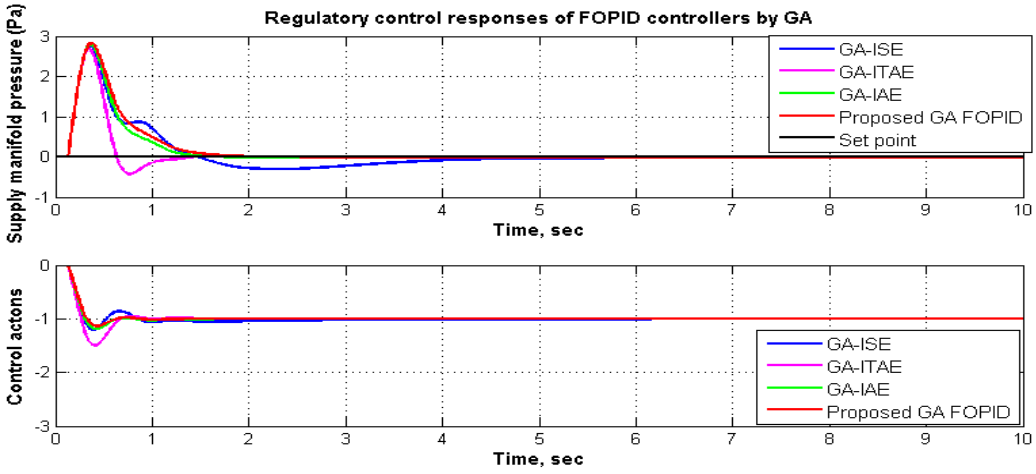

(b)

Figure 7.3 Control of supply manifold pressure using GA optimization method (a) Servo response and (b) Regulatory response.

A disturbance input of a unit positive step change is applied at time t = 0 sec. From Figure 7.3, it can be inferred that the FOPID controllers using GA optimization process are able to reject the disturbance quickly and bring the output back to the set point. The FOPID controller with proposed objective function able to reject the disturbance input more quickly and get back the response to the set point when compared to the responses of FOPID controllers with IAE, ISE and ITAE cost functions separately. Further, the variation of controller output is found to be smooth as shown in Figure 7.3(b).

A comparison of time domain and performance analysis is made between Padula et al [79] FOPID controller response from chapter 5 and proposed GA based FOPID controller response from chapter 7. Figure 7.4 show the comparison of proposed GA based FOPID and FOPID with Ms 1.4 [79] controller methods. Table 7.3shows the summary of performance comparison of proposed GA based FOPID and FOPID with Ms 1.4 [79] controller methods.

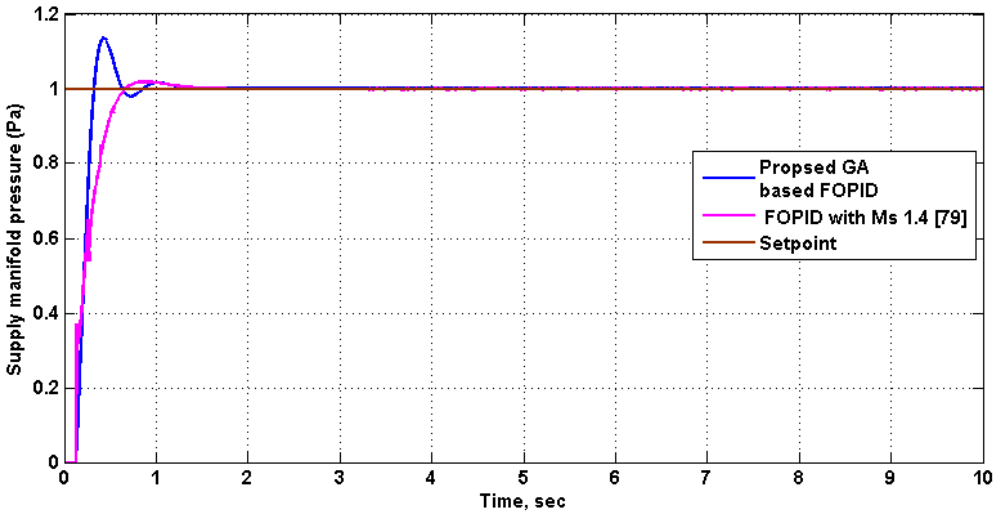

Figure 7.4 Comparison of Proposed GA based FOPID and FOPID with Ms 1.4[74] controller methods.

From table 7.3 and Figure 7.4 proposed GA based FOPID controller produces the better response in all performance parameters except peak overshoot when compared with sensitivity based FOPID controller.

Table 7.3 Summary of performance comparison of proposed GA based FOPID and FOPID with Ms 1.4[79] controller methods

Performance Parameters	Proposed GA based FOPID	FOPID with Ms 1.4 [79]
Rise time (sec)	0.148	0.3211
Peak time(sec)	0.430	0.8200
Settling time(sec)	0.743	1.1155
Peak Overshoot (%)	13.31	3.559
ISE	0.1908	0.1930
IAE	0.2535	0.2802
ITAE	0.0057	0.0607

7.4.1 Comparison of time scales of different controllers with time scale of open loop response

Time constant for open loop model response = 0.5275 sec

Table 7.4 Time constant values of controllers from this chapter

S.No	Type of controller	Time constant of the response in sec
1	GA based IAE	0.233
2	GA based ITAE	0.213
3	GA based ISE	0.226
4	Proposed Controller	0.240

Table 7.4 shows the time constant values of different controllers used in this chapter. When compare the time scales of different controller responses, the time constant of different controller responses from Table 7.4 are smaller than the time constant of the open loop response of the PEM fuel cell system.

7.5 Conclusions

This section presents the novel tuning method for the FOPID controller parameters using genetic algorithm (GA) based supply manifold pressure control of PEM fuel cell. The objective function

of the proposed genetic algorithm is designed according to the required control characteristics of supply manifold system. The FOPTD model of supply manifold pressure system is modeled and its response with the proposed GA tuning technique was obtained. The proposed GA tuning method has a better performance compared with the traditional GAs based IAE, ITAE and ISE indices. The proposed method gives a better response and satisfies the specified control characteristics of the supply manifold pressure controlled system.

Chapter 8
Design of Fuzzy self-tuning PID controller for control of oxygen excess ratio of PEM fuel cell

8.1 Introduction

A fuzzy logic controller (FLC) is widely accepted as an efficient controller, which is capable of controlling system without knowledge of its underlying dynamics and without using extensive mathematical analysis. Applications of FLCs in the literature witness that FLC is very efficient for nonlinear and uncertain systems. However, the design of FLC is difficult because it involves several parameters without a distinct method for tuning. The design parameters for FLC are input/output scaling factors, membership function parameters and the rule base. Several heuristic methods have been proposed for the design and tuning of FLCs usually involving trial and error methods. Here, a novel combining method based on conventional PID and fuzzy logic controllers is proposed. This proposal bears two major advantages: the strengths of both PID and fuzzy logic controllers are benefited while the hybrid controller suitably performs with uncertainties of nominal parameters of the PEMFC-based system. Fuzzy logic was firstly proposed by Lotfi A. Zadeh in 1965 to control plants that were difficult to model [81]. The application of fuzzy logic in control problems was firstly introduced by Mamdani in 1974 [82].A Fuzzy self-tuning PID controller is designed in order to regulate the oxygen excess ratio at a desired value when the stack current changes. The proposed control scheme is separated into two parts: fuzzy tuner and classical PID controller. The parameters of PID controller are adapted by means of fuzzy tuner.

8.2 Fuzzy Logic Control System

A simple fuzzy logic control system is shown is Figure 8.1. The fuzzy logic control system consists of two inputs error and change in error, error is obtained by comparing the reference input signal with output signal. This error is checked with respect to time that is called change in error and these are the basically two input of fuzzy logic controller.

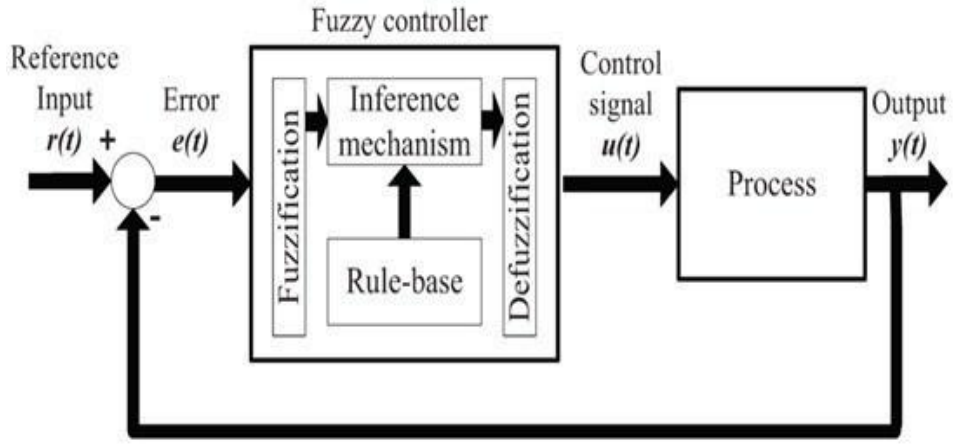

Figure 8.1 Fuzzy Logic Control System

The fuzzy logic controller consists of three components fuzzification, inference mechanism and DE fuzzification. When inputs (error and derivative error) are given to fuzzy logic controller then fuzzy logic controller decided what would be the output of this controller using fuzzy rules which are settled by fuzzy controller designer. Similarly, the fuzzy logic controller output is given to output motor or machine after processing mechanism.

8.2.1 Components of Fuzzy Logic Control System

The fuzzy logic control system consists of three main components,

Fuzzification: Fuzzification component consists of two components that are called as membership function and labels. Fuzzy logic controller converts input data or variable data into fuzzy membership function according to user defined chart such as temperature is too cold, motor speed is too low and assign the grade of this data value from 0 to 1. Different shapes could be used for membership function such as S, A, π and Z.

Inference Mechanism: Inference mechanism component of fuzzy logic control system consists of fuzzy rules which are settled by controller designer shown in Figure 8.1. Based on these fuzzy rules, controller decided the output of fuzzy logic controller. This is the main intelligent control of this system.

DE fuzzification: DE fuzzification component of fuzzy logic converts the fuzzy data values into real life data values after examining the fuzzy rules but these real-life data values depend upon the DE fuzzification method. Different methods are used for DE fuzzification process such center of gravity (SOG), weighted average method, mean of maxima (MOM) and smallest of

maxima (SOM). Each method has different advantages and disadvantages. These methods are set by the controller designer.

8.2.2 Conventional PID Controller

The control signal of a conventional PID controller is

$$u(t) = k_p e(t) + k_i \int_0^t e(t)d\tau + k_d \frac{de(t)}{dt} \quad 8.1$$

where error is denoted by e (t), k_p is the proportional, k_i is the integral and k_d is the derivative coefficient of the Equation 8.1.The general feedback control diagram of the PEMFC system is shown in Figure 8.2.

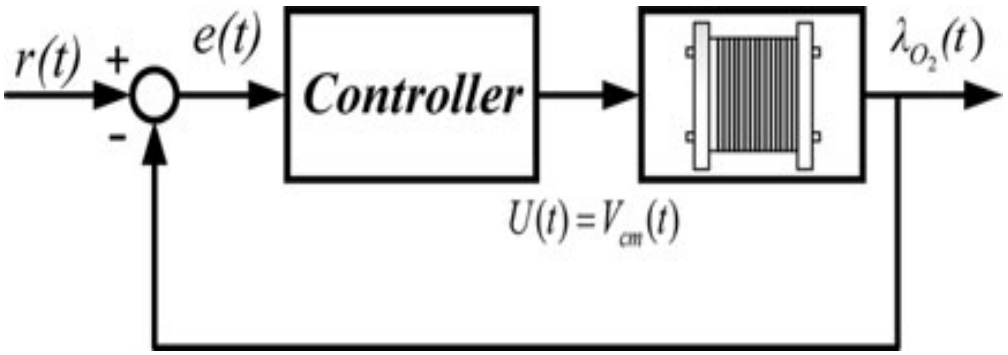

Figure 8.2 The general feedback control diagram of PEMFC system.

8.2.3 Control Objective

The main control objective for the PEM fuel cell system is regulating the oxygen excess ratio z_2, the air excess ratio is defined by the amount of oxygen provided $W_{O2,in}$ and the amount of oxygen reacted $W_{O2,ret}$i.e described as [15,37]

$$z_2 = \frac{W_{O_{2.in}}}{W_{O_{2,ret}}} \quad 8.2$$

If the value of z_2 is too low it is likely to cause "Oxygen Starvation". This phenomenon can cause a short circuit and hot spot on the surface of membrane cell. On the other hand, a higher value of z_2 will drive the auxiliary system to consume more power. It is necessary to use efficient control method to regulate the oxygen excess ratio in order to prevent oxygen starvation and reduce the extra parasitic power loss.

8.2.4 Design of fuzzy self-tuning PID controller

Fuzzy logic controller has two inputsto fuzzy inference: error *e(t)* and derivative of error *de(t)*, and three outputs for each PID controller parameters respectively K_p, $K_i$andK_d. Mamdani model is applied as structure of fuzzy inference with some modification to obtain the best value for K_p, $K_i$and$K_d$shown in Figure 8.3.

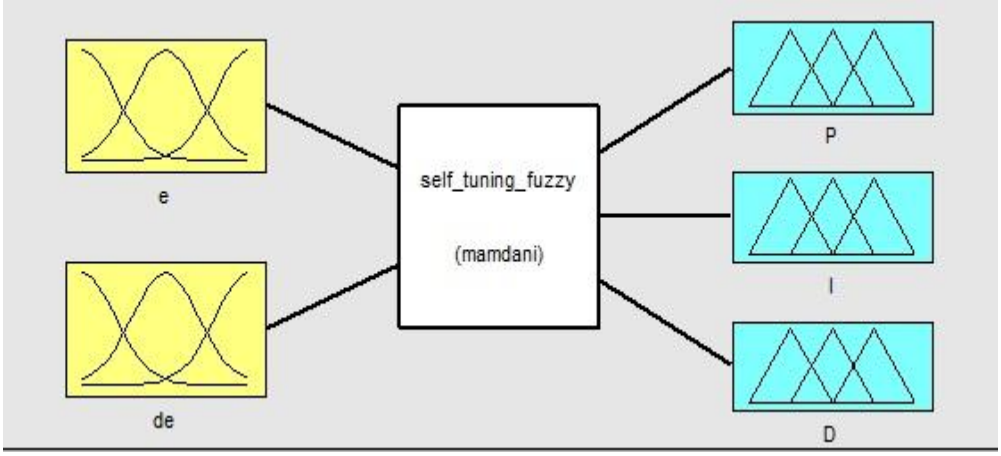

Figure 8.3 Fuzzy Inference System (FIS)

Fuzzy self-tuning PID controller means that the three term control K_p, K_i and K_d are tuned by using fuzzy tuner. The oxygen excess ratio control based on Fuzzy self-tuning PID controller is shown in Figure 8.4. Figure 8.5 shows the Fuzzy self-tuning PID controller structure for the control of oxygen excess ratio of PEM fuel cell system using Simulink.

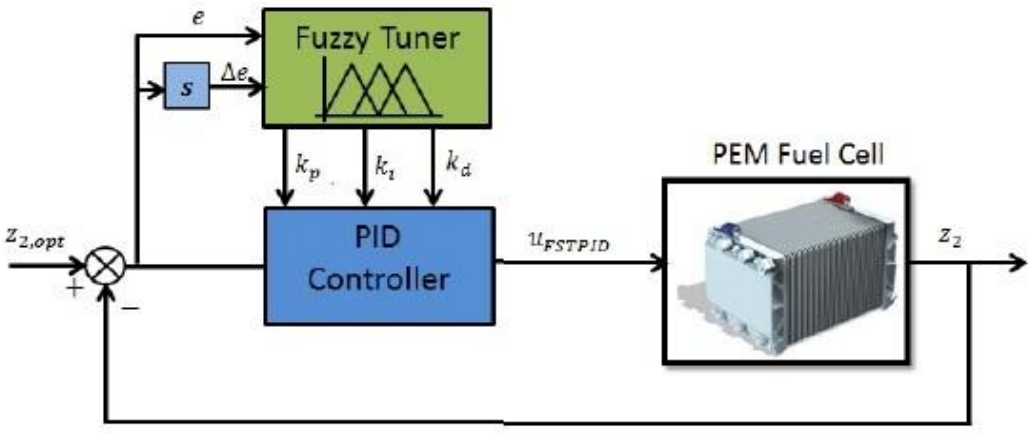

Figure 8.4 Fuzzy self-tuning PID controller structure for the control of oxygen excess ratio of PEM fuel cell system.

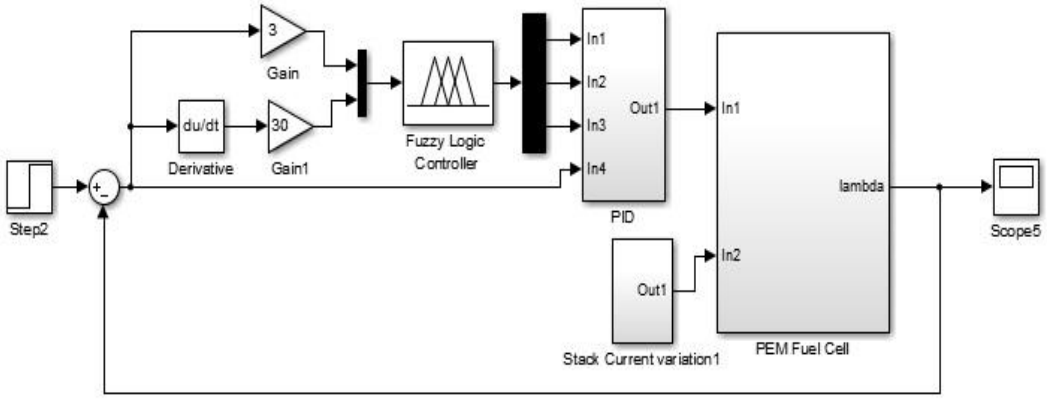

Figure 8.5 Implementation of Fuzzy self-tuning PID controller for the control of oxygen excess ratio of PEM fuel cell system using Simulink of MATLAB.

Where e is the error between oxygen excess ratio set point and its output and Δe is derivation of error. There are two inputs to fuzzy inference e and Δe , and three outputs k_p, k_i and k_d. the actual range of e and Δe is [-3, 3] and [-30, 30], which can be converted to [-1,1] by multiplying the factors. The output range k_p, k_i and $k_d$are [0, 1000], [0, 2000] and [0, 1] respectively. The fuzzy subsets of input are small, middle, and large and the output fuzzy subsets are small, middle, and large. The basic form of fuzzy control rule is " if the error $e$and the error derivation $\Delta e$is A and B, then the fuzzy control outputs are k_p, k_i and k_d ". The membership functions of inputs and outputs are respectively shown in Figure 8.6 and 8.7. And the fuzzy control rules are obtained by Table 8.1.

Table 8.1 Fuzzy rules for tuning PID parameters

		e		
	K_p, k_i, k_d	**SMALL (S)**	**MIDDLE (M)**	**LARGE (L)**
	SMALL	M S S	M S S	L S S
Δe	**MIDDLE**	L M M	M M S	M S S
	LARGE	L LL	M L S	S L S

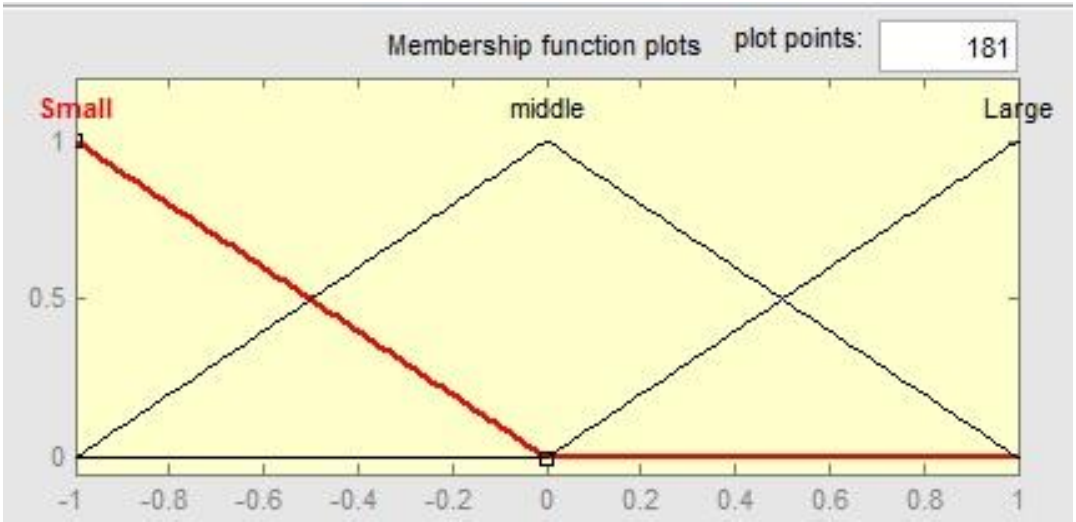

Figure 8.6 Membership functions for e and Δe

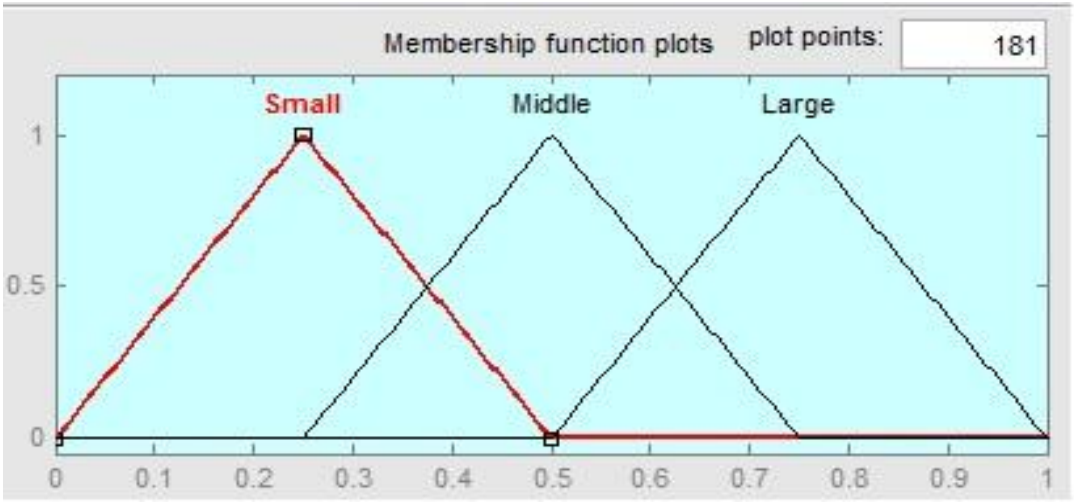

Figure 8.7 Membership functions for k_p, k_i and k_d

8.3 Simulation results and Discussion

To verify the performance of the Fuzzy self-tuning PID control strategy, simulations using MATLAB/SUMULINK are performed and analyzed. The Fuzzy self-tuning PID control strategy applied to 4th order `nonlinear model of the PEMFC system. The main aim of the design of these controllers is to regulate the oxygen excess ratio at a setpoint value, which is assumed

equal to 2. With this setpoint, it can be guaranteed that the PEMFC system works within the range of its maximum net power for each load variation while the oxygen starvation is avoided.

8.3.1 Comparative analysis

This subsection shows a comparison study between the control strategies i.e., Classical PID and fuzzy self-tuned PID controllers. Figure 8.8 shows the variation of stack current which is applied to the nonlinear PEM fuel cell model as load disturbance input. The stack current rises up from 50 A to 100 A at t = 5 s. Next, after 5 s, it increases by 100 to 150 A. This increment stopped when the stack current reaches 250 A. After 25 s, the current rises from 250 to 275A. Finally, at time 30 s the stack current 275 to 300 A

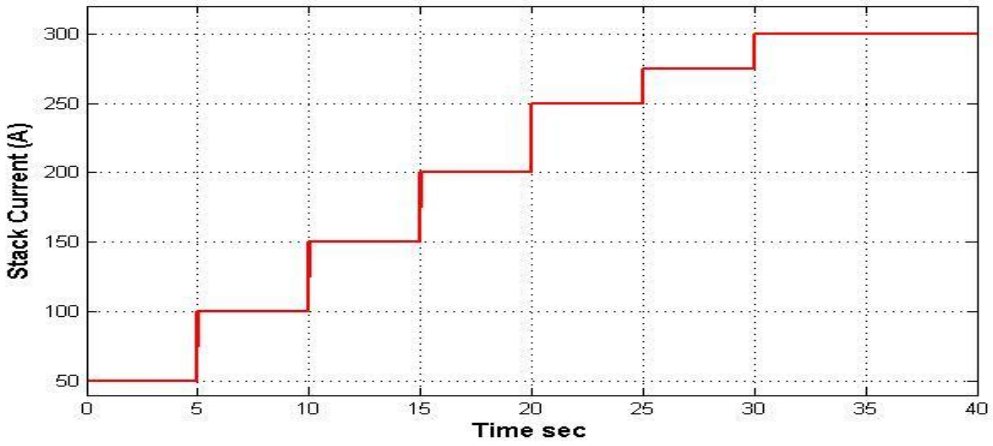

Figure 8.8 Stack current variation

Figure 8.9 shows the dynamic behavior of oxygen excess ratio under different stack current variation using PID controller and Figure 8.10 shows the response of oxygen excess ratio using Fuzzy Self tuning PID(FSTPID) controller under load current variation of Figures 8.8.

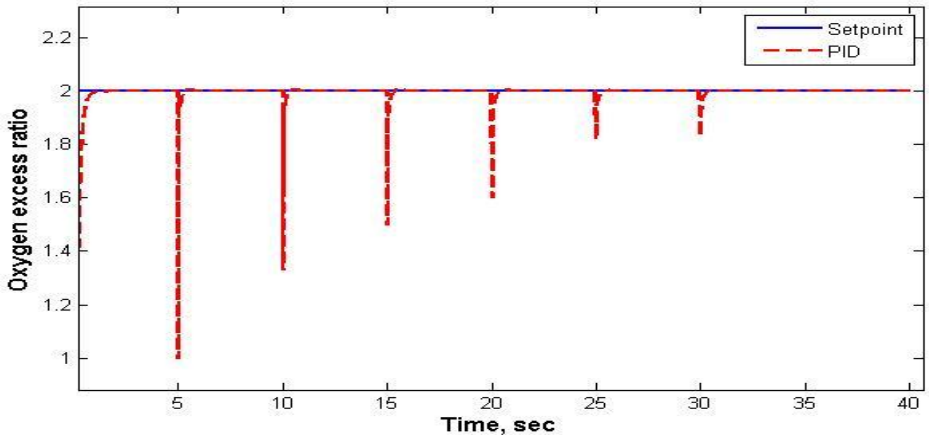

Figure 8.9 Response of oxygen excess ratio using classical PID controller.

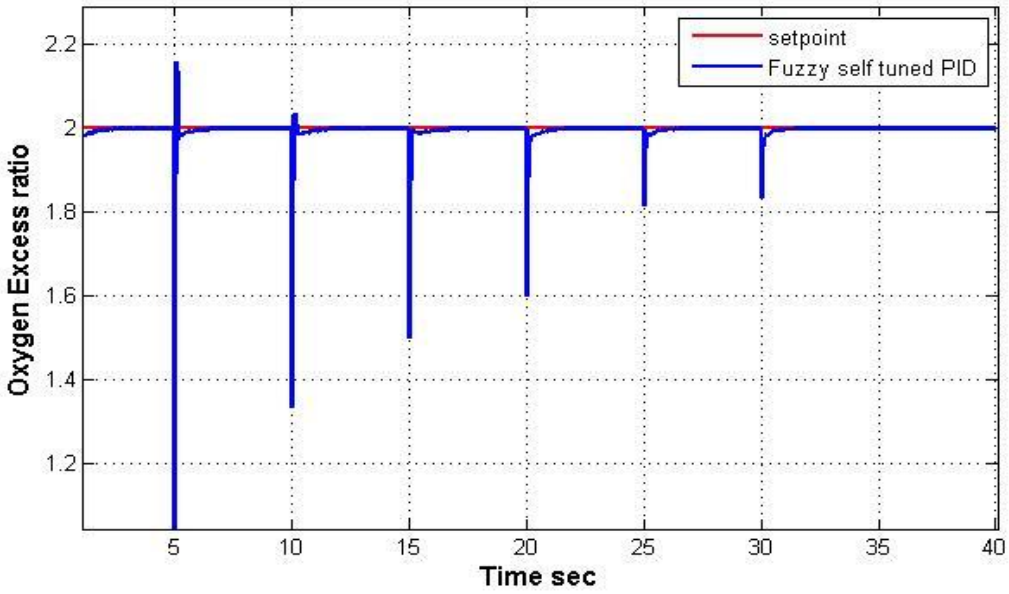

Figure 8.10 Response of oxygen excess ratio using fuzzy self tuning PID controller

It can be seen from Figure 8.11 that all the applied control strategies adjust oxygen excess ratio(z_2) at the setpoint with a satisfactory tracking performance. Figure 8.12 present the magnified plot of oxygen excess ratio when the stack current is increased from 100 A to 150 A (at t =10 s).

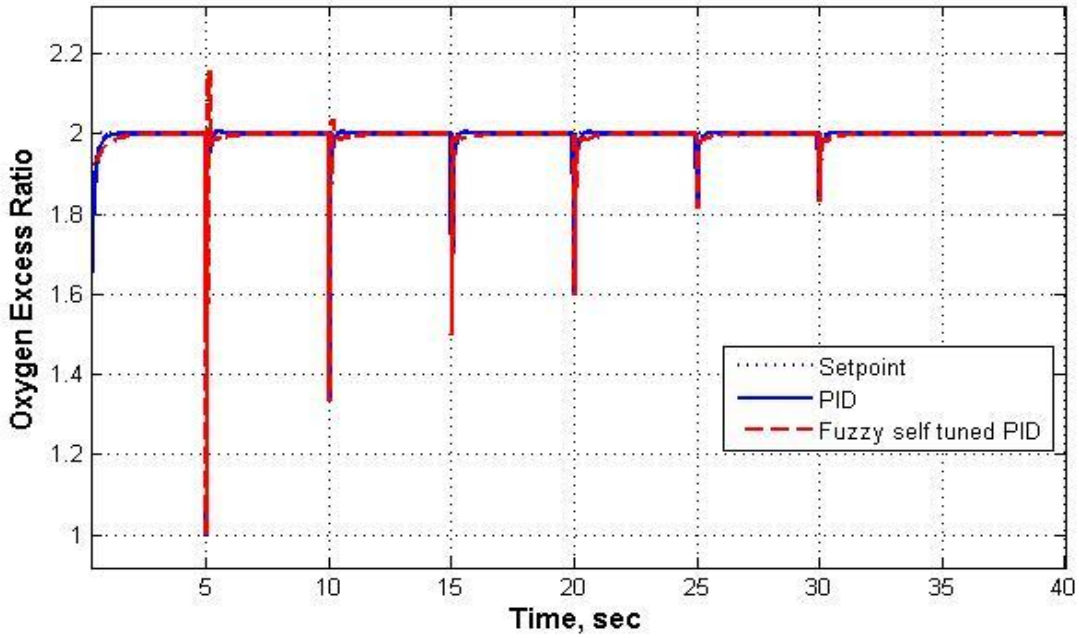

Figure 8.11 Response of oxygen excess ratio for PID and FSTPID control strategies.

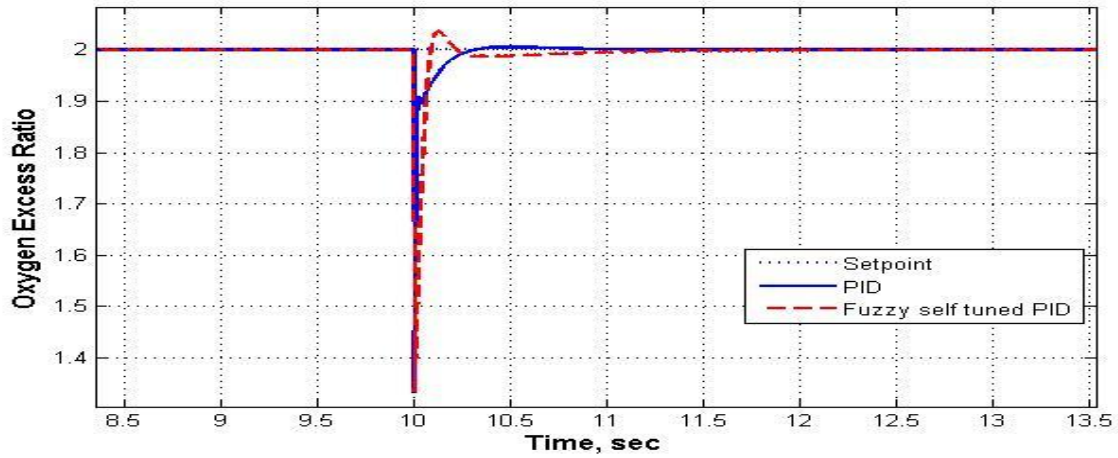

Figure 8.12 The magnified plot of oxygen excess ratio variation at t=10s

Comparison of time domain specifications of PID and FSTPID control schemes is given in Table 8.2. The settling time for classical PID 0.48 sec reduced to 0.3990 sec in the fuzzy self tuning PID control scheme. Percentage of peak overshoot for PID is 364.51 is reduced to 56.84 in the fuzzy self tuning PID controller.

Table 8.2 Comparison of time domain specifications.

Type of controller	Peak time	Settling time	Overshoot (%)
PID	0.0870	0.4800	364.51
FSTPID	0	0.3990	56.8409

8.4 Conclusions

In this chapter, a fuzzy self tuning PID controller is designed to control the oxygen excess ratio in order to avoid oxygen starvation when stack current suddenly change. The simulation results shows that fuzzy self tuning PID control has better control effort than the classical PIDcontrol

Chapter 9
Overall conclusions and Future work

In this thesis work, higher order PEM fuel cell model is approximated to FOPTD model for analysis and control design using one of the model reduction methods. The analysis of uncertainty for the FOPTD model was carried out to know the uncertainty of plant transfer function with varying operating conditions. From FOPTD model, Smith predictor controller was designed and compared with other tuning methods such as ZN-PI, Skogestad- Internal Model Control (SIMC)-PI, Improved SIMC-PID. Smith predictor produces better response in terms of percentage of peak overshoot compare to classical controllers. Model Predictive Controller was designed for the linearized SISO system of higher order model of PEM fuel cell to control the supply manifold pressure. Simulation results shows that the MPC controller produces very less overshoot but it produces slow rise time. Decentralized PI controller was designed for the linearized MIMO system to know the interactions of the plant outputs.

Different fractional order PI/PID controller tuning methods were applied to the approximated FOPTD model of PEM fuel cell and compared their performance in terms of performance indices and time domain indices. Tested the robustness of better fractional order controller on original non linear model of PEM fuel cell system for the control of supply manifold pressure. Simulation results shows that the proposed controller produces significant output response under load current disturbances.

Fractional order PID controller was designed for the supply manifold pressure control of Proton Exchange Membrane fuel cell based on minimization of IAE and constraint of maximum sensitivity 1.4 and 2.0. Compared with AMIGO PID and ZN FOPID controller tuning methods in terms of performance indices and time domain indices. Simulation results shows that the proposed controller produces better response under measurement noise.

Designed fractional order PID controller based on proposed objective function using Genetic Algorithm for the control of supply manifold pressure of PEM fuel cell system and compared its response with standard objective functions. From simulation results the proposed controller produces better response when compare to other methods of similar kind.

Fuzzy self tuning PID controller was applied for the original model of the PEM fuel cell system model to control the oxygen excess ratio and compared its response with classical PID controller. From the simulation results Fuzzy self tuning PID controller produces significant response when compare to classical PID controller under external disturbances are applied.

Future scope of the work

- Design of fuzzy fractional PI-PD controller for the control of oxygen excess ratio of PEM fuel cell.

For the given 4^{th} order model, we will design fuzzy fractional PI-PD controller using optimization methods to control the oxygen excess ratio of PEM fuel cell. And compare the performance of the designed controllers with other controllers worked out in the literature.

- Design of centralized controllers for MIMO system of PEM fuel cell.

In this work, we will design the different centralized controller methods for the MIMO system of PEMFC and compare the better results.

- Design of fractional order controllers for the MIMO system of PEM fuel cell.

We will design fractional PI controllers for the MIMO system of PEM fuel cell system using different optimization methods and compare the better results.

References

[1]. Matraji I, Laghrouche S, Jemei S, Wack M. Robust control of the PEM fuel cell air-feed system via sub-optimal second order sliding mode. Appl. Energy 2013; 104: 945–957.

[2]. Larminie J, Dicks A, McDonald MS. Fuel cell systems explained. vol. 2. New York: Wiley;2003.

[3]. Kunusch C, Puelston P.F, and MayoskyM.A., Sliding-mode control of PEM fuel cells. London: Springer; 2012.

[4]. ShahR.K., Introduction to Fuel Cells, In book: Recent Trends in Fuel Cell Science and Technology, Chapter 1, New Delhi, India: Anamaya Publishers; 2007.

[5]. Laughton M. A., Fuel cell, Power Engineering Journal, 2002; 16(1): 37-47.

[6]. Tang H, Peikang S, Jiang SP, Wang F, Pan M A., Degradation study of Nafion proton exchange membrane of PEM fuel cells. J Power Sources, 2007; 170(1):85–92.

[7]. Maher A.R. Sadiq Al-Baghdadi., Modelling of proton exchange membrane fuel cell performance based on semi-empirical equations. Renewable Energy, 2005; 30(10): 1587-1599.

[8]. Amphlett J, Mann R, Peppley B, Roberge P, Rodrigues A., A model predicting transient responses of proton exchange membrane fuel cells. J Power Sources, 1996; 61:183–188.

[9]. Barbir F, PEM fuel cells: theory and practice. Burlington, MA, USA: Elsevier; 2005

[10]. Mann R.F, Amphlett J.C, HooperM.A.I., JensenH.M., Peppley B.A and Roberge P.R, Development and Application of a Generalised Steady-State Electrochemical Model for a PEM Fuel Cel. Journal of Power Sources, 2000; 86:173 –180.

[11]. Tao W.Q, Min C.H, Liu X.L, He Y.L, Yin B.H and JiangW, Parameter Sensitivity Examination and Discussion of PEM Fuel Cell Simulation Model Validation Part I. Current Status of Modeling Research and Model Development. Journal of Power Sources, 2006;160(1): 359 – 373.

[12]. Boettner D.D, Paganelli G, Guezennec Y.G, RizzoniG. and Moran M.J., Proton Exchange Membrane Fuel Cell System Model for Automotive Vehicle Simulation and Control. Journal of Energy Resources and Technology, 2002; 124(21): 20 – 27.

[13]. Corrêa J.M, Farret F.A. Canha L.N, and Simões M.G., An Electrochemical-Based Fuel-Cell Model Suitable for Electrical Engineering Automation Approach, IEEE Transactions onIndustrial Electronics, 2004;51(5): 1103 – 1112.

[14]. Outeiro M.T, Chibante R, Carvalho A.S and de Almeida A.T., A Parameter OptimizedModel of a Proton Exchange Membrane Fuel Cell Including Temperature Effects, Journal ofPower Sources, 2008;185(2): 952 – 960.

[15]. Pukrushpan J.T, Stefanopoulou A.G, Peng H, Control of fuel cell breathing. IEEE Control Syst 2004; 24(2):30-46.

[16]. Grujicic M, Chittajallu K.M, Pukrushpan J.T. Control of the transient behaviour of polymer electrolyte membrane fuel cell systems. Proceedings of the Institution of Mechanical Engineers, Part D: Journal of Automobile Engineering. 2004;218(11):1239-50.

[17]. Bao C, Ouyang M, Yi B. Modeling and control of air stream and hydrogen flow with recirculation in a PEM fuel cell system—II. Linear and adaptive nonlinear control. International journal of hydrogen energy. 2006;31(13):1897-913.

[18]. Pukrushpan J.T, Peng H, Stefanopoulou A.G. Control-oriented modeling and analysis for automotive fuel cell systems. J. Dyn. Sys., Meas., Control. 2004;126(1):14-25.

[19]. Wang F.C, Yang Y.P, Huang C.W, Chang H.P, Chen H.T. System identification and robust control of a portable proton exchange membrane full-cell system. Journal of Power Sources. 2007; 164(2): 704-12.

[20]. Wang F.C, Chen H.T, Yen J.Y. Multivariable LQG control of a proton exchange membrane fuel cell system. IFAC Proceedings Volumes. 2008;41(2):10995-1000.

[21]. Wang F.C, Chen H.T, Yang Y.P, Yen J.Y., Multivariable robust control of a proton exchange membrane fuel cell system. Journal of Power Sources. 2008 ;177(2):393-403.

[22]. Niknezhadi A, Allu_Fantova M, Kunusch C, Ocampo-Martinez C., Design and implementation of LQR/LQG strategies for oxygen stoichiometry control in PEM fuel cells based systems. J Power Sour2011; 196(9): 4277-82.

[23]. Wang Y.X, Xuan D.J, Kim Y.B. Design and experimental implementation of time delay control for air supply in a polymer electrolyte membrane fuel cell system. International Journal of Hydrogen Energy. 2013;38 (30):13381-92.

[24]. Özbek M, Wang S, Marx M, Söffker D. Modeling and control of a PEM fuel cell system: a practical study based on experimental defined component behavior. Journal of Process Control. 2013; 23(3):282-93.

[25]. Al-Durra A, Yurkovich S, Guezennec Y. Study of nonlinear control schemes for an automotive traction PEM fuel cell system. International journal of hydrogen energy. 2010;35(20):11291-307.

[26]. Da Fonseca R, Bideaux E, Gerard M, Jeanneret B, Desbois-Renaudin M, Sari A. Control of PEMFC system air group using differential flatness approach: validation by a dynamic fuel cell system model. Applied energy. 2014 ;113:219-29.

[27]. Rios R, Ramos C, Jairo E. Non-linear state space model and control strategy for PEM fuel cell systems. Dyna. 2011;78(166):60-67

[28]. Na W.K, Gou B. Feedback-linearization-based nonlinear control for PEM fuel cells. IEEE Transactions on Energy Conversion. 2008;23(1):179-90.

[29]. Kunusch C, Puleston P, Mayosky M, and Riera J. Sliding mode strategy for PEM fuel cells stacks breathing control using a super-twisting algorithm. IEEE Trans on Control Systems Technology 2009; 17 (1): 167–174.

[30]. Kunusch C, Puleston PF, Mayosky M.A, Fridman L. Experimental results applying second order sliding mode control to a PEM fuel cell based system. Control Engineering Practice. 2013; 21(5):719-26.

[31]. Baroud Z,Benmiloud M, Benalia A. Sliding mode controller for breathing subsystem on a PEM fuel cell system. In2015 3rd International Conference on Control, Engineering & Information Technology (CEIT) 2015;1-6. IEEE.

[32]. Garcia-Gabin W, Dorado F, Bordons C. Real-time implementation of a sliding mode controller for air supply on a PEM fuel cell. J Process Control 2010; 20(3): 325-36.

[33]. Park G, Gajic Z. Sliding mode control of a linearized polymer electrolyte membrane fuel cell model. Journal of Power Sources. 2012 Aug 15;212:226-32.

[34]. Sankar K, Thakre N, Singh, S M, Jana, A K. Sliding Mode Observer based Nonlinear Control of a PEMFC Integrated with a Methanol Reformer. Energy 2017; 139: 1126 – 1143

[35]. Pilloni A, Pisano A, Usai E. Observer based air excess ratio control of a PEM fuel cell system via high order sliding mode. IEEE Trans Ind Electron 2015; 62(8): 5236-46.

[36]. Golbert J, Lewin DR. Model-based control of fuel cells::(1) regulatory control. Journal of power sources. 2004;135(1-2):135-51.

[37]. Gruber J K, Doll M, Bordons C. Design and experimental validation of a constrained MPC for the air feed of a fuel cell. Control Engineering Practice 2009; 17(8): 875-885.

[38]. Gruber J K, Bordons C, Oliva A. Nonlinear MPC for the airflow in a PEM fuel cell using a volterra series model. Control Engineering Practice 2012; 20(2): 205-217.

[39]. Vahidi A, Kolmanovsky I, Stefanopoulou A. Constraint management in fuel cells: A fast reference governor approach. InProceedings of the 2005, American Control Conference, 2005. 2005 ; 3865-3870. IEEE.

[40]. Vahidi A, Stefanopoulou A, Peng H. Model predictive control for starvation prevention in a hybrid fuel cell system. InProceedings of the 2004 American Control Conference 2004 vol. 1, 834-839. IEEE.

[41]. Zhao Y, Pistikopoulos E. Dynamic modelling and parametric control for the polymer electrolyte membrane fuel cell system. Journal of power sources. 2013;232:270-278.

[42]. Ha¨hnel C, Aul V, Horn J. Power Control of Efficient Operation of a PEM Fuel Cell System by Nonlinear Model Predictive Control. IFAC-Papers On Line 2015; 48(11): 174–179.

[43]. Baroud Z, Benmiloud M, Benalia A, Ocampo-Martinez C. Novel hybrid fuzzy-PID control scheme for air supply in PEM fuel-cell-based systems. Int. J. Hydrogen Energy 2017; 42(15): 10435 -10447.

[44]. Li C H, Sun Z H, Wang Y L, Wu X D. in Unifying Electrical Engineering and Electronics Engineering, Lecture Notes in Electrical Engineering, Vol. 238 (Eds. S. Xing, S. Chen, Z. Wei, J. Xia), Springer, New York, 2014, 933–942.

[45]. Aliasghary M. Control of PEM Fuel Cell Systems Using Interval Type-2 Fuzzy PID Approach. Fuel Cells 2018; 18: 449-456.

[46]. Ou K, Wang Y, Li Z, Shen Y, Xuan D. Feedforward fuzzy-PID control for air flow regulation of PEM fuel cell system. Int. J. Hydrogen Energy 2015; 40(35): 11686-11695.

[47]. Benchouia N E, Derghal A, Mahmah B, Madi B, Khochemane L, Aoul E H. An adaptive fuzzy logic controller (AFLC) for PEMFC fuel cell. Int. J. Hydrogen Energy 2015; 40(39): 13806-13819.

[48]. Abbaspour A, Khalilnejad A, Chen Z. Robust adaptive neural network control for PEM fuel cell. Int. J. Hydrogen Energy 2016; 41(44): 20385-95.

[49]. Rezazadeh A, Sedighizadeh M, Karimi M. Proton Exchange Membrane Fuel Cell ControlUsing a Predictive Control Based on Neural Network. International Journal of Computer and Electrical Engineering. 2010;2(1):81.

[50]. Methekar R.N, Prasad V, Gudi R.D. Dynamic analysis and linear control strategies for proton exchange membrane fuel cell using a distributed parameter model. J. Power Sources 2007; 165 (1): 152-170.

[51]. Zhiyang Liu, Jian Chen, Hao Chen, Chizhou Yan. Air supply regulation for PEMFC systems based on uncertainty and disturbance estimation.Int. J. Hydrogen Energy 2018; 43:11559 – 11567.

[52]. Chang Y.A, Moura S.J. Air flow control in fuel cell systems: An extremum seeking approach. In2009 American Control Conference 2009: 1052-1059. IEEE

[53]. Das S, Functional fractional calculus, 2nd ed, Springer; 2011.

[54]. Podlubny I. Fractional-Order Systems and $PI^{\lambda}D^{\mu}$ Controllers. IEEE Transactions on Automatic Control 1999; 44(1): 208-214.

[55]. Vinagre B M, Podlubny I, Dorcak L, Feliu V. On Fractional PID Controllers: A Frequency Domain Approach. Proceedings of IFAC Workshop on Digital Control: Past, Present and Future of PID Control 2000; Terrasa, Spain, 53-58.

[56]. Valerio D, Costa J S. Tuning of fractional PID controllers with Ziegler–Nichols type rules. Signal Processing 2006; 86:2771–2784.

[57]. Shahiri M, Ranjbar A, Karami M.R, Ghaderi R. Oxygen Excess Ratio control of PEM Fuel Cell System Based on a Fractional Order model Approximation. International Journal of Mechatronics, Electrical and Computer Technology2014; 4(13): 1524-1550.

[58]. Shahiri M, Ranjbar A, Karami M.R, Ghaderi R. Robust control of nonlinear PEMFC against uncertainty using fractional complex order control. Nonlinear Dyn 2014; 1–16.

[59]. Shahiri M, Ranjbar A, Karami M.R, Ghaderi R. Tuning method for fractional complex order controller using standardized K-chart: application to PEM fuel cell. Asian Journal of Control 2016; 18(3):1102–1118.

[60]. XueqinLü, Xing Miao, Yang Xue, Liang Deng, Min Wang, Dong xiaGu, Xinyu Li. Dynamic Modeling and Fractional Order $PI^{\lambda}D^{\mu}$Control of PEM Fuel Cell. Int. J. Electrochem. Sci 2017;12: 7518 – 7536.

[61]. PhaniTejaBankupalli, Subhojit Ghosh, Lalit Kumar, SusovonSamanta. Fractional order modeling and two loop control of PEM fuel cell for voltage regulation considering both source and load perturbations. Int. J. Hydrogen Energy 2018; 43: 6294-6309.

[62]. Taleb M.A, Godoy E, Bethoux O, Irofti D. PEM fuel cell fractional order modeling and identification. In: Prepr. 19th IFAC world congr 2014; 2125-31.

[63]. Taleb M.A, Bethoux O, Godoy E. Identification of a PEMFC fractional order model. Int. J. Hydrogen Energy 2016; 42(2): 1499-509.

[64]. Pukrushpan J.T., Stefanopoulou A.G. and Peng H., Control of fuel cell power systems: principles, modeling, analysis and feedback design, Springer; 2004.

[65]. Suh K.W., Modeling, analysis and control of fuel cell hybrid power systems, Ph.D. dissertation, Dept. Mech. Eng., Univ. Michigan, Ann Arbor, 2006.

[66]. Gruber J.K, Bordons C, Dorado F. Nonlinear control of the air feed of a fuel cell. In2008 American Control Conference 2008;1121-1126. IEEE.

[67]. Baroud Z., Benmiloud M., Benalia A., "Modelling and Analysis of Proton Exchange Membrane Fuel Cell System," in: 3rd International Conference on, Information Processing and Electrical Engineering (ICIPEE), 2014;1–6.

[68]. Liu J, Laghrouche S, Wack M. Differential flatness-based observer design for a PEM fuel cell using adaptive-gain sliding mode differentiators. In2013 European Control Conference (ECC) 2013; 2477-2482. IEEE.

[69]. Seborg. D. E, EdgarT. F., Mellichamp D. A. and Doyle F. J., "Process Dynamics and Control, 3rd ed. Wiley, New York, 2011

[70]. Sundaresan K.R, Krishnaswamy P.R. Estimation of time delay time constant parameters in time, frequency, and Laplace domains. The Canadian Journal of Chemical Engineering. 1978 56(2):257-62.

[71]. Sourdille P, O'Dwyer A. Implementation of new modified Smith predictor designs. In Conference papers 2004; (p. 31).

[72]. Smith, O.J.M. Closer control of loops with dead time. Chemical Engineering Progress,1957; 53, 217 -219.

[73]. Bemporad, A., Morari, M., Ricker, N.L. Model Predictive Control Toolbox for Matlab – User's Guide. Mathworks, 2004.

[74]. Tavakoli S, Griffin I, Fleming P.J. Tuning of decentralised PI (PID) controllers for TITO processes. Control engineering practice. 2006 ; 14(9):1069-80.

[75]. Chen Y, Bhaskaran T, Xue D. Practical tuning rule development for fractional order proportional and integral controllers. Journal of Computational and Nonlinear Dynamics. 2008; 3(2):021403.

[76]. Bhambhani V, Chen Y, Xue D. Optimal fractional order proportional integral controller for varying time-delay systems. IFAC Proceedings Volumes. 2008;41(2):4910-5.

[77]. Gude J.J, Kahoraho E. Simple tuning rules for fractional PI controllers. In2009 IEEE Conference on Emerging Technologies & Factory Automation 2009 ;1-8. IEEE.

[78]. Merrikh-Bayat F. General rules for optimal tuning the PIλDμ controllers with application to first-order plus time delay processes. The Canadian Journal of Chemical Engineering. 2012; 90(6):1400-10.

[79]. Padula F, and Visioli A. Tuning rules for optimal PID and fractional-order PID controllers. Journal of process control. 2011;21(1):69-81.

[80]. Åström K.J, Hägglund T. Revisiting the Ziegler–Nichols step response method for PID control. Journal of process control. 2004;14(6):635-50.

[81]. Zadeh LA. Fuzzy sets. Information and control. 1965; 8(3):338-53.

[82]. Mamdani E. Application of fuzzy algorithms for control of simple dynamic plant. Proc Inst ElectrEng 1974;121(3):1585-8.

[83]. Liu Z, Chen J, Chen S, Huang L, Shao Z. Modeling and control of cathode air humidity for PEM fuel cell systems. IFAC-PapersOnLine. 2017 Jul 1;50(1):4751-4756.

[84]. Deng H, Li Q, Cui Y, Zhu Y, Chen W. Nonlinear controller design based on cascade adaptive sliding mode control for PEM fuel cell air supply systems. International Journal of Hydrogen Energy. 2019 Jul 19;44(35):19357-69.

[85]. Sankar K, Jana AK. Nonlinear multivariable sliding mode control of a reversible PEM fuel cell integrated system. Energy Conversion and Management. 2018 Sep 1;171:541-65.

[86]. Zhao D, Xu L, Huangfu Y, Dou M, Liu J. Semi-physical modeling and control of a centrifugal compressor for the air feeding of a PEM fuel cell. Energy Conversion and Management. 2017 Dec 15;154:380-6.

[87]. Ziogou C, Voutetakis S, Georgiadis MC, Papadopoulou S. Model predictive control (MPC) strategies for PEM fuel cell systems–A comparative experimental demonstration. Chemical Engineering Research and Design. 2018 Mar 1;131:656-70.

[88]. Ou K, Wang YX, Li ZZ, Shen YD, Xuan DJ. Feedforward fuzzy-PID control for air flow regulation of PEM fuel cell system. International journal of hydrogen energy. 2015 Sep 21;40(35):11686-95.

[89]. Fan Z, Yu X, Yan M, Hong C. Oxygen excess ratio control of PEM fuel cell based on self-adaptive fuzzy PID. IFAC-PapersOnLine. 2018 Jan 1;51(31):15-20.

[90]. Li M, Lu J, Hu Y, Gao J. Oxygen Excess Ratio Controller Design of PEM Fuel Cell. IFAC-PapersOnLine. 2018 Jan 1;51(31):493-498.

[91] Chavan SL, Talange DB. System identification black box approach for modeling performance of PEM fuel cell. Journal of Energy Storage. 2018 Aug 1;18:327-32.

[92]. Ma Y, Zhang F, Gao J, Chen H, Shen T. Oxygen excess ratio control of PEM fuel cells using observer-based nonlinear triple-step controller. International Journal of Hydrogen Energy. 2019 Nov 21.

.[93]. Skogestad, S., Simple Analytic Rules for Model Reduction and PID Controller Tuning, J. Process Control 2003: 13: 291-309.

[94]. Åström KJ, Panagopoulos H, Hägglund T. Design of PI controllers based on non-convex optimization. Automatica. 1998 May 1;34(5):585-601.

[95] .Persson P, Åström KJ. Dominant pole design-a unified view of PID controller tuning. IFAC Proceedings Volumes. 1992 Jul 1;25(14):377-82.

[96] Åström KJ, Hägglund T, Astrom KJ. Advanced PID control. Research Triangle Park, NC: ISA-The Instrumentation, Systems, and Automation Society; 2006 Aug.

[97]. Cao JY, Liang J, Cao BG. Optimization of fractional order PID controllers based on genetic algorithms. In2005 international conference on machine learning and cybernetics 2005 Aug 18 (Vol. 9, pp. 5686-5689). IEEE.

Appendix A

Model parameters and constants

Table: I Simulation Parameters of PEMFC system

Parameter	Symbol	SI Units	Value
Atmospheric pressure	P_{atm}	*Pa*	101325
Saturation pressure	P_{sat}	*Pa*	3140.4
Average ambient air relative humidity	$\emptyset_{atm}$	--	0.5
Atmospheric temperature	T_{atm}	*K*	298. 15
Air-specific heat ratio	γ	--	1. 4
Stack temperature	T_{st}	*K*	353. 15
Specific heat of air	C_P	*J/kg/K*	1004
Universal gas constant	R	*J /mol/K*	8. 31451
Molar mass of oxygen	M_{O2}	*kg/mol*	32×10^{-3}
Molar mass of nitrogen	M_{N2}	*kg/mol*	28×10^{-3}
Molar mass of vapor	M_v	*kg/mol*	18×10^{-3}
Molar mass of air	$M_{a,atm}$	*kg/mol*	29×10^{-3}
Faraday's constant	F	*C/mol*	96485
Cathode volume	V_{ca}	m^3	0.01
Supply manifold volume	V_{sm}	m^3	0. 02
Air-supply compressor motor mechanical efficiency	η_{cp}	*%*	0.8
Air-supply compressor efficiency	η_{cm}	*%*	0.98
Air-supply compressor and motor inertia	J_{cp}	*N.m*	5×10^{-5}
Air-supply compressor motor resistance	R_{cm}	*ohm*	0. 82
Motor constant	K_t	*Nm/A*	0. 0153
Motor constant	K_v	*V/ (rad/sec)*	0. 0153
Cathode inlet orifice constant	$K_{ca,in}$	*kg/sec/Pa*	0.36×10^{-5}
Cathode outlet throttle discharge co efficient	C_D	---	0.0124

Cathode outlet throttle area	A_T	m^2	0.002
Number of cells in fuel cell stack	n	---	381
Oxygen mole fraction	$y_{O_2,atm}$	----	0.21

Table: II Constants of the PEMFC system model.

$c_1 = \frac{RT_{st}K_{ca,in}}{M_{O_2}V_{ca}}\left(\frac{x_{O_2,atm}}{1+\omega_{atm}}\right)$	$c_7 = \frac{RT_{st}n}{4FV_{ca}}$	$c_{13} = \frac{\eta_{cm}K_t}{J_{cp}R_{cm}}$
$c_2 = P_{sat}$	$c_8 = \frac{RT_{st}K_{ca,in}}{M_{N_2}V_{ca}}\left(\frac{1-x_{O_2,atm}}{1+\omega_{atm}}\right)$	$c_{14} = \frac{RT_{atm}\gamma}{M_{a,atm}V_{sm}}$
$c_3 = \frac{RT_{st}}{V_{ca}}$	$c_9 = \frac{\eta_{cm}K_tK_v}{J_{cp}R_{cm}}$	$c_{15} = \frac{1}{\eta_{cp}}$
$c_4 = M_{O_2}$	$c_{10} = \frac{C_pT_{atm}}{J_{cp}\eta_{cp}}$	$c_{16} = K_{ca\_in}$
$c_{5=M_{N_2}}$	$c_{11} = P_{atm}$	$c_{17} = \frac{C_DA_T}{\sqrt{RT_{st}}}\sqrt{\frac{2\gamma}{\gamma-1}}$
$c_6 = M_vP_{sat}$	$c_{12} = \frac{\gamma-1}{\gamma}$	$c_{18} = \frac{1}{\gamma}$
$x_{O_2,atm} = \frac{y_{O_2,atm}\,M_{O_2}}{M_{a,atm}}$	$\omega_{atm} = \frac{M_v}{M_{a,atm}}\frac{\phi_{atm}P_{sat}}{P_{atm}-\phi_{atm}P_{sat}}$	

Appendix B

Simulink diagram of the 4th order PEM fuel cell model used in Chapter 3 for deriving the open loop step response and deriving the FOPTD model.

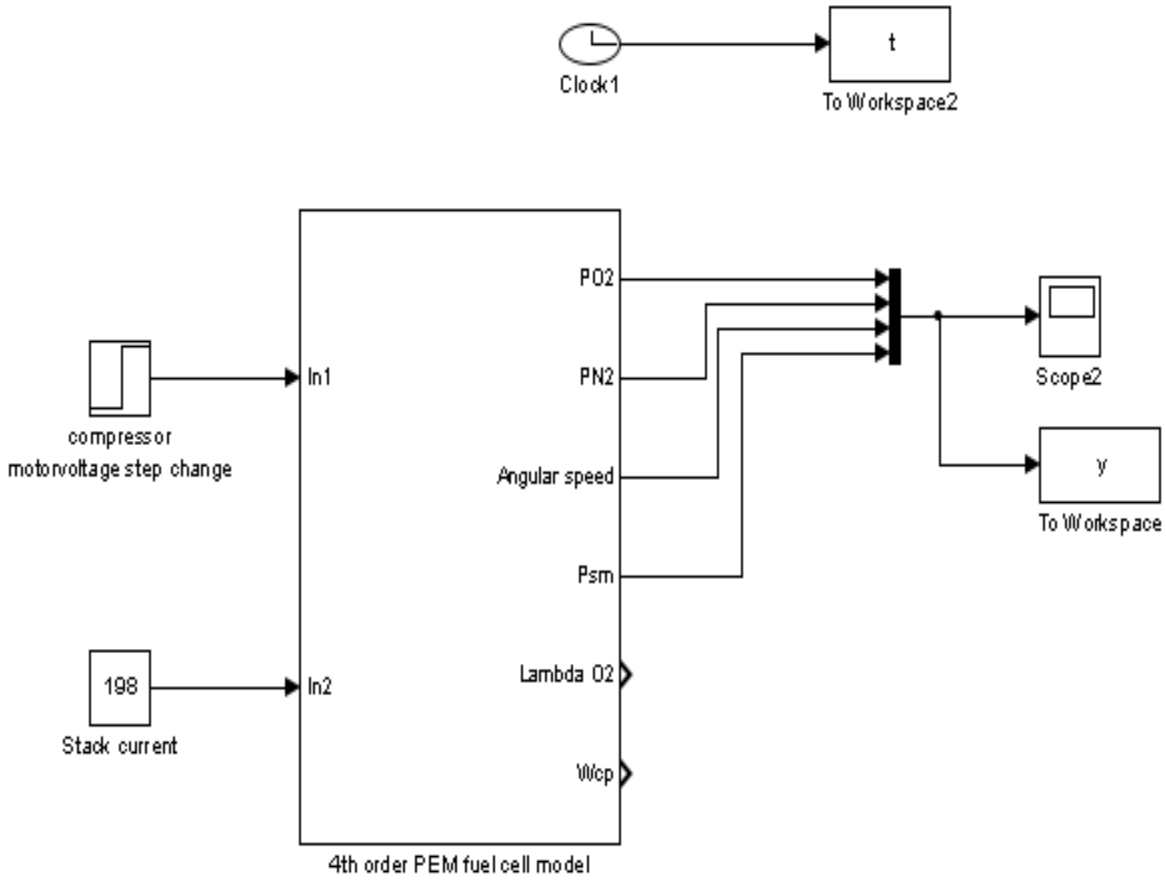

Simulink diagram of 4th order model divided into two parts 1) constants of the model and 2) state equations of the model.

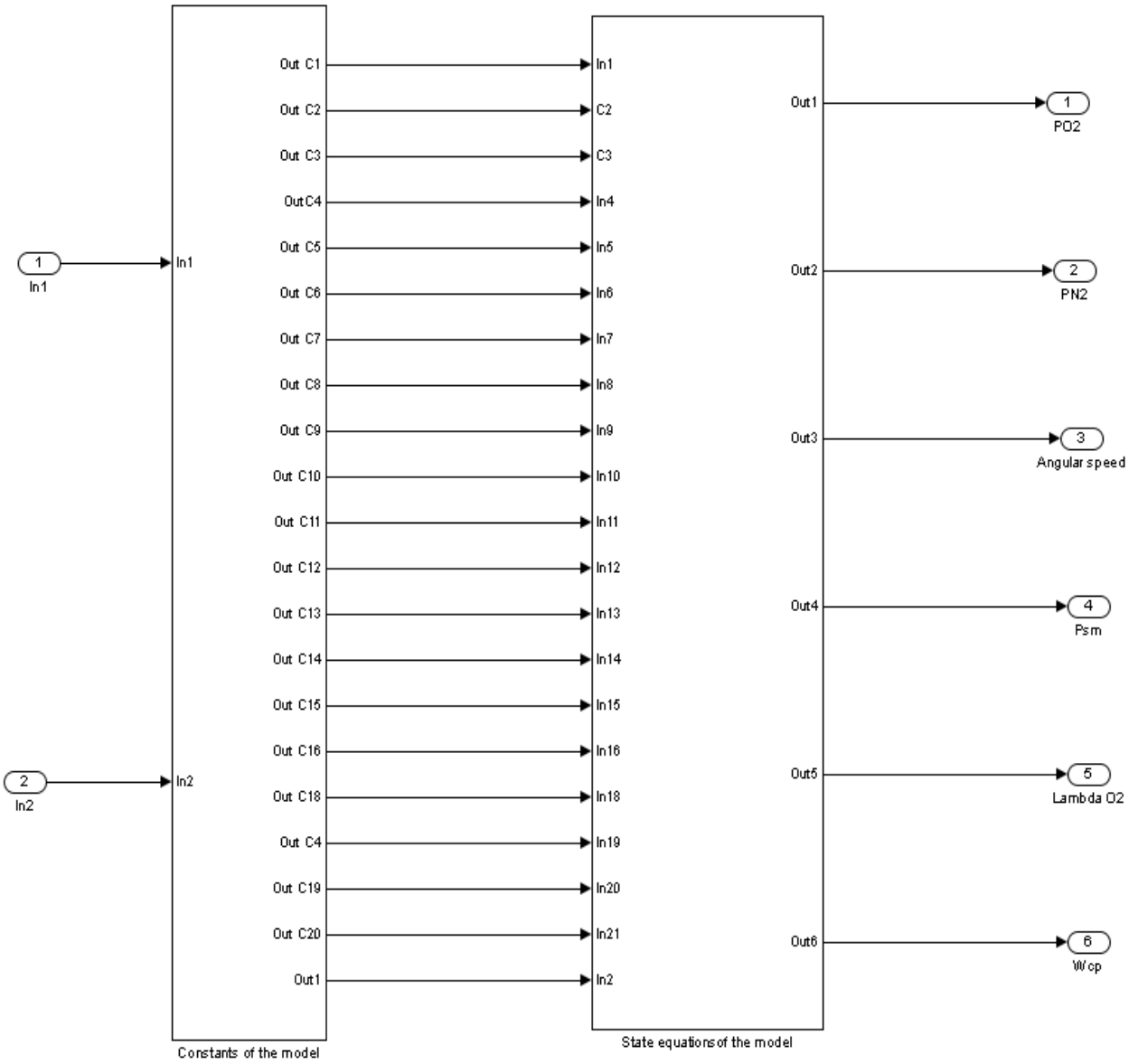

Simulink diagram for the constants of the model

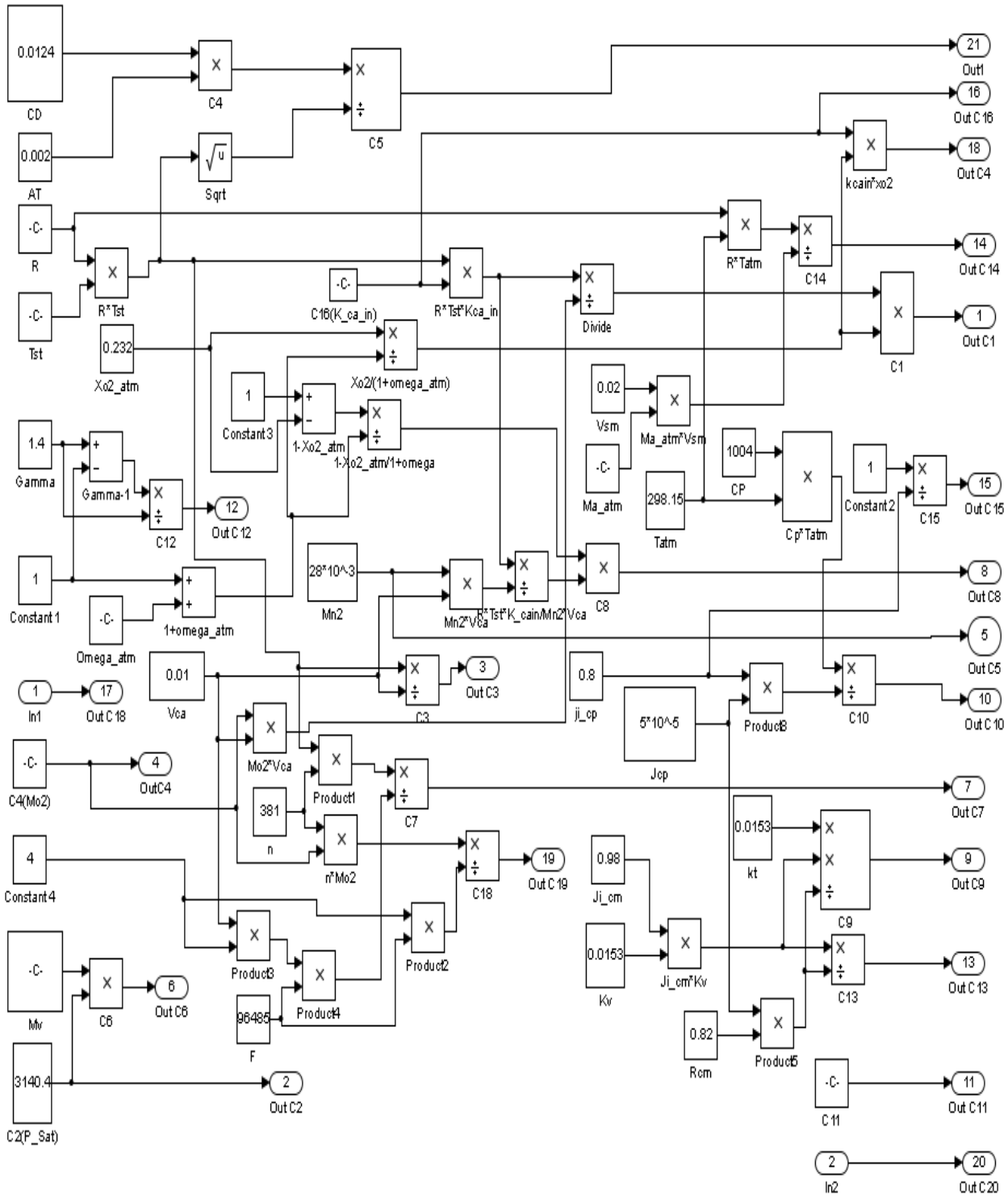

Simulink diagram for the state equations of the model

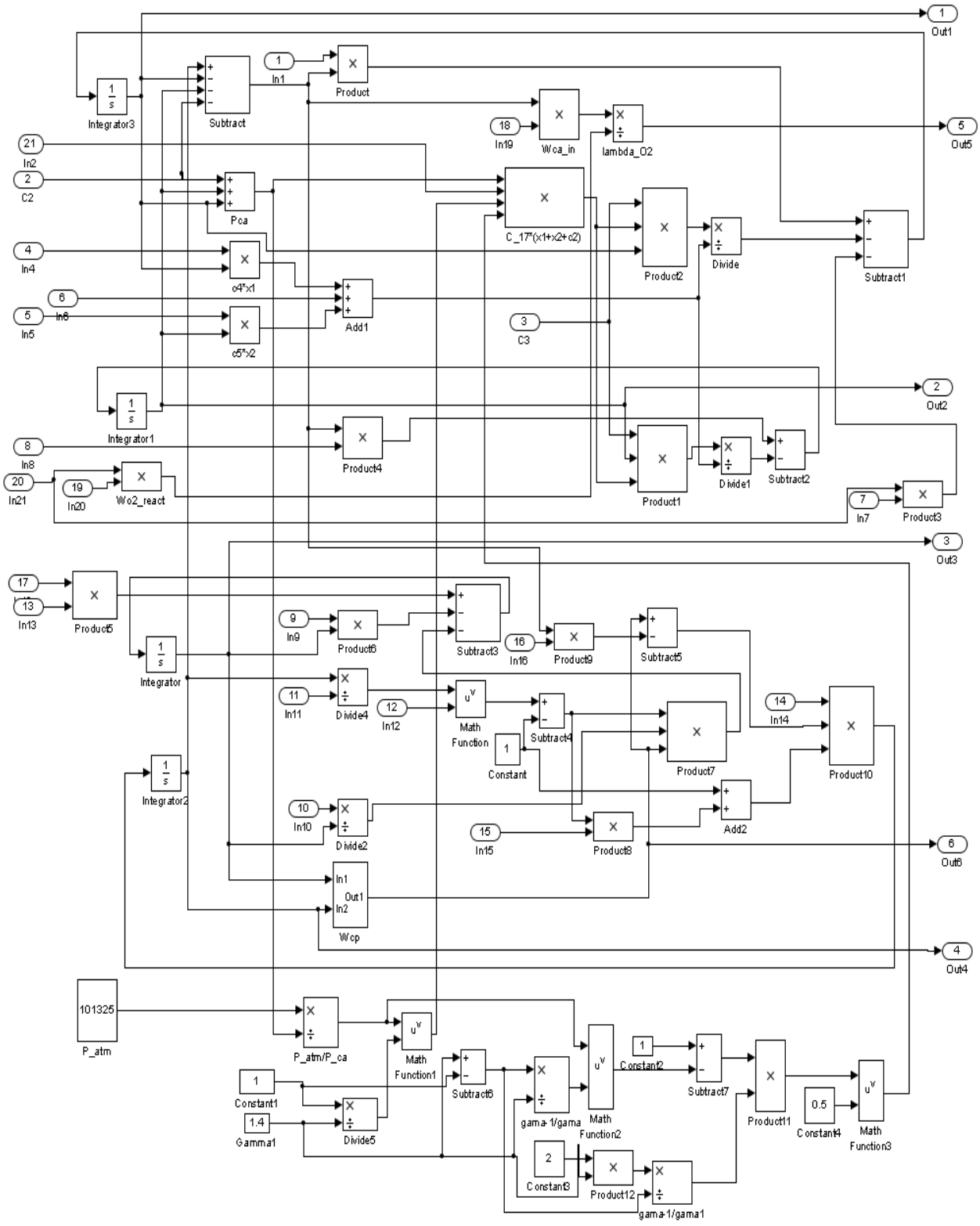

Simulink Block diagram for comparison of smith predictor with other methods used in Chapter 4

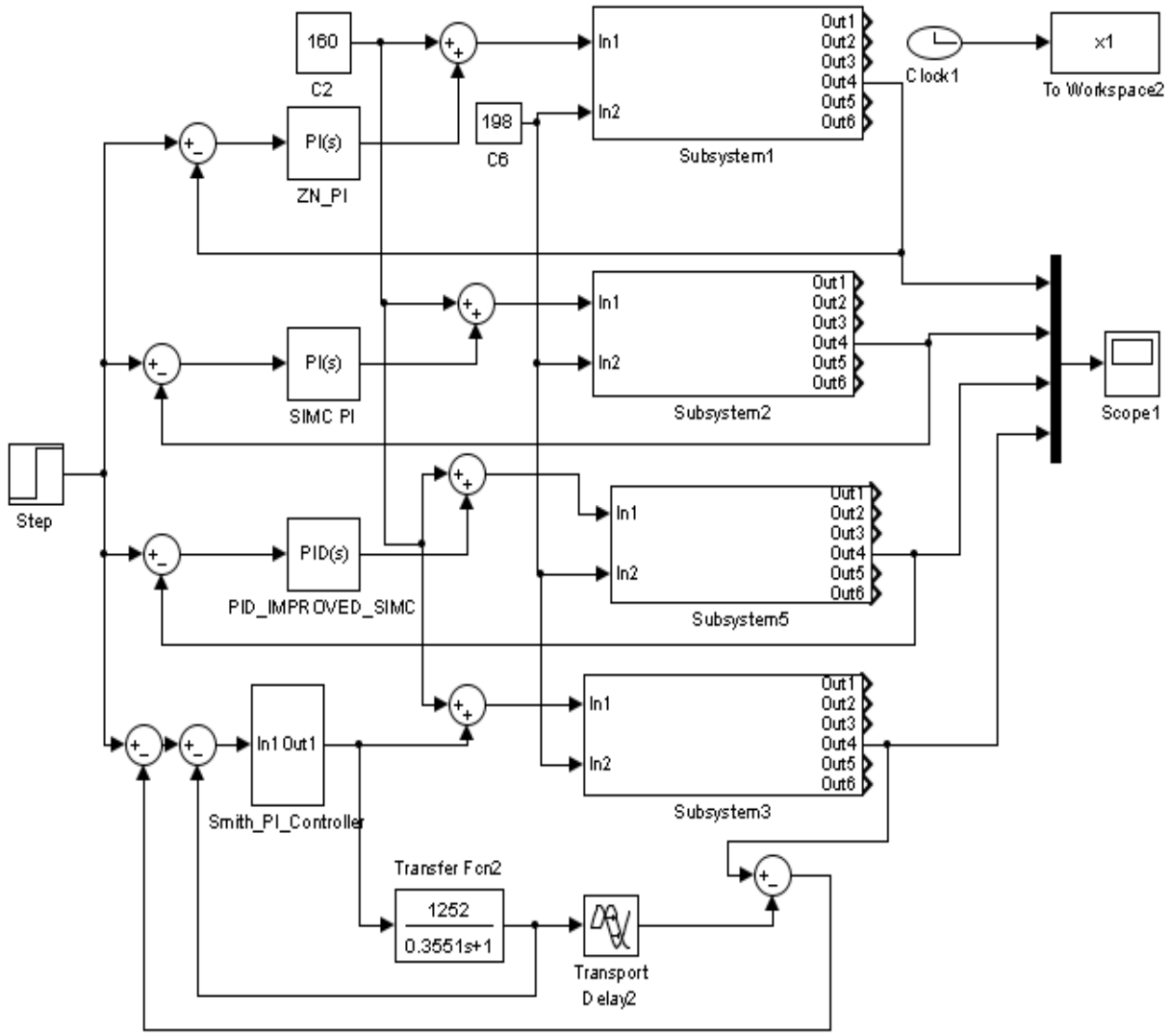

Simulink Block diagram for Decentralized controller for the MIMO system of PEM fuel cell which is used in Chapter 4

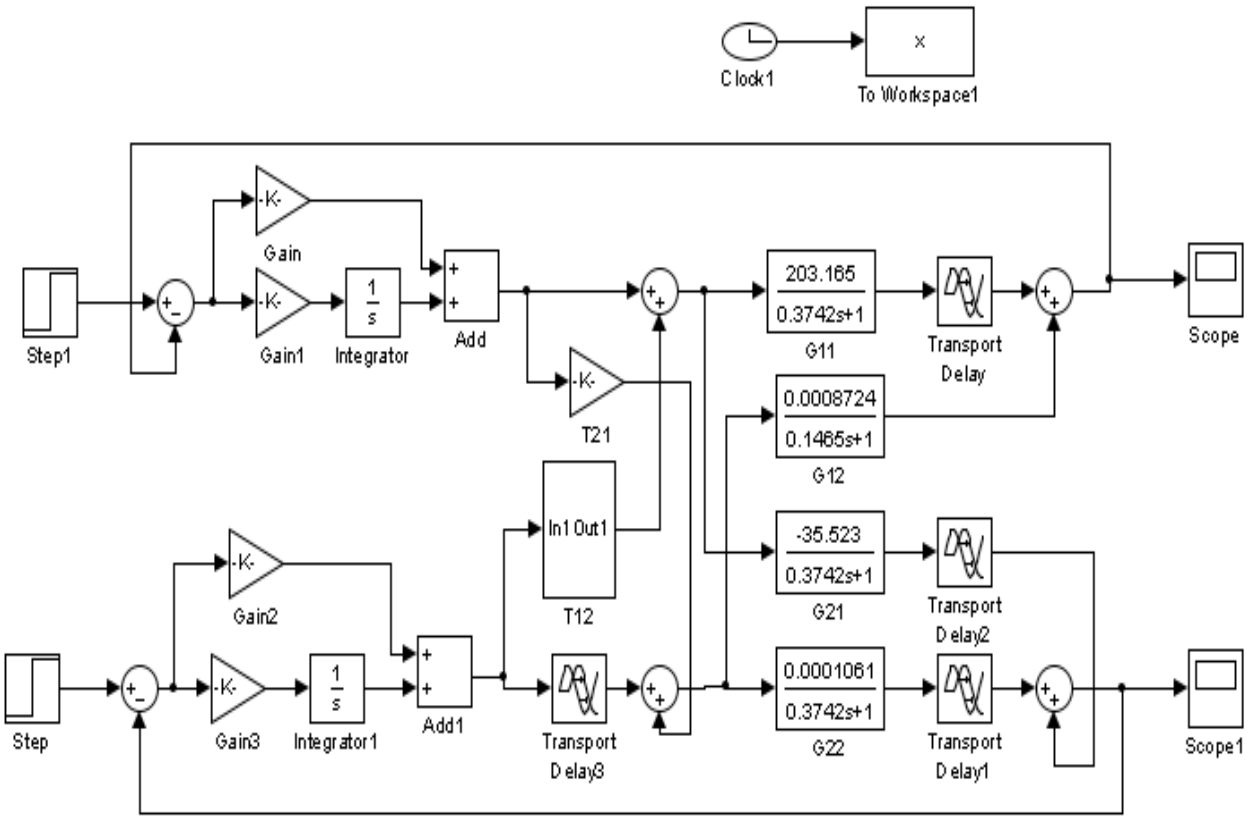

Simulink diagram for optimization using GA which is used in Chapter 7

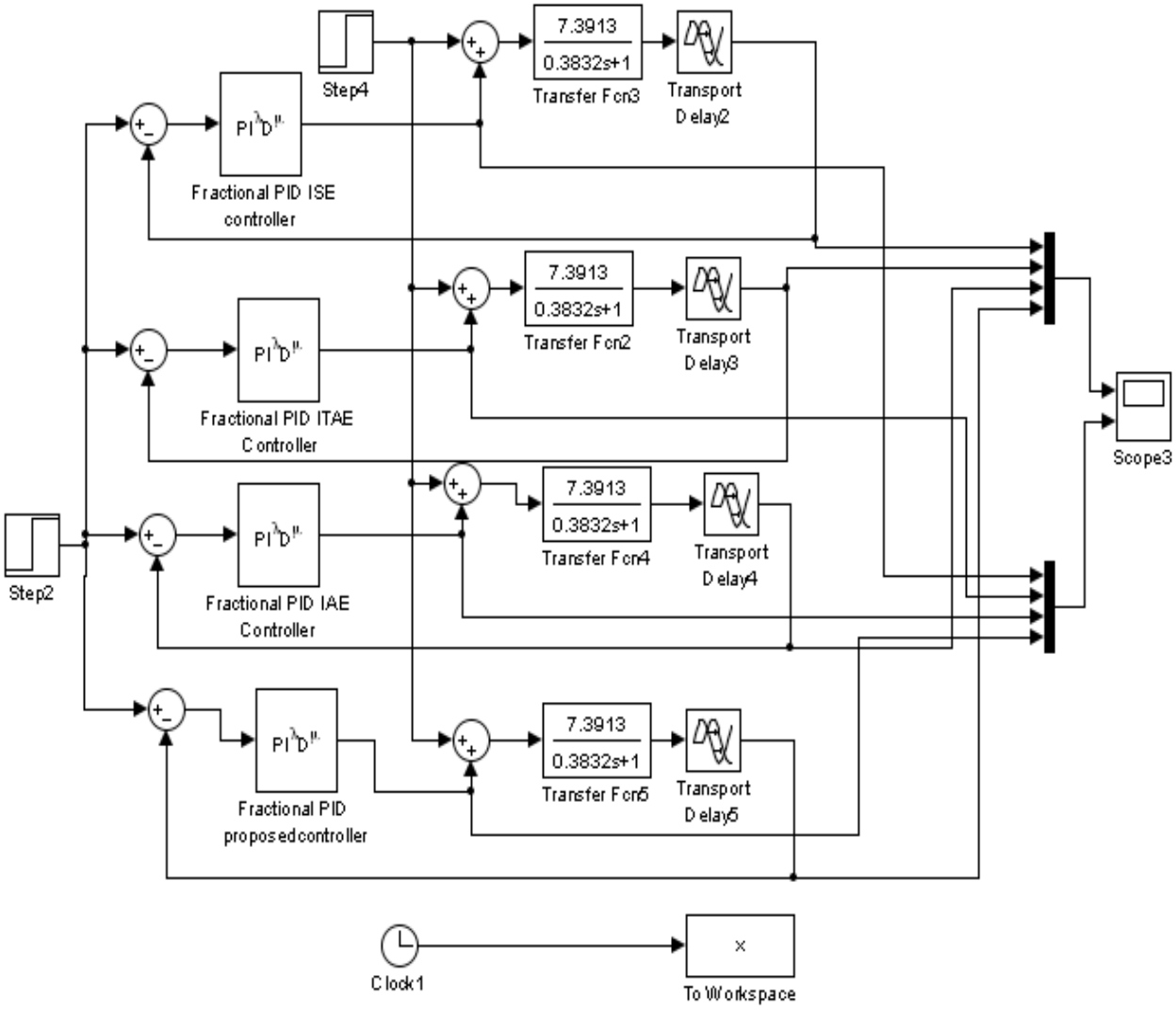

List of Publications

Journals

1. **SrinivasaraoDivi,** S. H. Sonawane &Shantanu Das, "Uncertainty analysis of transfer function of proton exchange membrane fuel cell and design of PI/PID controller for supply manifold pressure control", **Indian Chemical Engineer**, Vol 61(2): pp.138-152 (2019) DOI: 10.1080/00194506.2018.1510794

2. **SrinivasaraoDivi,** Shantanu Das, G. Uday Bhaskar Babu, & S.H. Sonawane, "Fractional order PID controller design for supply manifold pressure control of Proton Exchange Membrane fuel cell" was published online in the journal of **Chemical Product and Process Modeling (CPPM)** Vol 14(3) : (2019) DOI:10.1515/cppm-2018-0053.

International Conferences:

1. "Identification and Design of controller for PEM fuel cell system" Presented in international conference CHEMCON-2016 held on 27-30th, Dec-2016 at IIT Madras, Chennai.

Resume

Personal Details:

Name	SRINIVASARAO DIVI	**Address for Correspondence**
DOB	25-06-1981	Srinivasarao Divi, H.No:6-98, Bank of India Bazaar, Cherukupalli (post), Guntur Dist, AP-522309 Phone: 9949723988 Email-ID:divieie@gmail.com
Sex	Male	
Marital Status	Married	

Educational Qualifications:

Degree	Branch/ Specialization	College	University	Year of Admission	Year of Pass	% of marks
Ph.D	Instrumentation and Control	NIT Warangal	NIT Warangal	2015	2020	-
M.Tech	Instrumentation	NIT Kurukshetra	NIT Kurukshetra	2008	2010	8.32 CGPA
B.Tech	Electronics & Instrumentation Engg.	L.B.R College of Engg., Mylavaram, Krishna Dt.	JNT University, Hyderabad	2003	2006	61.20
DIPLOMA	Electronics & Instrumentation Engg.	S.G.P.R Govt. Polytechnic, Kurnool	SBTE&T, Hyderabad	1996	1999	66.00
SSC		Z.P.H School, Cherukupalli, Guntur Dist	SSC	-	1996	73.50

Title of the Ph.D Thesis: "Design of controllers and analysis of PEM fuel cell systems". Under the guidance of Dr. Shirish H Sonawane sir.

Experience Summary: Teaching: 6 Years 5 Months Industry: 2 Years 10 months
Research:

Total: 9 Years 3 Months

Teaching Experience

S.No.	College	University	Post held	Duration		Ratified (Y/N)	Date of Ratification	Exp. in yrs
				From	To			
1	VRSEC, Vijayawada	JNTUK	Assistant Professor	01-06-2012	15-07-2015	Y	22-08-2014	3.1 Y
2	SPCE, Tuni	JNTUK	Assistant Professor	11-11-2010	31- 05-2012	N	--	1.6 Y
3	SPCE, Tuni	JNTUK	Assistant Professor	25-06-2007	01- 07-2008.	N	--	1 Y
4	S.M.V.M Polytechnic, Tanuku	SBTE&T, Hyderabad	Associate Lecturer	15-06-2006	15-04-2007	N	--	10 M

Details of Industrial Experience:

- Worked as Technician Apprentice in Andhra Cements Ltd, Dachepalli, Guntur dist. From 20/11/2001 To 19/11/2002.
- Worked as Packing Machine Operator in Concept Foods Pvt Ltd, Medchal, Hyderabad From 10/01/2000 To 19/11/2001

Details of Publications/Conferences:

1. Srinivasarao Divi, S. H. Sonawane & Shantanu Das, "**Uncertainty analysis of transfer function of proton exchange membrane fuel cell and design of PI/PID controller for supply manifold pressure control"**, Indian Chemical Engineer (ICE), Vol 61(2): pp.138-152 (2019). DOI: **10.1080/00194506.2018.1510794**

2. SrinivasaraoDivi, Shantanu Das, G. Uday Bhaskar Babu, & S.H. Sonawane, "Fractional order PID controller design for supply manifold pressure control of Proton Exchange Membrane fuel cell" was published online in the journal of **Chemical Product and Process Modeling (CPPM)** Vol 14(3) : (2019) DOI:10.1515/cppm-2018-0053.

3. D.Srinivasarao, D. Kishore, and J.Nityanandam, "**Experimental Studies and Controller Design of Shell and Tube Heat Exchanger Using With and Without Insert**", International Journal of Engineering Research and Applications (IJERA), Vol.3, Issue 4, July-August 2013, 1126-1132 with Impact factor 1.69

4. Presented a paper titled **"Identification and Design of controller for PEM fuel cell system"** S.R. Divi and S.H. Sonawane in International Conference CHEMCON-2016 held on 27-30th Dec-2016 at IIT Madras, Chennai.

Courses Taught:

- Linear Control Systems
- Process Control Instrumentation
- Industrial Instrumentation
- Biomedical Instrumentation
- Circuit Analysis
- Electronic Devices & Circuits

R&D:

Publications	**Journal Publications**	**Conferences**
	International: 03 National: --	International: 01 National: --
Workshops/FDPs Attended:	(i) 1 Day: (2) (ii) 2 to 5 Days: (12) (iii) >5 Days: (1)	
Research Projects sanctioned, if any		
Books Published, if any		
Conferences/Workshops organized		
Awards, if any	Secured 493 rank in GATE 2007 INSTRUMENTATION with a score of 341. Secured 23 rank in state level E-CET entrance exam for B.Tech admission.	
Any other information		

ADDITIONAL SKILLS:

- Can work in teams.
- Willingness to learn.
- Responsible and dedicated

- Positive thinking.
- Learning from experiences.

DECLARATION

I hereby declare that the information given above is true and correct to the best of my knowledge and belief. If I am selected, I agree to abide by the Rules and Regulations of the institute/industry.

Date: -0 - 2020

Place: NIT Warangal **Signature of the Candidate**